2022

Characterization of Porcine Respiratory Epithelial Cells and Their Innate Immune Responses to Bacterial and Viral Ligands

Yam Prasad Gautam

South Dakota State University, yamprasad.gautam@sdstate.edu

Follow this and additional works at: https://openprairie.sdstate.edu/etd2

Part of the Bacteriology Commons, and the Virology Commons

Recommended Citation

Gautam, Yam Prasad, "Characterization of Porcine Respiratory Epithelial Cells and Their Innate Immune Responses to Bacterial and Viral Ligands" (2022). *Electronic Theses and Dissertations*. 398.
https://openprairie.sdstate.edu/etd2/398

This Thesis - Open Access is brought to you for free and open access by Open PRAIRIE: Open Public Research Access Institutional Repository and Information Exchange. It has been accepted for inclusion in Electronic Theses and Dissertations by an authorized administrator of Open PRAIRIE: Open Public Research Access Institutional Repository and Information Exchange. For more information, please contact michael.biondo@sdstate.edu.

CHARACTERIZATION OF PORCINE RESPIRATORY EPITHELIAL CELLS AND THEIR

INNATE IMMUNE RESPONSES TO BACTERIAL AND VIRAL LIGANDS

BY

YAM PRASAD GAUTAM

A thesis submitted in partial fulfillment of Master of Science

Major in Biological Sciences

Specialization in Microbiology

South Dakota State University

2022

THESIS ACCEPTANCE PAGE

Yam Prasad Gautam

This thesis is approved as a creditable and independent investigation by a candidate for

the master's degree and is acceptable for meeting the thesis requirements for this degree.

Acceptance of this does not imply that the conclusions reached by the candidate are

necessarily the conclusions of the major department.

Radhey Kaushik
Advisor   Date

Radhey Kaushik
Department Head   Date

Nicole Lounsbery, PhD
Director, Graduate School   Date

ACKNOWLEDGEMENTS

ABSTRACT

CHARACTERIZATION OF PORCINE RESPIRATORY EPITHELIAL CELLS AND
THEIR INNATE IMMUNE RESPONSES TO BACTERIAL AND VIRAL LIGANDS

YAM PRASAD GAUTAM

2022

In response to a pathogenic attack, the host produces a series of defense mechanisms through various intracellular signaling pathways. The byproduct of these signaling pathways helps tackle the invading pathogen and protects the body from getting into a diseased state. This system is called the immune system. The immune system can be divided into two branches namely the innate immune system and adaptive immune system. The groups of immune cells that provide protection regardless of the pathogen specificity constitute the innate immune system. The system that acts according to the pathogen specificity is called the adaptive immune response. The production of antibodies by B cells is a prime example of adaptive immune responses. Macrophages, neutrophils, and monocytes are a few examples of innate immune cells. Besides them, mucosal epithelial cells of the intestinal and respiratory systems are crucial in generating innate immune responses. Invading pathogens and their recognition by the host is pivotal in preventing the subsequent infection and diseases. Epithelial cells express various Pathogen Recognition Receptors (PRRs). These PRRs recognize pathogen-associated molecular patterns (PAMPs) or damage-associated molecular patterns (DAMPs). The binding of PAMPs and/or DAMPs to epithelial cells initiates intracellular signaling pathways that lead to the generation of innate immune responses through the regulation of gene expression. Porcine

respiratory epithelial cells and their expression of PRRs render them vital not only for the regulation of innate immune responses but also to study respiratory disease pathogenesis. Ironically, only a handful of studies can be found on these cells and the limited number of studies have hindered our understanding of the role of porcine respiratory cells in innate immunity.

In this study, we have characterized previously established porcine primary respiratory epithelial cells from nasal turbinate and trachea followed by their immortalization using hTERT and SV40 large T-antigen. We also studied their innate immune responses to various bacterial and viral ligands. Both the primary and immortalized cells showed typical epithelial cobblestone morphology with a heavy expression of cytokeratin indicating epithelial origin. Cells did not change their morphological characteristics even after immortalization. Immortalization was confirmed by immunofluorescence assay for SV40 and immunocytochemistry for hTERT. However, they did look more granulated than the primary cells. Growth curve analysis showed a faster growth rate of immortalized cells in comparison to the primary cells of both nasal and tracheal origin. Finally, we stimulated the primary cells with various bacterial and viral ligands. Upon stimulation, porcine primary respiratory cells mounted innate immune responses through modulation of the expression of various PRRs and the production of cytokines/chemokines. Modulation of gene expression on mRNA level was measured using ΔΔct method. The research findings may be vital in studying the role of respiratory epithelial cells in the pathogenesis of various respiratory diseases and innate immune responses in pigs.

TABLE OF CONTENTS

ABBREVIATIONS

AIMS: Absent in melanoma 2

AP: Activator protein

APC: Antigen presenting cell

APRIL: A proliferation inducing ligand

ASMA: Alpha smooth muscle actin

ATCC: American type culture collection

BAFF: B-cell activating factor

CARD: Caspase activation and recruitment domain

CD: Cluster of differentiation

cDNA: Complementary DNA

CpG: C-phosphate-G

CRD: Carbohydrate recognition domain

CT: Cycle Threshold

DAB: Diaminobenzidine

DAMP: Damage associated molecular pattern

DC: Dendritic cell

DC-SIGN: Dendritic Cell Specific Intracellular Adhesion Molecule-3-Grabbing Non-Integrin

DMEM: Dulbecco's Modified Eagle's Medium

DNA: Deoxyribonucleic acid

dsRNA: double stranded RNA

EGF: Epidermal growth factor

EDTA: Ethylenediaminetetraacetic acid

FBS: Fetal bovine serum

FLA: Flagellin

HA: Hemagglutinin

HDL: High density lipoprotein

ICAM: Intracellular adhesion molecule

IFA: Immunofluorescence Assay

IFN: Interferon

IgA: Immunoglobulin A

IgM: Immunoglobulin M

IgG: Immunoglobulin G

IHC: Immunohistochemistry

IkB: IkappaB

IKK: IkB kinase

IL: Interleukin

InAc: Inulin acetate

IPEC: Intestinal porcine epithelial cells

IPS: Interferon-beta promotor stimulator

IRAK: Interlukin-1 receptor -associated kinase

IRF: Interferon Regulatory Transcription factor

ITS: Insulin Transferrin Selenium

LPS: Lipopolysaccharide

MAP: Mitogen activated protein

MAPK: MAP kinase

MCP: Macrophage chemoattractant protein

MDA5: Melanoma differentiation-associated gene 5

MDP: Muramyl dipeptide

MHC: Major histocompatibility complex

MyD88: Myeloid differentiation primary response gene 88

NA: Neuraminidase

NF-kB: Nuclear Factor KappaB

NK: Natural Killer cells

NLRs: NOD-like receptors

NOD: Nucleotide-oligomerization domain

PAMP: Pathogen-associated molecular patterns

PBS: Phosphate buffered saline

PCR: Polymerase chain reaction

PGN: Peptidoglycan

PMDVS: Pathogen mimicking vaccine delivery system

PPNTECs: Pig primary nasal turbinate epithelial cells

Poly I:C: Polyinosinic-polycytidylic acid

PPTECs: Pig primary tracheal epithelial cells

PRRs: Pathogen recognition receptors

RD: Repressor domain

RICK: Receptor interacting serine/threonine protein kinase 2

RIG-I: Retinoic acid inducible gene-1

RLR: RIG-I like receptors

RNA: Ribonucleic acid

RT-qPCR: Reverse Transcriptase- Polymerase Chain reaction

RTU: Ready-to-use

SIgA: Secretory IgA

SEM: Standard error of mean

TAB: TAK-1 binding proteins

TAG: TRAM adaptor with gold domain

TAK: TGF-beta activated kinase

TICAM: TIR domain containing adaptor molecule

TIR: Toll-interlukin-1 receptor

TLR: Toll like receptors

TNF: Tumor necrosis factor

TRAF: TNF receptor associated factors

TRIF: TIR domain containing adaptor inducing interferon beta

TRIM: Tripartite motif

TH1: T-helper 1

LIST OF TABLES

LIST OF FIGURES

1   Chapter 1. Literature review

1.1 Mucosal surfaces and innate immunity

The mucosal surfaces of the body play a major role in innate immunity and host-pathogen interaction. The importance of the involvement of respiratory and intestinal mucosa and the epithelial surfaces in the host-pathogen interaction, anatomical and physiological barrier function as the first line of defense has been shown by overwhelming number of previous studies (1-4). Microorganisms are received by the digestive and respiratory mucosal epithelia mostly via ingestion/inhalation. The epithelial surfaces have unique receptors for the binding of pathogens and their entry. The unique receptors on the epithelial cell surfaces are called Pathogen Recognition Receptors (PRRs) that bind to specific Pathogen Associated Molecular Patterns (PAMPs) on microbe surfaces. The binding of PRRs to PAMPs initiates cell signaling followed by the activation of the innate immune responses (5, 6).

Intestinal and respiratory mucosal epithelial cells are continuously exposed to various microorganisms. All microbes are not pathogens because the commensals or the normal flora are the populations of microbes that benefit the host and do not have any pathogenic action toward the host (7, 8). The epithelial cells can sense the presence of pathogens or their metabolic products and mount the immunological responses against them while simultaneously inducing tolerance against the commensals which is a basis for balance and homeostasis. The sensing of pathogens or commensals is highly regulated as it is a way of knowing the microbial environment and the surrounding (9). The selective recognition of pathogens and the distinction between pathogens and commensals by the host is believed to be there because the surface epithelia cause the sequestration of indigenous microflora

and thus, the PRRs cannot be activated whereas the antigens/virulence factors on pathogens easily pass-through epithelial barriers and recognized by various PRRs on immune cells (10, 11).

1.1.1 Immune system and its components

To protect or defend us, a well-specialized and organized system exists that plays a role against infection, and this organized system is known as the immune system. The Immune system can fundamentally be differentiated into two branches. The innate immune system protects by using various innate immune cells like macrophages, neutrophils, and monocytes which are phagocytic and perform phagocytosis (12). Other cells including mast cells, NK-cells, basophils, and eosinophils are also components of the innate immune system and help in producing innate inflammatory responses to provide defense against infection by invading microbes. B cells and T cells are the major components of the adaptive immune system, the second branch of the immune system. The adaptive immune system is responsible for the humoral or antibody-based immune response against microbes (13). The innate immune system and its response play an important role in the removal of pathogens and in developing pathogen-specific adaptive immunity (14). Both branches of the immune system come together and work simultaneously and defend us against pathogens (5).

1.2 Pathogen recognition receptors

The invasion of a host by microorganisms initiates their recognition through germline-encoded receptors which are known as the pattern-recognition receptors (PRRs) (15). PRRs exist in a variety of classes and have a diverse range of immunological functionality. TLRs, NLRs, and RLRs are some common examples of PRRs. PRRs bind to their respective

ligands which lead to the activation of intracellular signaling and subsequent expression or upregulation of genes that are vital for the generation of immune responses (16-18).

Microbial components recognized by PRRs are called pathogen-associated molecular patterns (PAMPs). PAMPs are essential molecules that are required by pathogens for their survival. Different PAMPs are recognized by their respective PRRs and this binding activates specific signaling pathways to generate distinct antipathogenic responses (19).

1.2.1 Toll-like receptors

1.2.1.1 History

Out of several kinds of PRRs such as Toll-Like Receptors (TLRs), NOD-like receptors (NLRs), RIG-I like receptors (RLRs), C-type lectin receptors, absent in melanoma 2 (AIMS) like receptors, TLRs are the most powerful molecular receptors used by the innate immune system to sense the microbial environment and provide the necessary protection to the host. The 2011 Nobel prize award in medicine to Jules Hoffman and Bruce Beutler tells the impact and worldwide recognition of this landmark finding (20).

TLRs or the toll proteins were first identified in *Drosophila melanogaster* (21), and this discovery is marked as one of the most significant breakthroughs in host-pathogen interaction which led to a flurry of research and discoveries in the field of immunology. Initially, Toll receptors were discovered as a transmembrane receptors essential for the dorso-ventral polarity development in developing embryos of Drosophila (21). Nine genes in the *Drosophila* genome encode toll proteins (22). In humans, 10 TLRs have been identified. Human TLR1, TLR2, TLR3, TLR6, and TLR10 reside on chromosome number 4 while TLR4 and TLR5 reside on chromosomes 9 and 1, respectively. Similarly, TLR7 and TLR8 are in chromosome 10 while chromosome 3 encodes TLR9. The above

chromosomal locality reveals the dispersed nature of TLR genes throughout the human genome. TLR genes and their DNA sequence studies have shown the conserved nature of these genes across species and their independent evolution from a common ancestral gene (23-25).

Table 1. TLR Recognition of Microbial Components

Microbial Components	Species	TLR Usage
Bacteria		
LPS	Gram-negative bacteria	TLR4
Diacyl lipopeptides	*Mycoplasma*	TLR6/TLR2
Triacyl lipopeptides	Bacteria and mycobacteria	TLR1/TLR2
LTA	Group B *Streptococcus*	TLR6/TLR2
PG	Gram-positive bacteria	TLR2
Porins	*Neisseria*	TLR2
Lipoarabinomannan	Mycobacteria	TLR2
Flagellin	Flagellated bacteria	TLR5
CpG-DNA	Bacteria and mycobacteria	TLR9
ND	Uropathogenic bacteria	TLR11
Fungus		
Zymosan	*Saccharomyces cerevisiae*	TLR6/TLR2
Phospholipomannan	*Candida albicans*	TLR2
Mannan	*Candida albicans*	TLR4
Glucuronoxylomannan	*Cryptococcus neoformans*	TLR2 and TLR4
Parasites		
tGPI-mutin	*Trypanosoma*	TLR2
Glycoinositolphospholipids	*Trypanosoma*	TLR4
Hemozoin	*Plasmodium*	TLR9
Profilin-like molecule	*Toxoplasma gondii*	TLR11
Viruses		
DNA	Viruses	TLR9
dsRNA	Viruses	TLR3
ssRNA	RNA viruses	TLR7 and TLR8
Envelope proteins	RSV, MMTV	TLR4
Hemagglutinin protein	Measles virus	TLR2
ND	HCMV, HSV1	TLR2
Host		
Heat-shock protein 60, 70		TLR4
Fibrinogen		TLR4

Figure 1: Microbial components and their recognition by respective TLRs (19).
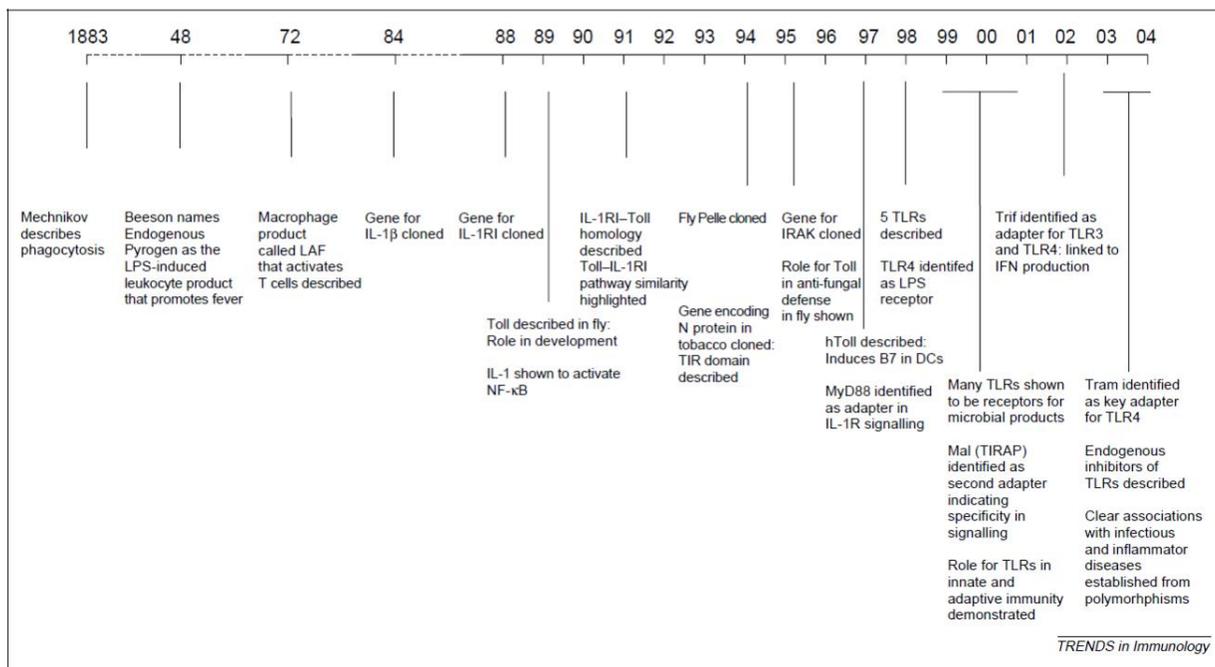
Figure 2: History of TLRs (26). Sequence of events starting from the discovery of TLRs to their roles in the innate immune system are described in a chronological order.

1.2.1.2 Types and distribution

Not long after *Drosophila* Toll protein was identified for the first time, a similar group of proteins sharing structural similarities to Toll protein in *Drosophila* was identified and was given the name Toll-like receptors (TLRs). TLRs have an extracellular domain with a leucine-rich repeat (LRR) and an intracellular domain with TIR. Out of all the TLRs identified to date, TLR4 is the one first identified. Lipopolysaccharide (LPS), a component of Gram-negative bacterial cell wall, was found to be recognized by TLR4 for the first time in 1998. This discovery was of immense significance and led to many more findings and discoveries of TLRs and their recognition of microbial components (21, 27).

Mammalian cells express several TLRs and different TLRs have their own tissue as well as cell-specific distribution pattern. To date, 13 different TLRs have been identified in mammals, 10 in humans, 10 in bovine, 10 in ovine, and 13 in mice (19, 28). Based on their expression TLRs are categorized into transmembrane receptors such as those expressed in epithelial cellular membranes, for example, TLR1, TLR-2, TLR-5, TLR-6, and those expressed intracellularly, for example, TLR-3, TLR-7, TLR-8, TLR-9, TLR-11, TLR-12, and TLR-13. Unlike other TLRs, TLR-4 is expressed extracellularly as well as intracellularly (29).

The mounting of the dysregulated innate immune response against commensals by the failure of recognition has been linked to severe diseases like inflammatory bowel disease and colorectal cancer (30). TLR2, TLR-4, TLR-5, and TLR-9 variants respectively have been linked to Crohn's disease and ulcerative colitis (31, 32). In conclusion, mutation, polymorphism, or any unwanted changes in these receptors have the potential to severely dysregulate homeostasis. The optimal expression of TLRs on intestinal and respiratory

epithelial cells is key in protecting the host through the activation of the innate immune response followed by adaptive immunity (33).

TLRs are categorized into 5 subfamilies on basis of amino acid sequence comparison. TLR2, TLR3, TLR4, TLR5, and TLR9 are the 5 different subfamilies. Based on their similarity in amino acid sequence and genomic structures, a phylogenetic tree is constructed as shown in the figure 3 below (21).

A variety of innate immune cells ubiquitously express mRNAs for TLR expression. Blood monocytes/macrophages express most TLRs. However, they do not express TLR3 (34). Mature dendritic cells and immature dendritic cells have different levels of expression of TLRs. Some TLRs are expressed more in immature cells while some are expressed at high levels in mature cells. For example, TLR1, 2, 4, and 5 expression is high initially in mature dendritic cells but as the cells mature, their expression is lowered with the maturity. The expression of TLRs on dendritic cells can be said to have a direct correlation with the maturation stages (35). Mast cells, also express TLRs including TLR2, TLR4, TLR6, and TLR8 (36, 37). The intestinal and respiratory epithelial cells express TLRs, but the expression is finely regulated and is less widespread when compared to immune cells. Regulated expression of TLRs on epithelial cells is crucial because immune cells or APCs are programmed to trigger an immune response against foreign organisms, but if epithelial cells also elicit an immune response like APCs, it will lead to unnecessary and overexpression of immune responses against billions of commensals throughout the mucosal surfaces. Thus, the expression of TLRs is selective and less widespread in mucosal epithelial cells. When encountered with a pathogen, mucosal epithelial cells can produce inflammatory cytokines and chemokines such as IL-6, IL-10, IL-1a, IL-1b, IL-13, TNF-a,

and thus, promote inflammation and protection against the pathogen. Mucosal epithelial cells can activate the innate and adaptive immune systems by producing factors like interferons, BAFF, and APRIL (38, 39).
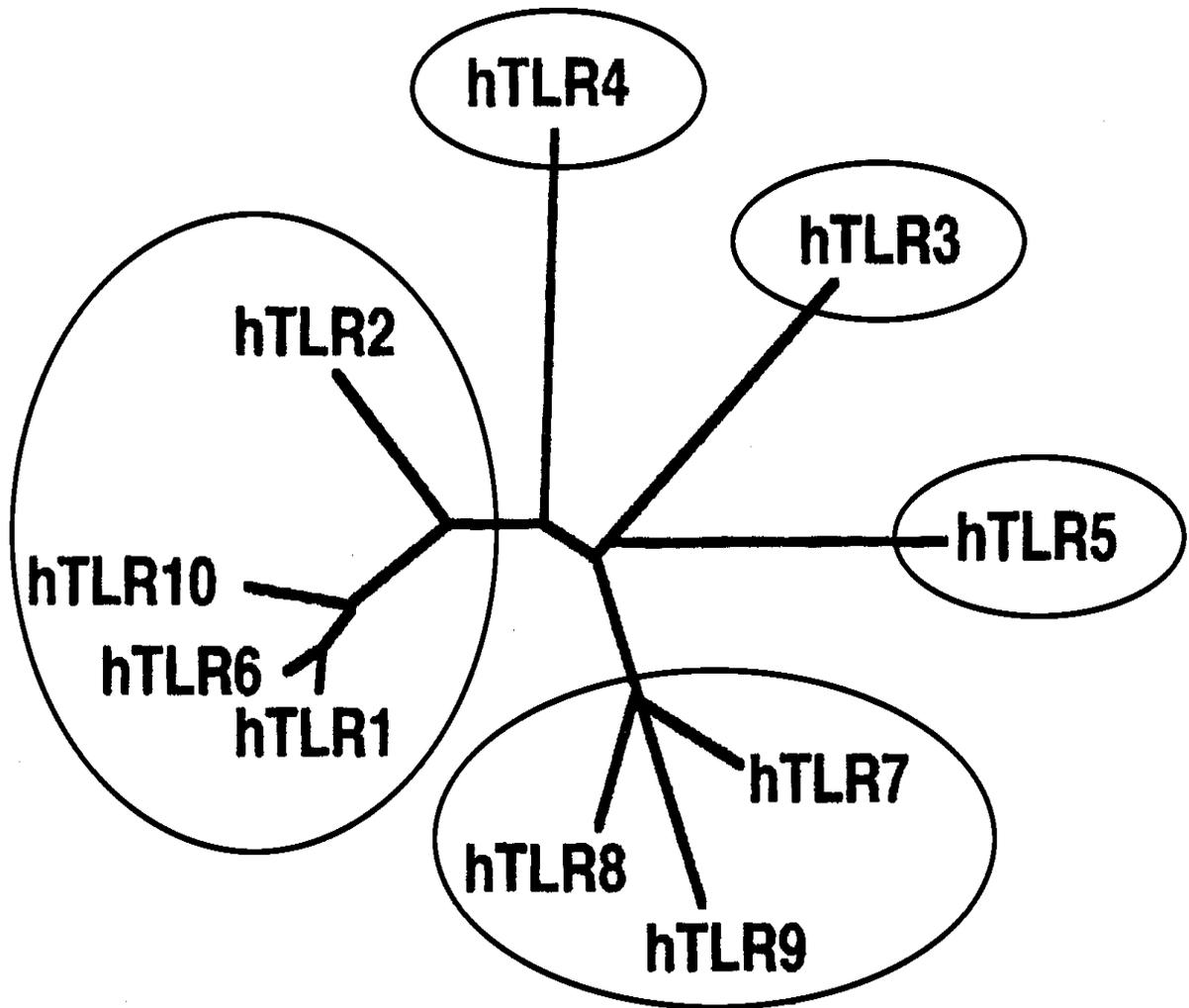
Figure 3: Phylogenetic tree of Human Toll-like receptors (21). The phylogenetic tree is designed on basis of genetic resemblances between TLRs.

1.2.1.3   TLR signaling
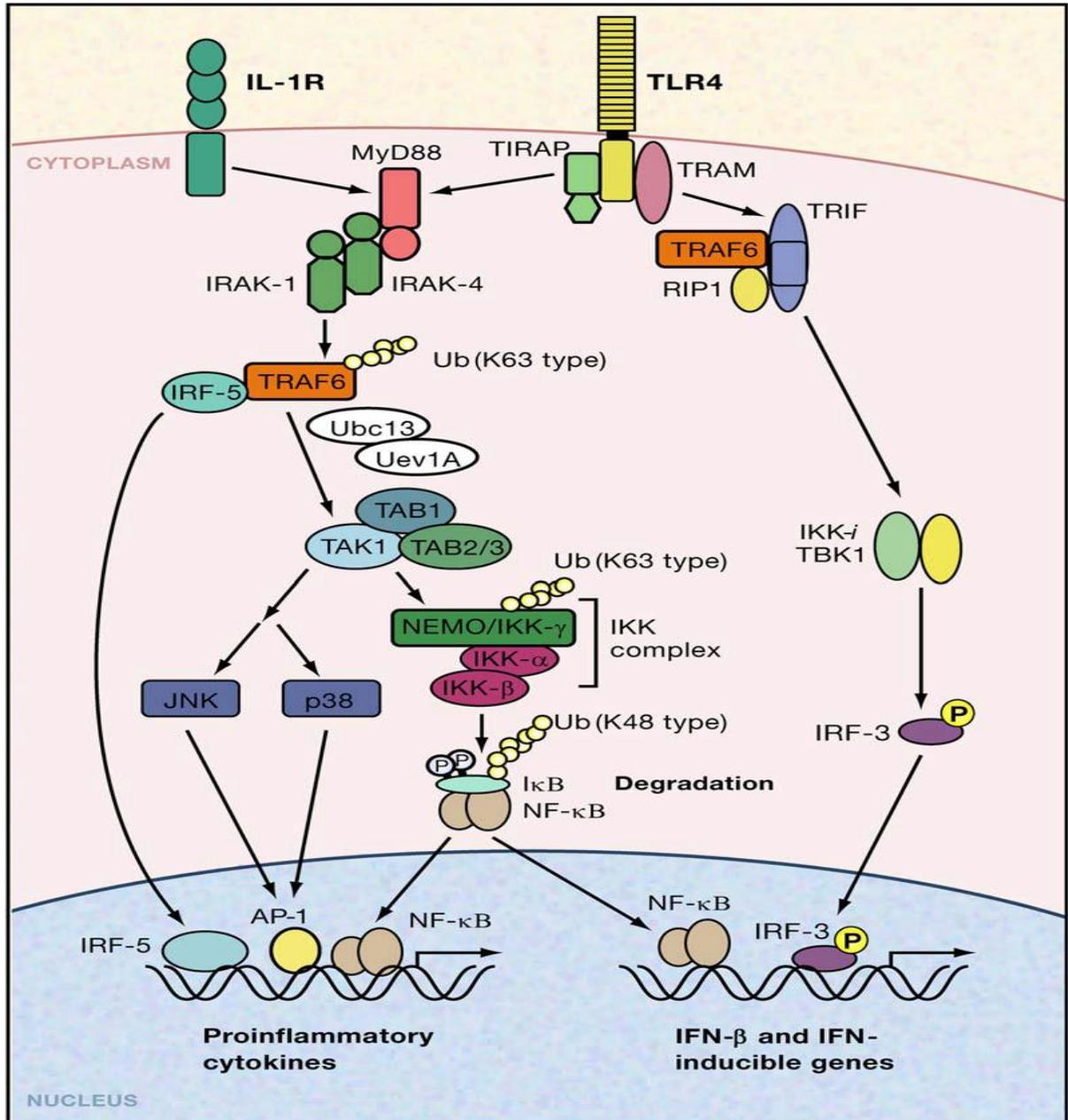
Figure 4: TLR signaling pathway (19). The figure shows both the MyD88 dependent signaling pathway and TRIF dependent signaling pathway leading to the transcription of proinflammatory cytokines and type-I Interferons.

PRRs recognize PAMPs or DAMPs leading to the activation of downstream signaling. The downstream signaling activates the innate immune system marked by the production of inflammatory cytokines, chemokines, and IFNs. These molecules not only contribute to the innate response but also the activation of the pathogen-specific adaptive immune response. TLRs recognition of PAMPs is facilitated by leucine-rich repeats (LRRs), an ectodomain of TLRs. TLRs also possess a cytoplasmic Toll/IL-1 receptor (TIR) domain responsible for the initiation of downstream signaling. Recognition of PAMPs promotes TIR domain-containing adaptor proteins recruitment by TLRs. Adaptor proteins such as MyD88 and TRIF commence signal transduction pathway that leads to the activation of the NF-kB pathway or MAP kinase pathway that regulates the expression of genes encoding cytokines, chemokines, and IFNs that contribute to the host defense (40-42).

1.2.1.3.1 MyD88 dependent signaling pathway

MyD88, an adaptor molecule central to the inflammatory signaling pathway, was first described as an upregulated gene during IL-6 induced myeloid differentiation (43, 44). MyD88 has a C-terminal portion consisting of the TIR domain and interacts with the TIR-domain containing molecules such as TLRs. Death Domain (DD), present in the N-terminus of MyD88, is associated with IL-1 receptor-associated kinase (IRAK). IRAK activity was described for the first time in 1994 (45). The first cloned IRAK molecule was IRAK1. But it was found that the mice lacking IRAK1 still were able to respond to IL-1, even though the response was very weak (46). Later, three other members of the IRAK family were identified namely IRAK2, IRAK-M, and IRAK4 (44, 47-49). When activated, IRAK1 undergoes autophosphorylation and interacts with TNF receptor-associated factor 6 (TRAF6). IRAK/TRAF6 interaction assembles a multiprotein signaling complex

consisting of TAK1, which is the mitogen-activated protein kinase kinase kinase (MAPKKK) and is associated with TAB1, TAB2, and TAB3 proteins, which are responsible for the regulation of activation of TAK1 kinase. Activation of TAK1 leads to the activation of IkB kinases (IKKs), p38, and JNKs, which ultimately leads to the activation of NF-kB and AP-1. NF-kB is a transcription factor, which translocate from the cytoplasm into the nucleus and thus, occurs the expression of proinflammatory cytokines IL-1, IL-6, and TNF-a. AP-1, an activator protein, and a transcription factor, activated via the MAPK family of proteins that are activated by TAK1, is also responsible for inducing the expression of innate immune response genes (19, 21, 50, 51).

1.2.1.3.2 TRIF-dependent signaling pathway

Toll/IL-1R domain-containing adaptor-inducing IFN-B or the TRIF-dependent signaling pathway plays important role in host defense and is responsible for the production of Type-I IFN alongside various mediators of the inflammatory immune response against pathogens independent of MyD88. TRIF is an adaptor molecule contributing to the activation of IRF-3 and subsequent IFN-B production (52, 53).

TICAM-1/TRIF comprises of an N-terminal domain, a TIR-domain, TRAF6-binding motif, and a receptor-interacting protein homotypic interaction motif (RHIM) (54). TIR domain of TICAM-1/TRIF binds to the TIR domain of TLR-3 leading to the activation of IRF-3, a transcriptional factor that later translocate into the nucleus and induces the production of type-I IFNs. Activation of the NF-kB pathway is believed to occur through the C-terminal domain (55). But it has been found that TICAM-2, another adaptor molecule like TICAM-1, is required for TICAM-1 to bind to TLR-4 for the activation of the TLR-4 mediated signaling pathway (52).

TRIF dependent signaling pathway is both negatively and positively regulated by various molecules. Molecules like CD16, CD14, Pellino (E3 ubiquitin ligase), TRIM56, and TRIM62 positively regulate the pathway by bolstering the activation or inhibiting the inhibitors of the pathway (56-59). Similarly, molecules like TAG (a TRAM variant), TRIM38, Pin1(Peptidyl-propyl isomerase), and HDL (High-density lipoprotein) negatively regulates the TRIF signaling pathway (54, 60-62).

1.2.2 NLRs and RLRs

Nucleotide-binding and oligomerization domain (NOD)-like receptors (NLRs) are another type of PRRs involved in the activation of NF-kB and MAPK signaling pathways. Unlike TLRs that recognize PAMPs present on the cell surface or in the endosomes, NLRs recognize PAMPs in the cytosol (63, 64). The microbial components successful in evading extracellular detection are detected in the cytosol by NLRs and RIG-like receptors (RLRs). NLRs are characterized by the presence of a conserved NOD (65). NLRs consist of NOD-1 and NOD-2 and are known to recognize products of bacterial peptidoglycan synthesis/degradation. γ-D-glutamyl-Meso-diaminopimelic acid (iE-DAP) is recognized by NOD1 while NOD-2 recognizes muramyl dipeptide (MDP) (66, 67).

Structurally, NLRs have a C-terminal leucine-rich repeat (LRR) responsible for the sensing of microbial particles. This sensing initiates the activation of the N-terminal caspase recruitment domain (CARD) and pyrin (P). The CARD domain activation leads to the recruitment of serine-threonine kinase (RICK) and the interaction of NOD1 and NOD2 with RICK induces the NF-kB and MAPK signaling pathway. In cooperation, NF-kB, and MAPK pathways regulate the innate and adaptive immune responses by upregulating the production of proinflammatory cytokines (68).

Like what NOD does, RLRs also recognize PAMPs in the cytoplasm and drive IFN-signaling. More specifically, RLRs interact with viral RNA ligands in the cytoplasm and contribute to the innate immune system through IFN-B production. Interestingly, RLRs play role in the adaptive immune response indirectly by driving IFN-B production which in turn activates B-cells and thus, antibody production (69). RIG-I and MDA-5 are two main RLRs expressed in a broad variety of cells and play a prominent role in activating the innate immune system. In addition to IFN-B production, RLRs also trigger the expression of genes having antiviral properties and play role in inducing antiviral response. In cells, the expression levels of RLRs differ significantly with or without the viral infection where the latter induces a high level of expression (70). Structurally, RLRs are like NODs and have an N-terminal CARD, a central RNA helicase domain involved in the unwinding of viral RNA molecules, and a C-terminal domain with a repressor domain (RD) within and is thought to be regulating the autoregulation in RIG-I (70).

According to Cui et al (71), the amino acid sequence ranging from 802-925, in the C-terminal domain, binds to the 5'-triphosphate ends of the viral dsRNA. This binding brings a conformational change in CARD, which is sequestered from any interaction in absence of viral infection. The conformational change enables CARD to interact with the adaptor protein IPS-1. This interaction leads to the phosphorylation of IRF-3 and IRF-7 by TBK1, subsequent translocation of IRF-3 and IRF-7 into the nucleus, and finally the expression of genes responsible for IFN-B production (72). RLRs and their signaling are highly regulated both positively and negatively and destabilization of RLRs signaling has been linked to various autoimmune disorders and cytokine storms (73).

1.2.3 Other PRRs

1.2.3.1 C-type lectins

C-type lectins are the type of lectins important in pathogen recognition. They have carbohydrate recognition domains (CRDs) that bind carbohydrate molecules in a calcium-dependent manner (74). C-type lectins are either produced as transmembrane proteins or are secreted as soluble proteins. Depending on the N-terminus end, they are divided into type-I and type-II C-type lectins, where the type-II has its N-terminus pointed outside of the cell cytoplasm and the type-I has its N-terminus towards the cytoplasm (75). Varieties of C-type lectins exist, and they perform varieties of functions. Transmembrane lectins have 3 main categories namely selectins mostly important for cell-cell interaction (76), collectins that are involved in pathogen recognition and innate immunity, and the dendritic cell-specific ICAM-3 grabbing non-integrin (DC-SIGN), which can act both as cell adhesion receptor and pathogen recognition receptor (77). C-type lectins contribute to innate immunity by recognizing the pathogens and their killing by the macrophages. Also, the antigen processing and presentation to MHC molecules lead to the activation of the adaptive immune system. Evidence of crosstalk between TLRs and C-type lectins has been found and this crosstalk is believed to be important in antigen tolerance or immune response (78, 79).

1.2.3.2 DNA-binding PRRs

The recognition of CpG DNA by TLR-9 is well known PAMP-PRR interaction for the induction of immune response against pathogens. However, recent studies have found several other molecules that can bind DNA and induce the immune response. Absent in melanoma (AIM2) mediated induction of IL-1B and IL-18 production independent of the TLR signaling through caspase-1 activation by the assembly of inflammasomes is an example of such molecules (80). Similarly, RNA polymerase III and DEDX/H box helicases also activate the NF-kB pathway without relying on TLR signaling (81). DNA recognition becomes vital in the identification, pathogenesis, and in eliciting of the immune response against DNA viruses (82).

1.3 Cytokines and Chemokines

Cytokines are protein molecules synthesized by immune cells that are actively involved in case of an infection or invasion as part of host immune responses. To regulate the host cell function, cytokines are important molecules that act non enzymatically in nanomolar concentration. Alongside neurotransmitters and hormones, cytokines are one of the largest intracellular signaling molecules (83). There are several categories in which cytokines can be classified. Interleukins are a type of cytokine that is involved in the activation of T cells, B cells, mast cells, neutrophils, and many other immune cells. Not only activation, but cytokines also play important role in their growth, development, and differentiation. Interferons are another class of cytokines that are important in macrophage activation and antiviral immune responses. Cellular adhesion, cellular response to stimulation, and in some cases cellular translocations are also controlled by cytokines. Based on inflammatory properties, cytokines can be divided into two classes. Proinflammatory cytokines are those

that induce inflammatory responses. IL-1, TNF-α, INF-α, IL-12, and IL-18 are some examples of proinflammatory cytokines. Anti-inflammatory cytokines are those that suppress inflammatory responses. Cytokines like IL-4, IL-10, and IL-14 are a few examples of anti-inflammatory cytokines (84, 85). The target cell membranes have receptors specific for a cytokine that facilitates their binding, and this receptor binding activates signal transduction pathways leading to the regulation of gene expression (86).

Chemokines are one of the families of cytokines with a chemoattractant property. They are vital in cellular trafficking and inflammatory immune response. Chemokines and their receptors are expressed by a wide variety of immune cells. To date, there are 40 to 50 human chemokines identified. Chemokines are small proteins ranging from 8 to 12 KD in molecular weight. Chemokines have four major subfamilies mainly C, CXC, CC , and CX_3 C. The division into families is based on structural and genetic properties. Mostly all chemokines are similar in their structure and have at least three β-pleated sheets indicated as β1-3 and a C-terminal α-helix. Most chemokines possess at least four cysteines in conserved positions. In the CXC chemokine family, a single amino acid separates the two cysteines nearest the N-termini of family members. In the CC chemokine family, the two cysteines nearest the N-termini of these proteins are adjacent. Lymphotactin is a structurally related chemokine having only one cysteine near its N-terminus and is said to belong to the C chemokine family. The CX_3C chemokine has a typical chemokine-like structure at its N-terminus except for the placement of three amino acids between the first two cysteines. IL-8 and MCP-1 are two common examples of chemokines. Apart from being a chemoattractant, chemokines are actively involved in functions like monocytes and

neutrophil adhesion, antimicrobial responses, and inflammatory immune responses (87, 88).

1.4 Pig Primary cells for research, and their characteristics

A recent pig heart transplantation into a human in a hospital in Baltimore, Maryland tells us that pigs have a close resemblance to humans and are immensely important tools not only for organ transplantation but also for studying human diseases and disease pathogenesis as a biomedical model.

Compared to other animals, pigs share many physiological and anatomical characteristics like size, structure, immunology, and genome with humans. The respiratory, digestive, vascular, and urinary systems of humans and pigs are similar which provides us with the opportunity to study the immune system in pigs and its significance in humans (89, 90).

Primary cells maintain the genetic and phenotypic characteristics, and functional markers just like present in in-vivo but, cell lines sometimes lose these properties and could misrepresent the in-vivo environment. Several examples can be found where the loss of genetic or phenotypic character is seen on various cell lines, for example, the mass-spectrometry based comparative study of Hepa1-6 cell line with primary hepatocytes found that the cell line exhibited a re-arrangement of metabolic pathways with a deficiency in mitochondria (91, 92). At the same time, maintaining primary cells comes with a challenge as it is arduous and sensitive. Primary cells and their growth require more effort and care because primary cells are adapted to live in an in-vivo membrane-bound environment and their establishment in culture takes time and is extremely sensitive as they need better optimization of culture conditions and nutrient requirements (93).

1.4.1   Role of Porcine respiratory epithelium in innate immunity

The epithelial cells of the respiratory mucosal layers act as a physical and immunological barrier. Antigen-specific mucosal-induced secretory immunoglobin (S-IgA) and ciliary movement generated by cilia on epithelial cell surfaces for antigen removal are two major mechanisms for the neutralization of various respiratory infections. Inflammatory cytokines and Type I IFNs production is another non-specific immune response in respiratory mucosal surfaces mediated by respiratory epithelial cells (94, 95). Inflammatory cytokines like IL-1, TNF-α, IL-12 produced in respiratory mucosa are vital for inflammatory responses against pathogenic infections (84). PRRs and their expression are vital for not only pathogen recognition, but also subsequent intracellular signaling processes. The porcine respiratory epithelial cells express various PRRs like TLRs, RLRs, and NLRs, and help in pathogenic recognition and generation of innate immune responses through intracellular signaling pathways. Production of cytokines/chemokines by the epithelial cells in the respiratory mucosa is pivotal for the activation of T cells and B cells, their maturation, migration, and differentiation (83). Furthermore, the commensal microorganisms residing in the respiratory mucosa compete with the invading pathogenic microbes incoming through ingestion/inhalation, for food and shelter and this competition between the commensals and pathogens sometimes leads to the production of toxins or metabolic products by the commensals which in turn kill the pathogens benefiting the host by reducing the chances of new infections. For example, *S. salivarius,* a commensal microbe produces bacteriocins, which is antagonistic to *S. pneumoniae.* Along with bacteriocins, it is seen that *S. salivarius* reduces the *S. pneumoniae* colonization by blocking the adhesion sites of *S. pneumoniae* (96-98).

1.5   Immortalization of primary cells

The senescence of primary cells after a limited growth duration because of a gradual loss of telomeric DNA after each cell division is known as the Hayflick Limit (99). Primary cells have a finite life span and after reaching a certain point, they stop proliferating (100). A sudden pause in primary cell proliferation may cause an unwanted delay in achieving research goals. Thus, it becomes immensely important to immortalize the primary cells to overcome replicative senescence.

The shortening of telomeric DNA is a major cause of primary cell senescence. Immortalization of primary cells can be done through the introduction of the human telomerase reverse transcriptase gene (hTERT) or viral oncogenes like the SV40 large T-antigen gene (101). Previous studies have shown that cells can be successfully immortalized using hTERT or SV40 large T-antigen genes (102, 103). Primary cells transformed with SV40 large T-antigen genes continue to provide valuable insights of the cellular behavior with altered expression of oncogenes and inhibition of tumor suppressor genes. The use of human papillomavirus (HPV) E6 and E7 genes have been seen to achieve immortalization of primary cells. HPV E6 and E7 genes work in a similar manner to SV40 large T-antigen gene (104). hTERT immortalization introduces the reverse transcriptase activity that prevents the shortening of the chromosome by the addition of telomeric DNA at the end of the chromosomes thus, resulting in the continuous proliferating of cells without replicative senescence (102). One important aspect of immortalization is preserving the original morphological and phenotypical characteristics. Changes in phenotypic characteristics after immortalization might render the cells unusable as they

cannot be trusted to provide the replica of primary cells. It is thus important to characterize the cells after the immortalization and evaluate any noticeable phenotypic changes.

1.6 Objectives of this study

1. To characterize the established porcine primary and immortalized respiratory epithelial cells

2. To study the growth kinetics of porcine primary and immortalized respiratory epithelial cells

3. To study the innate immune responses of porcine primary respiratory epithelial cells upon stimulation with various bacterial and viral ligands

2   Characterization of pig primary and immortalized nasal turbinate and tracheal epithelial cells

2.1 Abstract

Pig primary epithelial cells act as a barrier against various respiratory and enteric pathogens. Respiratory epithelial cells are means of primary immune defense system against pathogens by regulating both the innate immune system and the adaptive immune system. The respiratory epithelial cells mediate inflammatory immune reactions against pathogens in the respiratory system by producing various inflammatory cytokines like IL-1, TNF-α, IL-25, and IL-33 when stimulated by the pathogen. Many airborne pathogens are inhaled through the respiratory tract. Respiratory epithelial cells provide a physical barrier and play role in producing cytokines, chemokines, and various other antimicrobial components to prevent the host from becoming infected. However, the availability of a limited number of respiratory cell lines has significantly hindered clarity in roles played by pig primary respiratory epithelial cells in immunity. In this study, we developed and characterized a primary epithelial cell culture systems originating from the nasal turbinate and trachea of a day-old gnotobiotic piglet. Growth kinetics and phenotypic properties of the cells were studied before and after immortalizing the cells using hTERT and/or SV40 large T-antigen-based immortalization method. Overall, we successfully established and characterized both the primary and immortalized pig nasal turbinate and tracheal epithelial cell cultures. Both primary and immortalized porcine nasal turbinate and tracheal cells expressed epithelial cell marker cytokeratin and immortalized porcine nasal turbinate and tracheal cells showed enhanced growth kinetics with a shorter doubling time compared to

primary epithelial cells. These cell cultures may serve as a good model for studying host-pathogen interactions and innate immune responses to respiratory pathogens.

2.2 Introduction

The establishment and use of cell lines in scientific research are not new and have been employed for several decades. The use of cell lines may be beneficial considering their easy growth and adaptation to the artificial culture milieu. However, cell lines derived from various tumors are often susceptible to genotypic and phenotypic drift, and thus, prone to behave differently in comparison to primary cells (105). Primary cells, on the other hand, maintain the in-vivo physiological properties and thus, are better suited to be employed in biological research. Even though primary cells have comparatively limited growth ability and high mitotic activity, their exact replication of the in-vivo environment is indispensable in scientific research. The use of primary cells to study the physiological, biological, and immunological properties of mammals can be found as early as the 1960s (106).

Understanding mucosal immunity in respiratory mucosal surfaces becomes pivotal in minimizing respiratory diseases and viral infections. Respiratory mucosal surfaces are the second-largest mucosal surfaces after the digestive tract and thus, respiratory immune responses and mucosal surfaces are indispensable when it comes to the immune system in the respiratory tract (107). The respiratory tract can be divided into the upper and lower parts. The upper respiratory tract consists of the nose, nasal cavities, and pharynx. This part of the respiratory tract is always in direct exposure to the exterior environment. The lower respiratory tract consists of mainly the trachea and lungs and is sterile in normal conditions. The diseased condition is declared when the microbes pass through the upper respiratory tract, colonize the lower respiratory tract and cause infections. The mucosal surfaces come into play in preventing or restricting respiratory diseases and viral infections (108).

There are hundreds of bacteria, viruses, and fungi that can cause respiratory infections. Viruses like the influenza virus, corona virus, respiratory syncytial virus, parainfluenza virus, rhinovirus, and adenovirus are some of the most common respiratory viruses and can cause viral pneumonia. Secondary bacterial infections of the respiratory tract following viral pneumonia are common and are mostly caused by *Streptococcus pneumoniae*, *Staphylococcus aureus*, *Streptococcus pyrogenes*, and *Haemophilus influenzae*. Apart from viruses and bacteria, respiratory fungal infections are a major clinical issue, especially in immunocompromised patients. Fungal pathogens like *Cryptococcus, Aspergillus,* and *Pneumocystis* are known to cause severe lung infections mostly in immunodeficient individuals such as HIV/AIDS patients, cancer chemotherapy receiving patients, and those undergoing immunosuppressive treatment (109, 110). Respiratory pathogens grow and replicate on respiratory epithelial cells and thus, it becomes immensely important to fully understand the immunology of respiratory mucosal epithelial surfaces and corresponding epithelial cells to better understand the respiratory disease progression and pathogenesis (111, 112).

The expression and distribution of PRRs and other important biomolecules are found to be similar between pigs and humans. The proximity between pigs and humans and similar size and anatomy of major organs are vital in using pigs as an animal model and pig respiratory cells in studying respiratory infections and immune responses in-vitro. The selection of animal models depends on various factors like cost, anatomy, proximity/similarity, feasibility, ethical reasons, and availability. Physiological and anatomical similarity, easy availability, and feasibility contribute to choosing pigs as an animal model. Using humans or human samples is an impractical and unethical way of

conducting research and thus, animal models fill that void and are more practical and ethical (89).

The use of pigs as an animal model for in-vitro immunological studies is not new and has been ongoing for decades. Historically, most of the studies are conducted in intestinal epithelial cells. Only a handful of studies have been carried out on respiratory cells to find out their role in innate immune responses. More specifically, hardly any studies can be found on the porcine respiratory epithelial cells and their contribution to the immune system. Therefore, we hypothesized that both the pig primary and immortalized nasal turbinate and tracheal epithelial cells established and characterized in this study express epithelial markers and may serve as a good in-vitro models for studying the innate immune responses to bacterial and viral ligands.

2.3 Materials and Methods

2.3.1 Culturing of established pig primary nasal turbinate and tracheal epithelial cells

Using tissues collected from a day-old gnotobiotic piglet, primary nasal turbinate and tracheal cell cultures were established in the previous study (113). Dulbecco's Modified Eagle Medium-F12 (DMEM/F-12) medium supplemented with 5 % fetal bovine serum (FBS), 1% insulin-transferrin-selenium (ITS) (Invitrogen, Grand Island, NY), 5ng/ml mouse epidermal growth factor (EGF) (Invitrogen, Grand Island, NY), and 1% antibiotics (Penicillin-streptomycin) was used for culturing cells at 37◦ C, and 5 % CO_2. Trypsin (0.125%) was used to remove any fibroblast contamination.

2.3.2 Immunocytochemistry

Immunocytochemistry-based characterization of both the pig primary nasal turbinate epithelial cells (PPNTECs) and pig primary tracheal epithelial cells (PPTECs) and respective immortalized cell lines was performed using monoclonal antibodies against cell markers such as cytokeratin, vimentin, alpha-smooth muscle actin (ASMA), and desmin. From 10^6 cells/ml cell suspension, 120ul of the cell suspension was used and cytospins were made. Cytospins were air-dried for 1-2 hours and fixed in acetone for 7 mins. To block endogenous peroxidase activity, slides were immersed in 1X PBS with 0.3% hydrogen peroxide and 0.1% sodium azide. Slides were incubated in 1% goat serum for about 20 mins to block the non-specific protein binding. The endogenous biotin activity was blocked by using the avidin/biotin kit (Vector Laboratories). Cells were treated with either the primary antibody or the isotype control antibody. Primary mouse monoclonal antibodies at a concentration of 1µg/ml were made and cells were treated for 1 hour with 100µl of 1µg/ml antibody solutions specific against cytokeratin (mAb C6909; IgG2a isotype), vimentin (mAb V5255; IgM isotype), alpha-smooth muscle actin (mAb A2457; IgG2a isotype), or desmin (mAb D1033; IgG1 isotype) at room temperature. For isotype control, M9144 (IgG2a isotype), M5170 (IgM isotype), and M9269 (IgG1 isotype) antibodies were used. All these antibodies were obtained from Sigma-Aldrich. After an hour, cells were washed with 1X PBS and incubated for 30 mins with isotype-specific biotinylated goat-anti mouse IgG2a, IgM, or IgG1 antibodies (Caltag Laboratories) at 1:2000 dilutions. Cells were further incubated for 30 mins with streptavidin-horseradish peroxidase (Vector Laboratories). Ready-to-use (RTU) DAB (Diaminobenzidine) substrate was added to the cells. Horseradish peroxidase cleaves this substrate and produces

brown color indicating a positive reaction. Using hematoxylin, nuclear counterstaining was done. Slides were dried overnight and mounted in mounting media, and images were taken using a BX53 upright microscope.

2.3.3   SV40 immortalization of PPNTECs and PPTECs

To start with, half a million PPNTECs and PPTECs were separately cultured in four wells of a 6-well plate using DMEM/F-12 culture media. After 18 hours of incubation, all four wells were washed twice with sterile 1X PBS. To all four wells, 2 ml of serum-free OPTI-MEM media (Gibco) was added. A microcentrifuge tube was labeled as tube 1 and 485ul of OPTI-MEM along with 15ul of Lipofectamine (Invitrogen) was added and the tube was incubated at room temperature for 10 minutes. To a second microcentrifuge tube labeled as tube 2, 205 µl of Lipofectamine-OPTI-MEM mixture was transferred and 45 µl of pSV3-neo (ATCC) plasmid vector with SV40 gene was added. After gently mixing the contents in tube 2, it was incubated for 30 minutes at room temperature. To the first two wells labeled as well 1 and well 2, 125ul of tube 1 contents without plasmid was added. To wells 3 and 4, 125 µl of the plasmid-lipofectamine mixture was added from tube 2. The 6 well plates were then incubated at 37° C for 6 hours. After incubation, cells were washed with 1X PBS, and OPTI-MEM media was replaced by DMEM/F-12 media. Except for the first well which is a positive control for normal cell growth, 40 µl of G418 antibiotic (Thermo Fischer, Cat. no. 10131-035) was added to all labeled wells at a concentration of 1000ug/ml. After the antibiotic addition, the plate was incubated at 37° C for 24 hours and colonies resistant to the antibiotic were observed under the microscope. Antibiotic-resistant colonies from well 3 and 4 were trypsinized and transferred to a T-25 flask and cultured and maintained in DMEM/F-12 media in presence of the selection antibiotic G418.

2.3.4   hTERT immortalization of PPTECs

Half-million PPTECs were cultured in the 3 wells of a 6-well plate and incubated for 18 hours at 37° C. After incubation, cells were washed with 1X PBS. Two Eppendorf tubes were taken and labeled as tube 1 and tube 2. In tube 1, 15 µl of Lipofectamine reagent was mixed with 485 µl of OPTI-MEM media. This mixture was then incubated for 15 minutes at room temperature. In tube 2, 205 µl of the mixture from tube 1 was mixed with 45 µl of 100ng/µl pGRN-145 plasmid (ATCC) containing the hTERT gene. In the first and second well, 125 µl of the non-plasmid mixture from tube 1 was added. In the third well, 125 µl of the plasmid containing mixture from tube 2 was added. Cells were incubated for 6 hours at 37° C and washed with 1x PBS. Cells in the second and third wells were again incubated with 2 ml of DMEM/F12 medium containing Hygromycin B at a concentration of 100 µl/ml. Cells in the first well were used as a positive control for normal cell growth and only DMEM/F12 medium was added without any selection antibiotics. After 14 days of observation, antibiotic-resistant colonies were transferred to a T-25 flask and continued to grow in DMEM/F12 medium as hTERT immortalized PPTECs.

2.3.5 Confirmation of immortalization

2.3.5.1   Polymerase chain reaction (PCR)

For SV40 immortalization, DNA was extracted from SV40 immortalized pig nasal turbinate epithelial cells (PNTECs) and pig tracheal epithelial cells (PTECs) using DNeasy Blood and Tissue Kit (Qiagen, cat. no.69504). A Nanodrop ND-1000 spectrophotometer was used to measure the DNA concentration. Using specific primers for the SV40 gene and Taq PCR Kit (New England Biolabs, cat. no. E5000S), PCR was performed (table 1). The PCR cycle consisted of initial denaturation at 95° C for 5 minutes, followed by 30

cycles of denaturation at 95° C for 30 seconds, annealing at 55° C for 1 minute, and extension at 72° C for 1 minute. The final extension was done at 72° C for 10 minutes. PCR products were resolved on 1.5 % agarose gel. Gel images were taken to further verify the successful transfection.

For hTERT immortalization of PPTECs, using DNeasy Blood and Tissue Kit (Qiagen, cat. no. 69504), DNA was isolated. Using specific primers for the hTERT gene (Table 1), PCR was done. The following PCR conditions were used; initial denaturation at 95° C for 10 min, followed by 40 cycles of denaturation, annealing, and extension at 95° C for 30 sec, 60° C for 30 sec, 72° C for 60 sec, and final extension at 72° C for 60 sec. The products obtained were resolved in an agarose gel and visualized using the ODYSSEY-FC gel imaging system.

2.3.5.2 Immunocytochemistry for confirmation of hTERT protein expression

Cytospins were prepared using $1x10^5$ cells. Using the earlier described IHC protocol (28), immunocytochemical staining was conducted to confirm of expression of hTERT proteins. Rabbit anti-TERT polyclonal IgG at a concentration of 1.25 µg/ml (Santa Cruz Biotechnology Inc; SC 7212) was used for hTERT protein detection. Normal Rabbit IgG (SC3888) was used for isotype-matched control. Slides were incubated with 100 µl of either rabbit anti-TERT or normal rabbit IgG overnight at 4°C. After incubation, slides were washed three times with 1X PBS. After washing, 100 µl of biotinylated goat-anti-rabbit IgG (1:1000 diluted) was added and incubated for 30 minutes followed by washing with 1X PBS three times. Slides were again incubated with the streptavidin-HRP solution for 30 minutes followed by the addition of DAB substrate for colorimetric detection of hTERT

protein. Hematoxylin was used for nuclear counterstaining, and images were taken using Olympus BX53 upright microscope.

Table 1: Primers used in the amplification of SV40 large T-antigen or hTERT gene

Primers	Product size
For SV40: Forward: 5'- AGCAGACACTCTATGCCTGTGTGGAGTAAG- 3' Reverse: 5'- GACTTTGGAGGCTTCTGGATGCAACTGAG- 3'	706 BP
For hTERT: Forward: 5'-CGGAAGAGTGTCTGGAGCAA-3' Reverse: 5'-GGATGAAGCGGAGTCTGGA-3'	125 BP

2.3.5.3 Indirect Immunofluorescence assay for confirmation of SV40 immortalization

A 12 well-plate was used for the assay. In the first two wells labeled as well 1 and well 2, 50 thousand PPNTECs were added and in the next two wells labeled as well 3 and well 4, 50 thousand SV40 immortalized PNTECs were added. The 12 well-plate was incubated at 37° C for 24 hours. After 24 hours of incubation, cells were fixed with 1:1 acetone: methanol (250ul/chamber) at -20° C for 10-15 minutes, washed three times with 1X PBS and blocked with 1% goat serum for 20 minutes. 250µl (4µg/ml) of either mouse IgG2a isotype control (M9144) or mouse anti-SV40 monoclonal IgG2a antibody was added to respective wells and incubated at 37° C for 1 hour. All wells were treated with Alexa Fluor 488 conjugated goat anti-mouse IgG secondary antibody (Invitrogen, a11011) at 1:200 dilution and incubated for 1 hour in dark. Cells were washed with 1X PBS and nuclear staining was performed using 250 µl of propidium iodide (1:1000 dilution) per well. After 5 minutes, cells were washed again and mounted in permafluor mounting medium, and images were taken using Olympus BX53 upright microscope at 20X magnification. The same procedure was repeated for indirect immunofluorescence assay of primary and SV40 immortalized tracheal epithelial cells.

2.3.6 Growth Kinetics study

Two 6-well plates were taken, one for culturing PPNTECs and another for culturing SV40-immortalized PNTECs. To the 5 wells in each of the two 6-well plates, 20 thousand PPNTECs and SV40 PNTECs were added respectively. The plates were incubated at 37° C for 48 hours. Beginning on day 2, the number of cells on each well of both 6-well plates was counted until day 6. The same procedure was repeated two more times with both cell

types. Population doubling time (DT) was calculated using the formula: DT=T ln2/ln(X2/X1), where T is the incubation time in hours, X1 is the cell number at the beginning of the incubation time and X2 is the cell number at the end of the incubation time. The same procedure was repeated for the growth kinetics study of pig primary and SV40 immortalized tracheal cells.

2.4 Results

2.4.1 Phenotypic characterization of primary and SV40 immortalized pig primary nasal turbinate and tracheal epithelial cells revealed typical epithelial morphology/phenotype

Pig primary nasal turbinate and tracheal cells obtained from a day-old piglet (113) were cultured in DMEM/F12 media. The initial cells used in this study were fibroblast contaminated and thus, treated with 0.125% trypsin for 3 minutes to remove fibroblast contamination, and obtain a homogenous population of cells. Cells showed typical cobblestone morphology indicative of epithelial phenotype (Figure 5). Primary cells were immortalized using the SV40 large T-antigen gene and hTERT gene. After a successful transfection, cells were grown using similar culture conditions and they showed primary cells like typical cobblestone morphology indicative of being epithelial (Figure 5-6). However, cells did look more granulated after immortalization and started growing in multiple small clusters.

Immunocytochemistry was performed to further verify the epithelial nature using cytokeratin as universal epithelial cells marker. Primary and SV40 immortalized nasal turbinate and tracheal epithelial cells strongly stained positive (>90%) for cytokeratin (Figure 7-10). Less than 10% of the cells stained positive for vimentin which had been seen across different epithelial cell lines in-vitro. Staining specificity was verified by negative staining of isotype controls. Expression of desmin and alpha-smooth muscle actin were virtually none on both primary and SV40 immortalized cells in both cell types.

2.4.2 SV40 immortalization of PPNTECs and PPTECs was confirmed by conventional PCR and indirect immunofluorescence

DNA was extracted from both primary and SV40 immortalized cells. Using SV40 large T-antigen gene-specific primers, conventional PCR was performed, and the PCR products were tested on an agarose gel to confirm the presence of SV40 large T-antigen gene on SV40 immortalized cells. Gel image revealed the presence of SV40 large T-antigen gene (Figure 11) with the product size around 706 bp.

An indirect Immunofluorescence assay (IFA) was done to further verify the SV40 immortalization based on SV40 protein expression. The assay used SV40 specific primary antibody and Alexa fluor488 conjugated secondary antibody. SV40 immortalized cells were strongly positive for SV40 protein expression. Primary cells along with isotype controls were negative for SV40 protein expression (Figures 13 and 14). We were able to successfully culture primary PPNTECs and PPTECs up to 16 passages. Immortalized PPNTECs and PPTECs were grown up to 50 passages.

2.4.3 hTERT immortalization of PPTECs confirmed by conventional PCR and immunocytochemistry

DNA was extracted from both primary and hTERT immortalized tracheal cells. Using hTERT gene-specific primers, conventional PCR was performed, and the PCR products were resolved on an agarose gel to confirm the presence of the hTERT gene on hTERT immortalized cells. The gel image revealed the presence of the hTERT gene (Figure 11).

Immunocytochemistry (ICC) was done to further verify the hTERT immortalization based on hTERT protein expression. hTERT immortalized cells were strongly positive for hTERT protein expression. Primary cells stained slightly positive for hTERT protein.

Isotype controls were negative for hTERT protein expression (Figure 12). hTERT immortalized PPTECs were cultured up to passage number 16 successfully in DMEM/F-12 culture media.

2.4.4 Growth kinetics showed a shorter mean doubling time for immortalized cells

Using the protocol described earlier, a growth kinetics study was conducted on both primary and SV40 immortalized nasal turbinate epithelial cells and tracheal epithelial cells. The mean doubling time was 27.47 ± 0.26 hours for SV40 immortalized PPNTECs and 32.65 ± 9.16 hours for primary PPNTECs. For primary tracheal epithelial cells, the mean doubling time was 35.57 ± 5.935 hours and for SV40 immortalized PPTECs, it was 28.99 ± 3.575 hours. After immortalization, cells started to grow faster as shown by the mean doubling time for the immortalized PPNTECs and PPTECs. Graphs were made using GraphPad Prism software version 8.4.2 (Figure 15).
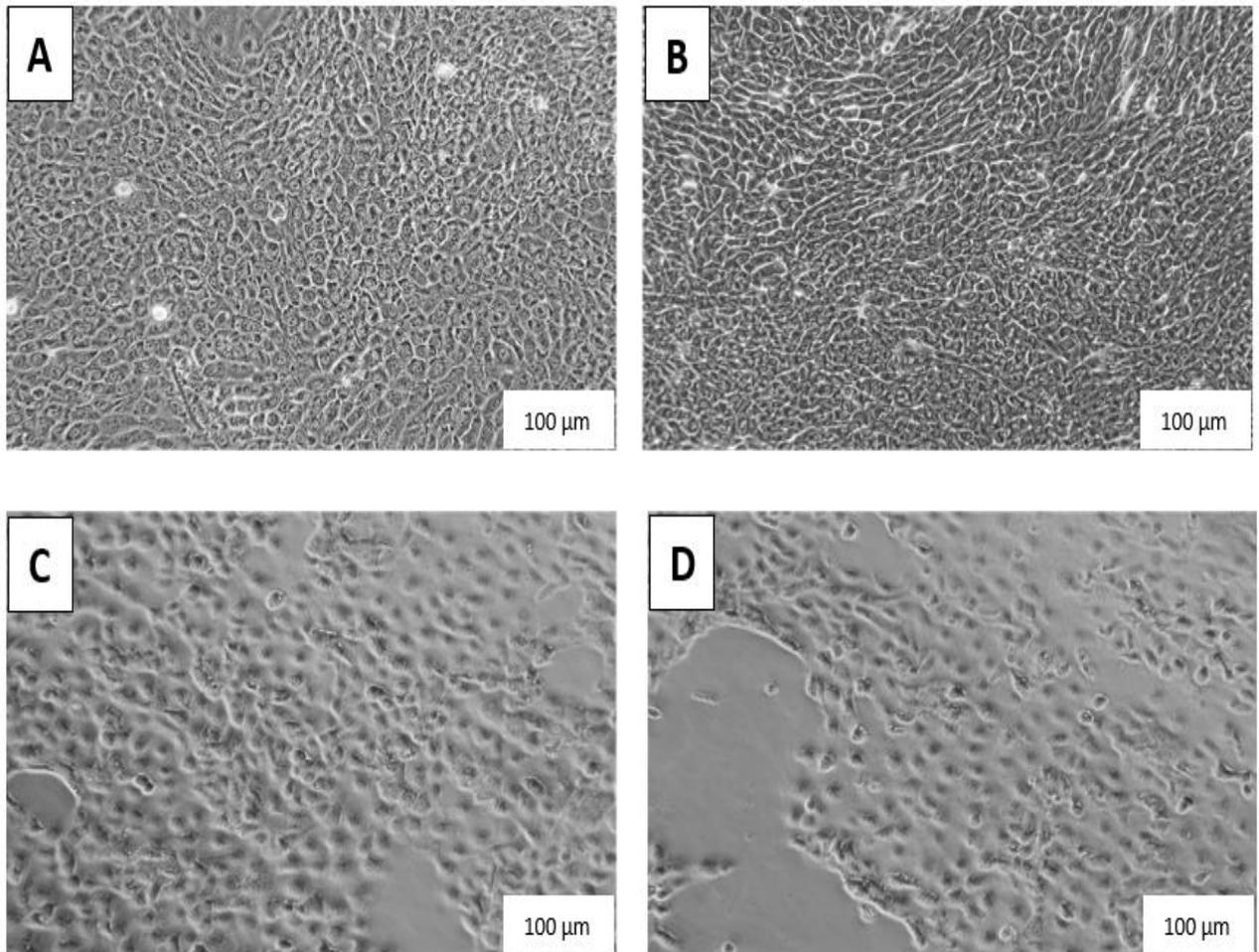
Figure 5: Porcine primary and immortalized epithelial cells. A. Pig primary nasal turbinate epithelial cells (PPNTECs). B. Pig primary tracheal epithelial cells (PPTECs). C. SV40 immortalized PPNTECs. D. SV40 immortalized PPTECs. Magnification 10x. Scale bars represent 100 µM.
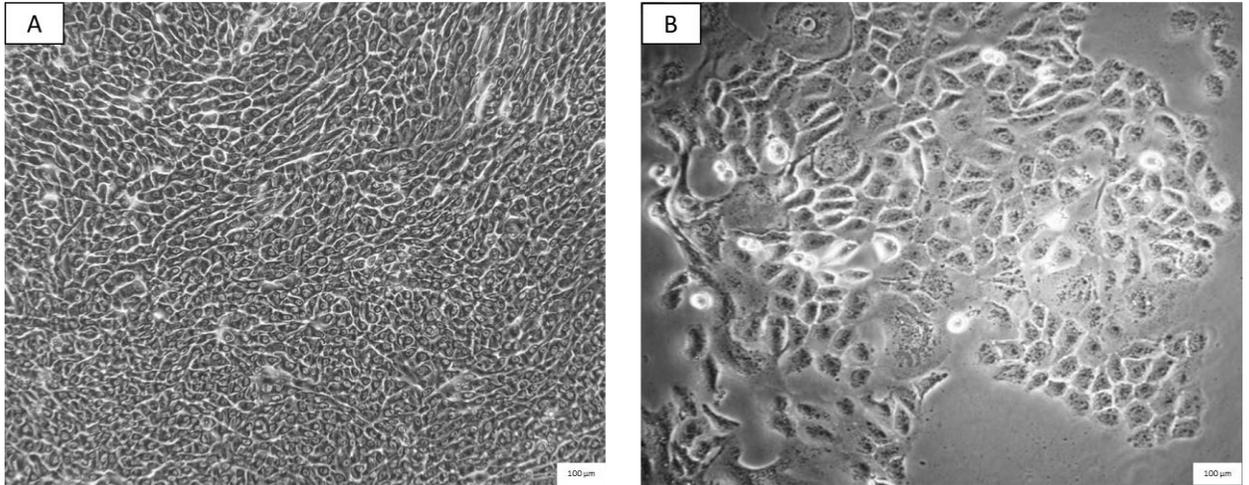
Figure 6: Porcine primary and hTERT immortalized respiratory epithelial cells. A. Pig primary tracheal epithelial cells (PPTECs). B. hTERT immortalized PPTECs.
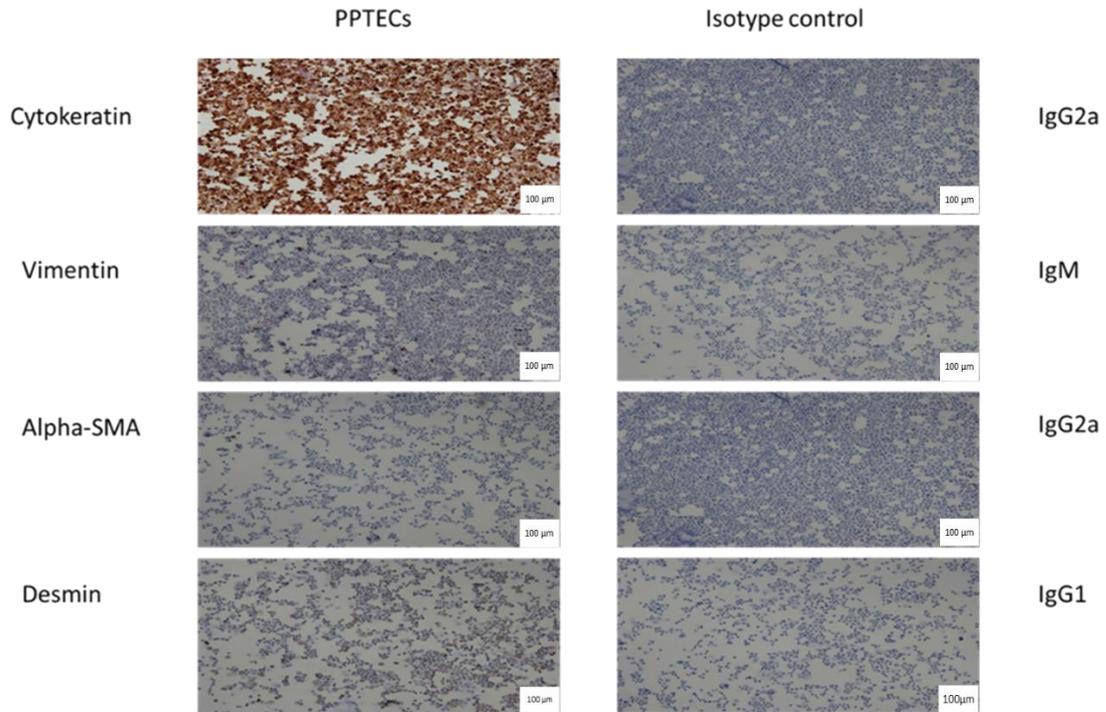
Figure 7: Immunocytochemistry-based characterization of porcine primary tracheal epithelial cells. Cytokeratin staining produced strong brown color indicating DAB substrate breakdown and positive staining (top left). Staining against vimentin, alpha-SMA, desmin, and isotype controls produced negative results (staining did not produce brown color) validating the epithelial nature of the cells. Magnification 10x, Scale bars represent 100 µM.
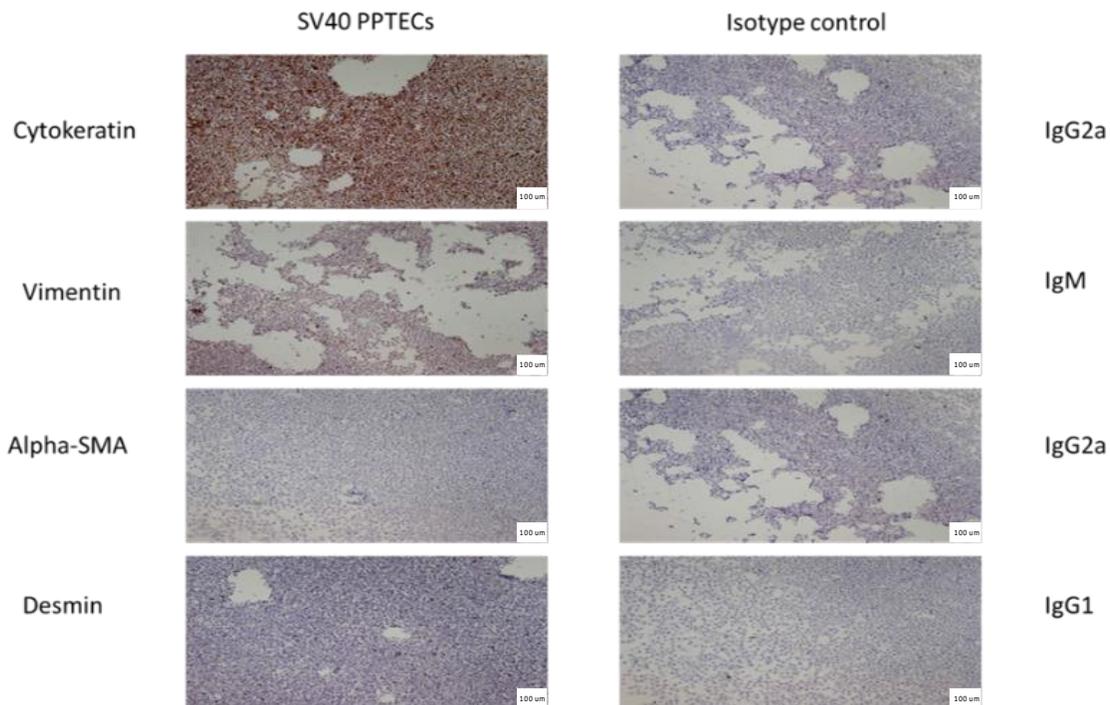
Figure 8: Immunocytochemistry-based characterization of porcine SV40 immortalized tracheal epithelial cells. Cytokeratin staining produced strong brown color indicating DAB substrate breakdown and positive staining (top left). Staining against vimentin, alpha-SMA, desmin, and isotype controls produced negative results (staining did not produce brown color) validating the epithelial nature of the cells. Magnification 10x, Scale bars represent 100 µM.
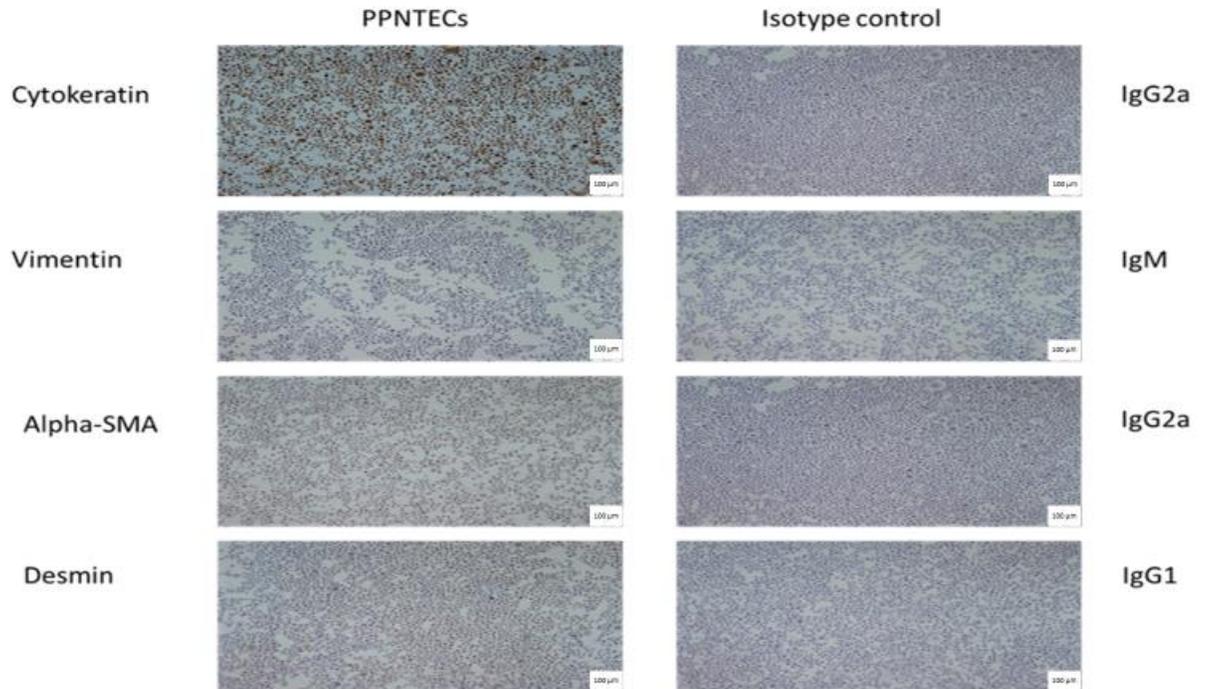
Figure 9: Immunocytochemistry-based characterization of porcine primary nasal turbinate epithelial cells. Cytokeratin staining produced strong brown color indicating DAB substrate breakdown and positive staining (top left). Staining against vimentin, alpha-SMA, desmin, and isotype controls produced negative results (staining did not produce brown color) validating the epithelial nature of the cells. Magnification 10x, Scale bars represent 100 µM.
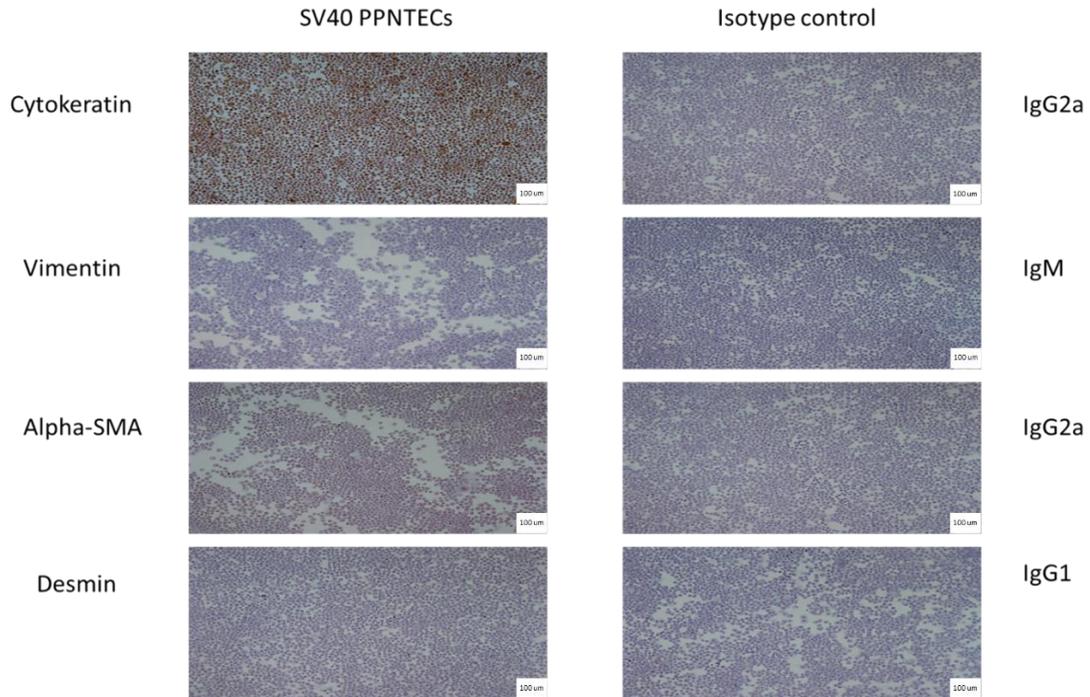
Figure 10: Immunocytochemistry-based characterization of porcine SV40 immortalized nasal turbinate epithelial cells. Cytokeratin staining produced strong brown color indicating DAB substrate breakdown and positive staining (top left). Staining against vimentin, alpha-SMA, desmin, and isotype controls produced negative results (staining did not produce brown color) validating the epithelial nature of the cells. Magnification 10x, Scale bars represent 100 µM.
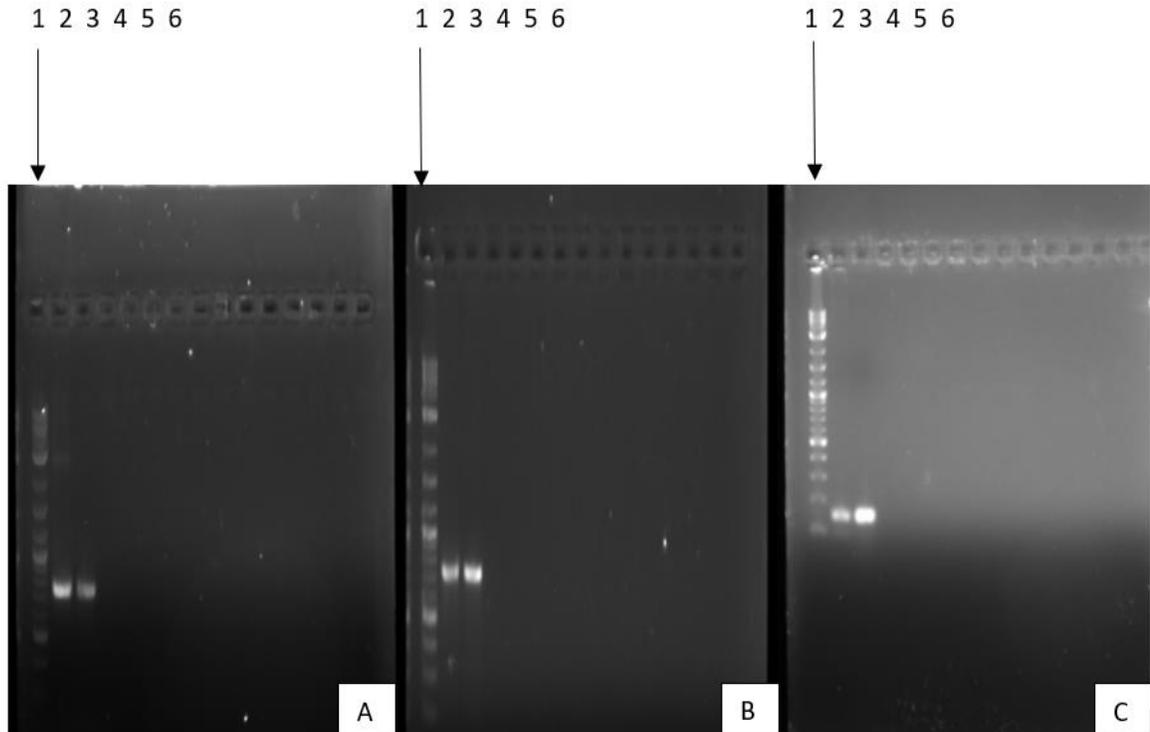
A. SV40 PPNTECs.	B. SV40 PPTECs	C. hTERT PPTECs
Lane 1: DNA ladder	Lane 1: DNA ladder	Lane 1: DNA ladder
Lane 2: SV40 plasmid	Lane 2: SV40 plasmid	Lane 2: pGRN145
Lane 3: SV40	Lane 3: SV40	plasmid
immortalized	immortalized PPTECs	Lane 3: hTERT
PPNTECs	Lane 4: PPTECs	immortalized PPTECs
Lane 4: PPNTECs	Lane 5: No template	Lane 4: PPTECs
Lane 5: No template	control	Lane 5: No template
control		control

Figure 11: Polymerase Chain Reaction (PCR) and agarose gel electrophoresis. A. Pig primary and SV40 immortalized nasal turbinate epithelial cells. B. Pig primary and SV40 immortalized tracheal epithelial cells. C. Pig primary and hTERT immortalized tracheal epithelial cells.
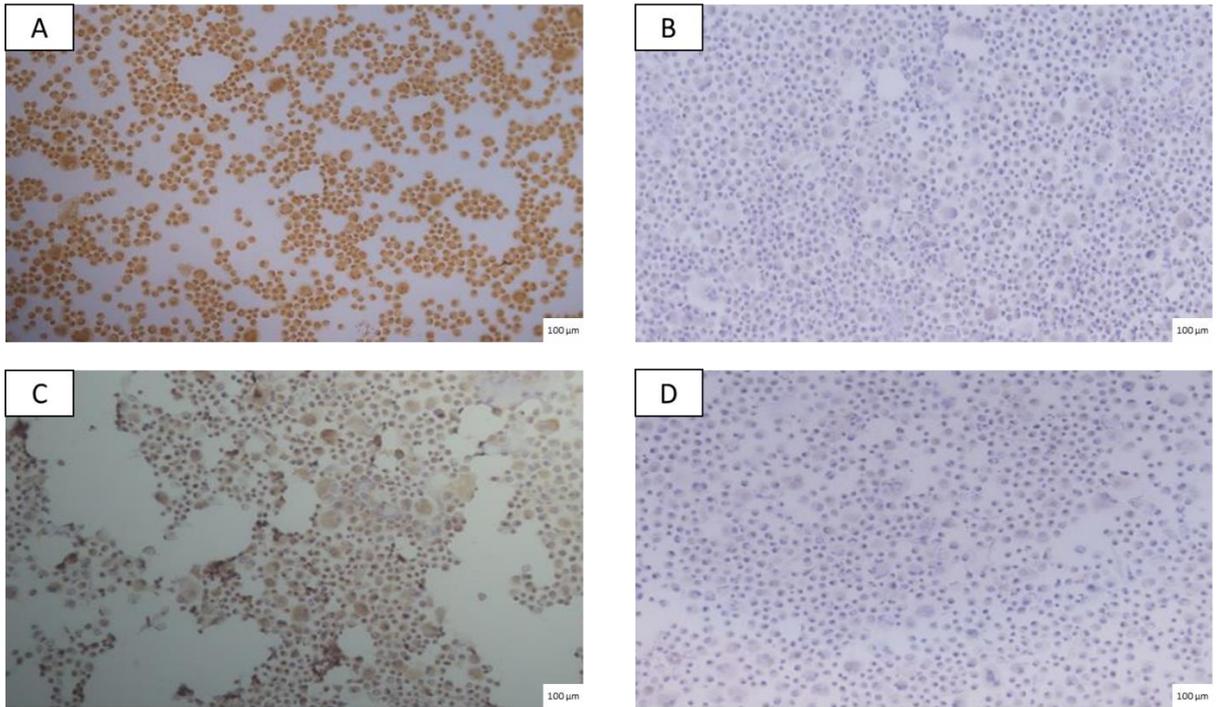
Figure 12: Immunocytochemistry for confirmation of hTERT protein expression. A and B, hTERT-PPTECs staining against hTERT specific antibody and isotype-matched control respectively. C and D, Primary tracheal cells staining against hTERT specific antibody and isotype-matched control respectively. Scale bar represents 100 µM, magnification 10X.
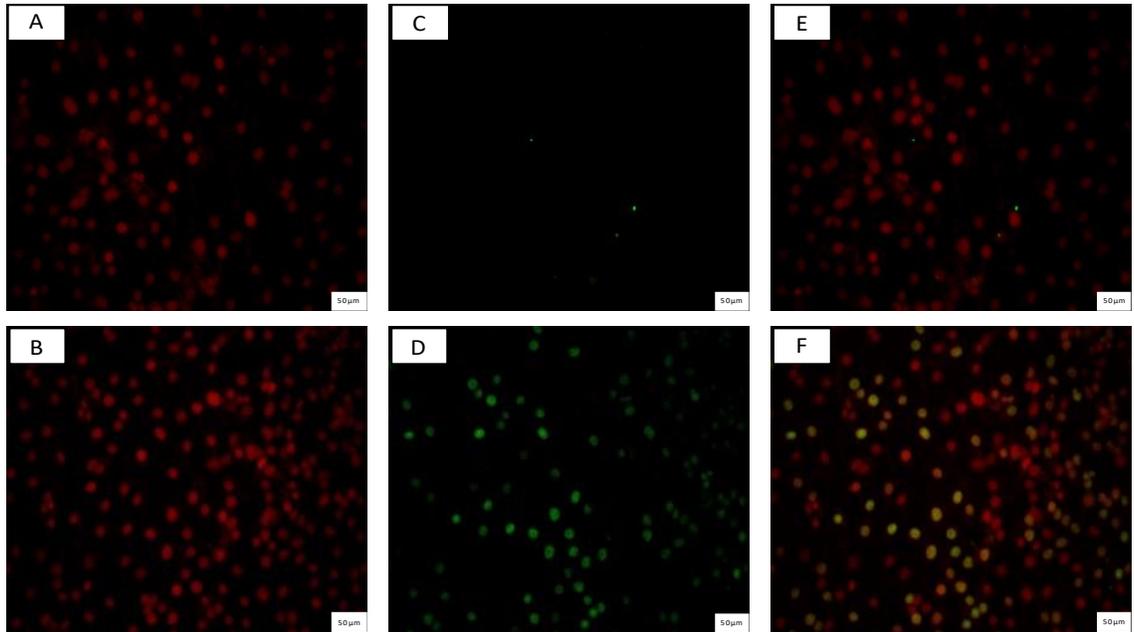
Figure 13: IFA revealed expression of SV40 protein by SV40 immortalized nasal turbinate epithelial cells. A & B: Pig primary and SV40 immortalized nasal turbinate epithelial cells nuclear staining respectively. C & D: Pig primary and SV40 immortalized nasal turbinate epithelial cells stained with SV40 specific primary Ab and Alexa 488 conjugated secondary Ab. E & F: Merged pictures. Scale bar 50 µM.
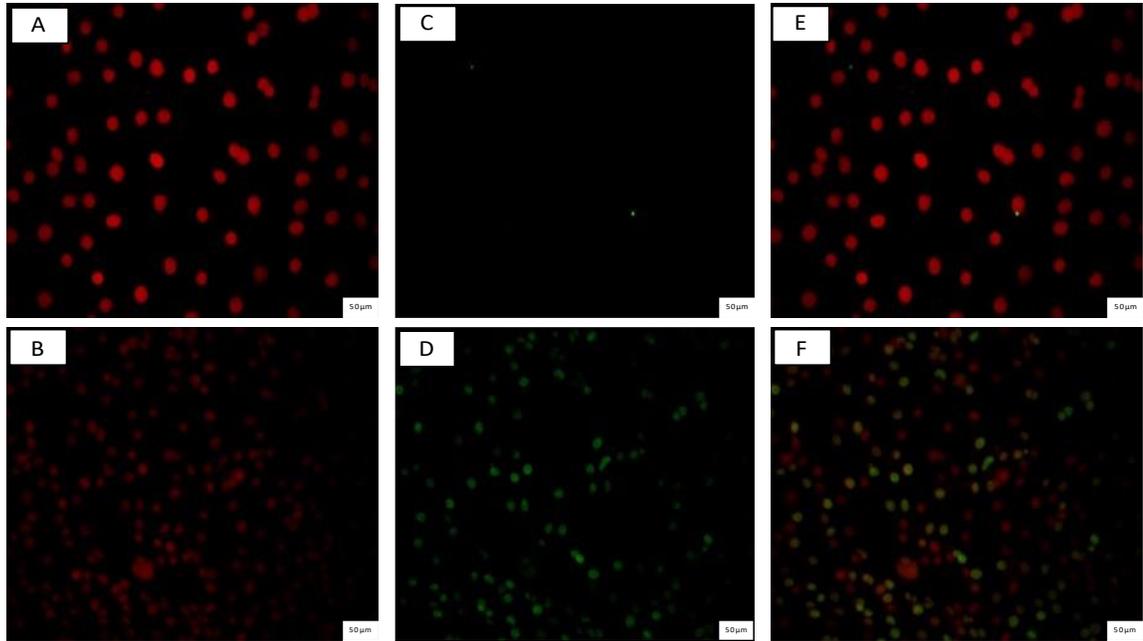
Figure 14: IFA revealed expression of SV40 protein by SV40 immortalized tracheal epithelial cells. A & B: Pig primary and SV40 immortalized tracheal epithelial cells nuclear staining respectively. C & D: Pig primary and SV40 immortalized tracheal epithelial cells stained with SV40 specific primary Ab and Alexa 488 conjugated secondary Ab. E & F: Merged pictures. Scale bar 50 µM.

.
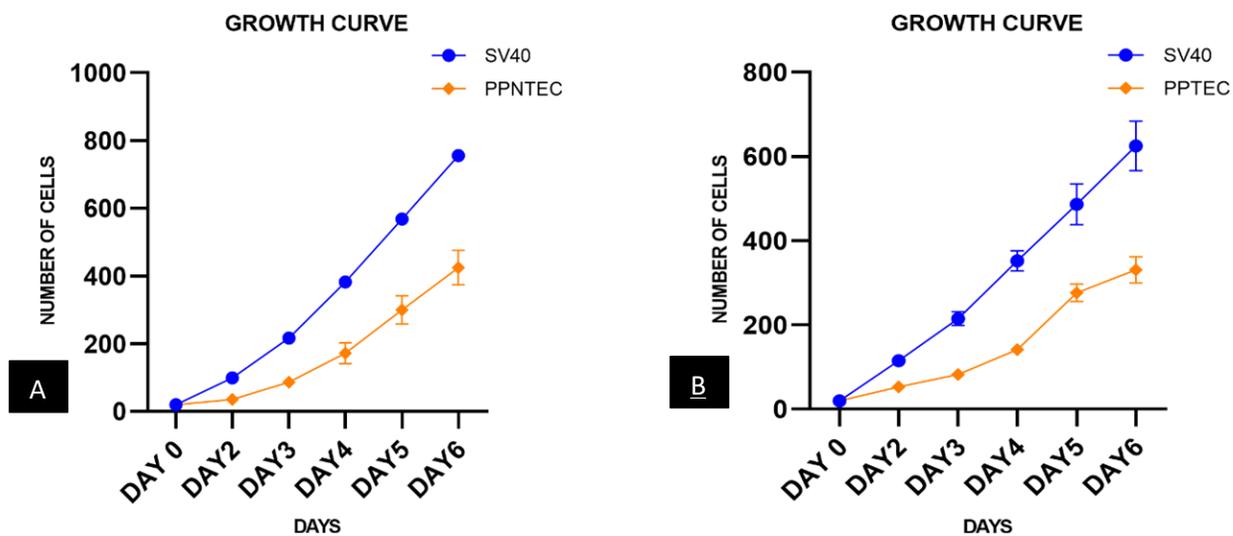
Figure 11: A. Growth kinetics study of PPNTECs and SV40 immortalized PPNTECs. The orange line represents the primary cells, and the blue line represents the SV40 immortalized cells. 20,000 cells were cultured on day 0 and beginning on day 2, until day 6, cells were counted using a hemocytometer. B. Growth kinetics study of PPTECs and SV40 Immortalized PPTECs. The orange line represents the primary cells, and the blue line represents the SV40 immortalized cells. 20,000 cells were cultured on day 0 and beginning on day 2, until day 6, cells were counted using a hemocytometer. The number of cells is in thousands.

2.5 Discussion

In this study, we have characterized pig primary respiratory epithelial cells from the trachea and nasal turbinate and established SV40 and hTERT immortalized pig respiratory epithelial cell lines. Primary cells have limited growth ability, and they tend to undergo cell senescence after a certain age. Discovered by Hayflick almost 40 years ago, the phenomenon where primary cells become senescent after a limited growth duration because of a gradual loss of telomeric DNA after each cell division is known as Hayflick Limit (99). Even though primary cells are indispensable tools in the immune system, an in-vitro study of the immune system might be jeopardized by primary cell senescence. Thus, the establishment of immortalized cell lines becomes immensely important (114). In this study, immortalized cell lines were generated using the SV40 and hTERT immortalization methods. SV40 immortalization is based on the transfection of primary cells with the SV40 large T-antigen whereas the hTERT method uses pGRN145 plasmid for hTERT gene transfection. Successful SV40 transfection leads to the expression of an oncoprotein and thus, allows the cells to bypass replicative senescence (115). Both primary and immortalized cells exhibited cobblestone morphology, a typical epithelial phenotypic characteristic but, immortalized cells appeared more granulated and started growing in multiple small clusters, unlike primary cells. It has been seen that the transfected cells can display different structural and functional morphologies upon SV40 T-antigen transfection (116). In a study conducted on human mammary epithelial cells, SV40 immortalization resulted in frequent aneuploidy and chromosomal abnormalities (117). Even though we did not study the changes at genomic levels, the granulated appearance of the immortalized cells might be a result of genomic changes and subsequent expression of proteins

responsible for the morphological appearance of the cells. Apart from that, both the primary and immortalized cell lines expressed heavy cytokeratin, a universal epithelial cell marker thus, confirming the epithelial nature of both cell types. After immortalization, cells were able to grow faster possibly because primary cells require a close to the in-vivo environment with complex culture conditions and different growth factors for their sustained growth (118). However, immortalized cells require comparatively less monitoring, and they tend to divide faster than primary cells in the same culture conditions. Fibroblast contamination of the epithelial cell culture was a common problem in this study. Pig respiratory cells from trachea and nasal turbinate isolated in a previous study (113) were fibroblast contaminated (<10%). By exploiting the differences in adherence pattern of the fibroblast cells and epithelial cells, fibroblast cells were removed from the epithelial cell culture. Fibroblast cells are more sensitive to trypsin treatment because they loosely adhere to the surface. Thus, cell culture flasks were treated with trypsin for 3 to 5 minutes and all the detached cells were removed. This method seemed to be effective and has been employed previously (113, 118, 119) but, needed to be repeated multiple times to get rid of most of the fibroblast contamination.

3 Chapter 3. Innate immune responses of porcine primary nasal turbinate and tracheal epithelial cells upon stimulation with bacterial and viral ligands

3.1 Abstract

Respiratory epithelial cells express various pathogen recognition receptors (PRRs), cytokines and chemokines, and play an important role in the innate immune responses against respiratory pathogens. The primary objective of this study was to evaluate the expression of various PRRs, cytokines and chemokines using RT-qPCR method in pig primary nasal turbinate epithelial cells (PPNTECs) and pig primary tracheal epithelial cells (PPTECs) in response to bacterial and viral ligands. The findings of this study indicated that the porcine respiratory epithelial cells from both the nasal turbinate and trachea constitutively expressed PRRs and various cytokines and chemokines, and expression of specific PRRs, cytokine and chemokine genes were modulated upon stimulation with bacterial and viral ligands. Therefore, the porcine respiratory epithelial cells from nasal turbinate (PPNTECs) and trachea (PPTECs) may serve as a good model for studies involving innate immune responses to pathogens and their mechanism for respiratory disease pathogenesis. However, as we did not study the mechanistic details of our observations at gene level, further studies are recommended to fully validate our findings.

3.2 Introduction

The discovery of PRRs was a breakthrough for the field of immunology especially in studying their role in the innate immune system. TLRs, RLRs, and NLRs are some of the most studied PRRs and among them, TLRs were the first identified PRRs. TLRs initiate host defense through their signaling pathways against foreign microbial particles (26). As of now, mammals are known to express 13 different TLRs with different functions and localization. Mostly, TLRs are expressed either on epithelial membranes or expressed intracellularly. The expression of TLRs on mucosal epithelial surfaces is finely regulated and this regulation is important for the controlled elicitation of innate immune responses by antigen presenting cells (APCs) (29). NLRS and RLRs are involved in the activation of NF-kB and MAPK signaling pathways followed by IFN-B production, a major cytokine of the innate immune system. Additionally, IFN-B helps in the activation of B cells for antibody production and thus, activation of adaptive immune response (66, 67). PRRs, cytokines and chemokines genes and their expression are vital for generation of the innate immune responses. Through various signaling pathways, PRRs, cytokines and chemokines modulate the innate immune system and its response to pathogenic infections/invasions (95).

Even though, respiratory epithelium is indispensable when it comes to innate immune responses in porcine respiratory mucosa, very few studies have been conducted in porcine respiratory epithelial cells. More importantly, there's a lack of sufficient information on porcine respiratory epithelial cells and their roles in respiratory immune responses and respiratory diseases. To shed more light on roles of porcine respiratory cells on porcine respiratory immune system and various porcine bacterial and viral respiratory diseases, in

this study, we established and characterized primary and immortalized cultures of porcine respiratory epithelial cells obtained from nasal turbinate and trachea of a day old gnotobiotic piglet using various immunological and biochemical techniques and stimulated them with bacterial and viral ligands to study their response towards the pathogenic ligand stimulation. The primary and immortalized porcine respiratory cell cultures characterized and stimulated with various bacterial and viral ligands may serve as a good model for understanding the innate immune responses against respiratory pathogens and respiratory diseases caused by them.

3.3 Materials and methods

For the ligand stimulation assay, various bacterial and viral ligands were used to stimulate the PRRs, cytokines and chemokine genes in PPNTECs and PPTECs (Table 2). The bacterial ligands included Lipopolysaccharide (LPS catalog: LG529) from *Escherichia coli O55: B55* at 5µg/ml concentration, peptidoglycan (PGN, catalog: tlrl-pgn) from *Staphylococcus aureus* at 10µg/ml concentration, Flagellin (FLA, catalog: tlrl-stfla) from *Salmonella typhimurium* at 100µg/ml concentration, Muramyl dipeptide (MDP, catalog: tlrl-mdp) at 10µg/ml concentration and γ-D-glutamyl-meso-diaminopimelic acid (iE-DAP, catalog: tlrl-dap). A TLR-4 agonist inulin acetate nanoparticle (InAc) synthesized from plant polysaccharide inulin was also used in the ligand stimulation assay (120). For the viral ligand study, viral nucleoside analogs; imiquimod (catalog: tlrl-imqs) at 5µg/ml concentration, polyinosonic: polycytidylic acid (Poly I:C, catalog: tlrl-pic) at 5µg/ml, and poly I:C with lyovec (Poly I:C/lyovec, catalog: tlrl-piclv) at 1µg/ml concentration were used to stimulate various PRRs. These ligands were obtained from InvivoGen (San Diego, USA).

Table 2: Ligands used in the stimulation of PPNTECs and PPTECs.

Ligands	name of receptors	Source	Concentration
Lipopolysaccharide	Surface; TLR4	*Escherichia coli O55: B55*	5 µg/ml
Peptidoglycan	Surface; TLR2	*Staphylococcus aureus*	10 µg/ml
Flagellin	Surface; TLR5	*Salmonella typhimurium*	100 µg/ml
Muramyl dipeptide	Cytoplasm; NOD2	Mycobacteria	10 µg/ml
γ-D-glutamyl-meso-diaminopimelic acid	Cytoplasm; NOD1	Gram-positive and gram-negative bacteria	10 µg/ml
Inulin acetate	Surface; TLR4	A plant product inulin	250 µg/ml
Poly I:C	Endosomes; TLR3	Synthetic analogue of double stranded RNA	5 µg/ml

| Poly I:C with lyovec | Cytoplasm; RIG-I | Poly I:C with transfecting reagent lyovec | 1 µg/ml |
| Imiquimod | Endosomes; TLR7/8 | Synthetic nucleotide analogue | 5 µg/ml |

3.3.1 RNA extraction and cDNA preparation

Cells were grown on a 6-well plate until 80% confluent, washed with 1X PBS, stimulated with bacterial and viral ligands for 3 and 24 hours, and trypsinized using 0.125% trypsin EDTA. The harvested cells were pelleted by centrifugation at 1200 rpm for 5 minutes. Following the RNeasy Mini Kit (Qiagen, catalog: 74101) protocol, RNA was extracted. Extracted RNA was quantified using a Nanodrop 2000 and stored at -80° C. For cDNA preparation, 1 ug RNA was reverse transcribed using a TaqMan reverse transcriptase kit (Applied Biosystems, catalog: N8080234) following the manufacturer's protocol. The resulting cDNA was diluted 5 times for further application. Each experiment was repeated 3 times.

3.3.2 Real-Time quantitative PCR (RT-qPCR)

In an Eppendorf tube, the master mix was made using 5 µl of SYBR green master mix (RT^2 SYBR Green ROX, catalog: 330523. Qiagen Sciences, Maryland, USA), 0.5 µl of forward and reverse primers, and 3 µl of nuclease-free water. 9 µl of master mix and 1 µl of diluted cDNA were mixed to make a final volume of 10µl and the RT-qPCR reaction was carried out on a 96-well PCR plate using Quantstudio™ Flex Real-Time PCR System (Applied Biosystems, NJ, USA). Gene expression analysis of various TLRs, RLRs, NLRs, and

cytokines/chemokines were studied using the specific primers (Table 3) Cyclophilin-A gene was used as a housekeeping gene. All the primers used in this study were designed in previous studies (121-123).

Table 3: List of genes and respective primers used in the stimulation assay.

Gene	Primer sequence (5'-3')	Accession number	Annealing Tempera-ture (◦ C)	Reference
TLR1	F: TGCTGGATGCTAACGGATGTC R: AAGTGGTTTCAATGTTGTTC AAAGTC	AB219664	55	(124)
TLR-2	F: TCACTTGTCTAACTTATCATC CTCTTG R: TCAGCGAAGGTGTCATTATTGC	AB085935	55	(124)
TLR-3	F: AGTAAATGAATCACCCTGCC TAGCA R: GCCGTTGACAAAACACATA AGGACT	DQ266435	55	(124)
TLR-4	F: GCCATCGCTGCTAACATCATC R: CTCATACTCAAAGATACACC ATCGG	AB188301	55	(124)
TLR-5	F: CCTTCCTGCTTCTTTGATGG R: CTGTGACCGTCCTGATGTAG	NM_001123202	55	(125)
TLR-6	F: AACCTACTGTCATAAGCCTTC	AB085936	55	(124)

	ATTC R: GTCTACCACAAATTCACTTTC TTCAG			
TLR-7	F: ACAATGATATCGCCACCTCC ACCA R: TGCCCAAGGAGAGAGTCTT CAGAT	NM_001097434	55	(126)
TLR-9	F: CACGACAGCCGAATAGCAC R: GGGAACAGGGAGCAGAGC	AY859728	57	(124)
NOD-1	F: CTGTCGTCAACACCGATCCA R: CCAGTTGGTGACGCAGCTT	NM_001114277	55	(127)
NOD-2	F: GAGCGCATCCTCTTAACTTTCG R: ACGCTCGTGATCCGTGAAC	NM_001105295	55	(127)
RIG-I	F: TATCCGAGCCGCAGGCTTTG ATGA R: AGTTTAGGGTTCTCGTTGTTG CTGGGA	NM_213804	60	(128)
Beta defensins11	F: TGCCACAGGTGCCGATCT R: CTGTTAGCTGCTTAAGGAATA AAG GC	XM_003362075	55	(129)

Beta defensins2	F: CCAGAGGTCAAACCACTACA	NM_214442	55	(129)
	R: GGTCCCTTCAATCCTGTTGAA			
MDA-5	F: TGCCCTTTCCCAGTGGATTA CTGA	NM_001100194	60	(128)
	R: TGTGTCCAGCTCCAATCAG ATTTG			
IL-1a	F: AGAATCTCAGAAACCCGAC TGTTT	M86725	57	(127)
	R: TTCAGCAACACGGGTTCGT			
IL-1b	F: GCCCTGTACCCCAACTGGTA	NM_86722	60	(127)
	R: CCAGGAAGACGGGCTTTTG			
IL-6	F: TGGATAAGCTGCAGTCACAG	AB035380	57	(127)
	R: ATTATCCGAATGGCCCTCAG			
IL-8	F: TTCGATGCCAGTGCATAAATA	L20001	55	(124)
	R: CTGTACAACCTTCTGCACCCA			
IL-10	F: TGGGTTGCCAAGCCTTGT	L35765	60	(127)
	R: GCCTTCGGCATTACGTCTTC			
TNF-a	F: CGACTCAGTGCCGAGATCAA	NM_214214	60	(127)
	R: CCTGCCCAGATTCAGCAAAG			
IFN-a	F: CCCCTGTGCCTGGGAGAT	X57191	60	(127)
	R: AGGTTTCTGGAGGAAGA			

	GAAGG			
IFN-b	F: AGTTGCCTGGGACTCCTCAA R: CCTCAGGGACCTCAA AGTTCAT	M86762	60	(127)
MCP-1	F: ACCAGCAGCAAGTGTCC TAAAG R: GTCAGGCTTCAAGGCTTCGG	55	NM_001077213	(127)
CYCLO-a	F: CCTGAACATACGGGTCCTG R: AACTGGGAACCGTTTGTGTTG	NM_214353.1	55	(127)

3.3.3   Statistical analysis

Experiments were conducted 3 times for reproducibility. Cyclophilin-A was used as an internal control to normalize cycle threshold (Ct) obtained from RT-qPCR reaction for various PRRs genes. mRNA fold change was calculated using the following formula: $2^{-\Delta\Delta Ct} = 2^{-\text{(CT value of target gene of the treatment-CT value of housekeeping gene of treatment)- (CT value of the negative control- CT value of housekeeping gene of the negative control)}}$. A two-tailed student's t-test was used to analyze the average fold change of three repeats. P values < 0.05 were considered significant for the study. Graphing was accomplished using GraphPad Prism software version 8.4.

3.4 Results

3.4.1 Changes in gene expression following bacterial ligand stimulation of pig primary nasal turbinate epithelial cells

Using specific primers, changes in gene expression of 8 different TLRs in response to various bacterial ligands were examined. Expression of various RLRs and NLRs, and defensins were also tested along with different cytokines/chemokines. Real-time reverse transcription (RT-qPCR) was performed, and Cyclophilin-A was used as a housekeeping gene.

Twenty-four hours of LPS stimulation significantly increased the expression of TLR-1. TLR-2, TLR-5, and TLR-6 expression increased both at 3 hours and 24 hours of LPS stimulation, but the changes were statistically non-significant. In contrast, 3 hours of LPS stimulation caused a decrease in TLR-7 and TLR-9 expression, but the changes were non-significant (Figure 16). Three hours of LPS stimulation significantly increased the expression of Beta-defensins 2. LPS stimulation for 24 hours caused a huge spike in RIG-I gene expression. However, high variation rendered the spike statistically non-significant. LPS stimulation had little effect on MDA-5, NOD-1, NOD-2, and Beta-defensins 1 gene expression as the changes were statistically non-significant (Figure 21). LPS significantly increased IL-10 expression after 24 hours and significantly increased TNF-alpha expression at 3 hours. MCP-1 gene expression decreased after 3 hours of LPS stimulation significantly. LPS stimulation had little effect on other cytokines/chemokines (Figure 26).

There were no significant changes in TLRs, RLRs, NLRs, and defensins gene expression upon PGN stimulation at both 3 hours and 24 hours' time point (Figure 17 and 22). Except

for significantly decreased expression of MCP-1 gene after 3 hours, PGN did not induce further significant changes in the rest of the cytokine and chemokine genes (Figure 27).

FLA caused TLR-2 and IL-1b gene expression to spike after 3 hours of stimulation with statistical significance. Apart from that, FLA did not induce further significant changes in gene expression for any other PRRs, cytokines and chemokines (Figure 18, 23 and 28). Out of all the PRRs, cytokines and chemokines tested, MDP only caused a significant decrease in the expression of IFN-beta gene after 24 hours of stimulation (Figure 19, 24 and 29). In addition to a significant decrease in NOD-2 gene expression after 24 hours, iE-dap caused IL-6 gene expression to change significantly both after 3 and 24 hours of stimulation (Figure 20, 25 and 30).

3.4.2 Changes in gene expression following viral ligand stimulation of pig primary nasal turbinate epithelial cells

There was a significant increase in TLR-6 expression after 3 hours of Poly I:C stimulation. However, Poly I:C stimulation did not induce any further significant changes in the rest of the PRRs, cytokines and chemokines (Figure 31, 35, and 39). Poly I:C with lyovec (Figure 32, 36 and 40) and imiquimod (Figure 34, 38 and 42) treatment were ineffective in producing any changes in any of the PRRs, cytokines and chemokines gene expression. Along with the viral ligands, a TLR-4 agonist inulin acetate nanoparticles were used to stimulate the cells. Inulin acetate significantly (Figure 33) downregulated the gene expression by causing TLR-1, TLR-2, and TLR-5 genes to decrease in their expression significantly after 24 hours of stimulation. Similarly, inulin acetate after 24 hours, caused a significant decrease in the expression of MDA-5, RIG-I, NOD-2, and Beta-defensin 2 genes (Figure 37). Inulin acetate also caused the significant downregulation of IL-10 and IFN-alpha after 24 hours of stimulation (Figure 41). Thus, inulin acetate affected specific PRRs, cytokines and chemokines, and caused their significant downregulation.

Figure 12: Various TLRs and their changes in gene expression based on LPS stimulation in PPNTECs. Bar graphs are the mean of three independent experiments and error bars represent the standard error of mean (SEM). Using delta-delta Ct method, fold change was calculated. Significant changes are represented by an asterisk (*), $p<0.05$.

Figure 13: Various TLRs and their changes in gene expression based on PGN stimulation in PPNTECs. Bar graphs are the mean of three independent experiments and error bars represent the standard error of mean (SEM). Using delta-delta Ct method, fold change was calculated. Significant changes are represented by an asterisk (*), $p < 0.05$.

Figure 14: Various TLRs and their changes in gene expression based on FLA stimulation in PPNTECs. Bar graphs are the mean of three independent experiments and error bars represent the standard error of mean (SEM). Using delta-delta Ct method, fold change was calculated. Significant changes are represented by an asterisk (*), p<0.05.

Figure 15: Various TLRs and their changes in gene expression based on MDP stimulation in PPNTECs. Bar graphs are the mean of three independent experiments and error bars represent the standard error of mean (SEM). Using delta-delta Ct method, fold change was calculated. Significant changes are represented by an asterisk (*), $p < 0.05$.
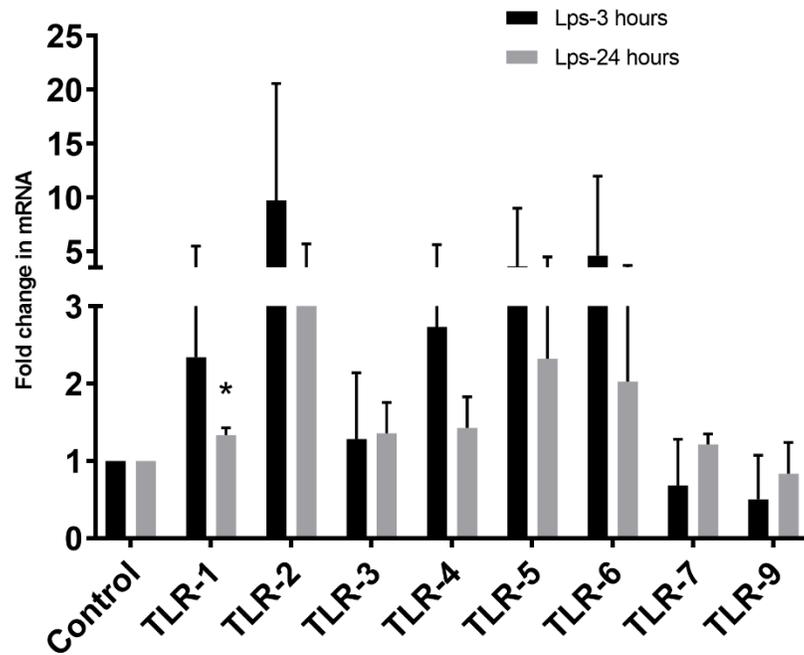
Figure 16: Various TLRs and their changes in gene expression based on iE-dap stimulation in PPNTECs. Bar graphs are the mean of three independent experiments and error bars represent the standard error of mean (SEM). Using delta-delta Ct method, fold change was calculated. Significant changes are represented by an asterisk (*), p<0.05.

Figure 17: RLRs, NLRs and other PRRs, and their changes in gene expression based on LPS stimulation in PPNTECs. Bar graphs are the mean of three independent experiments and error bars represent the standard error of mean (SEM). Using delta-delta Ct method, fold change was calculated. Significant changes are represented by an asterisk (*), $p < 0.05$.

Figure 18: RLRs, NLRs and other PRRs, and their changes in gene expression based on PGN stimulation in PPNTECs. Bar graphs are the mean of three independent experiments and error bars represent the standard error of mean (SEM). Using delta-delta Ct method, fold change was calculated. Significant changes are represented by an asterisk (*), $p < 0.05$.
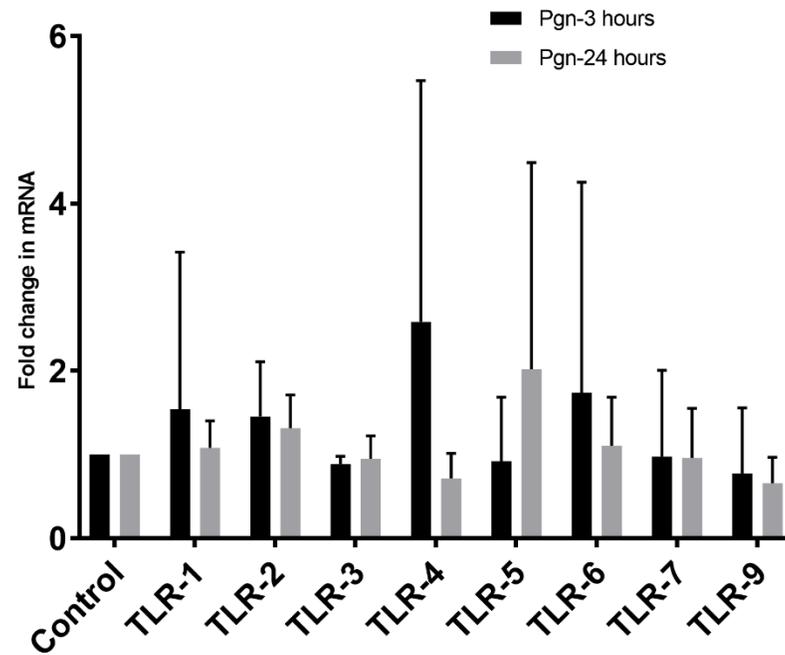
Figure 19: RLRs, NLRs and other PRRs, and their changes in gene expression based on FLA stimulation in PPNTECs. Bar graphs are the mean of three independent experiments and error bars represent the standard error of mean (SEM). Using delta-delta Ct method, fold change was calculated. Significant changes are represented by an asterisk (*), $p < 0.05$.
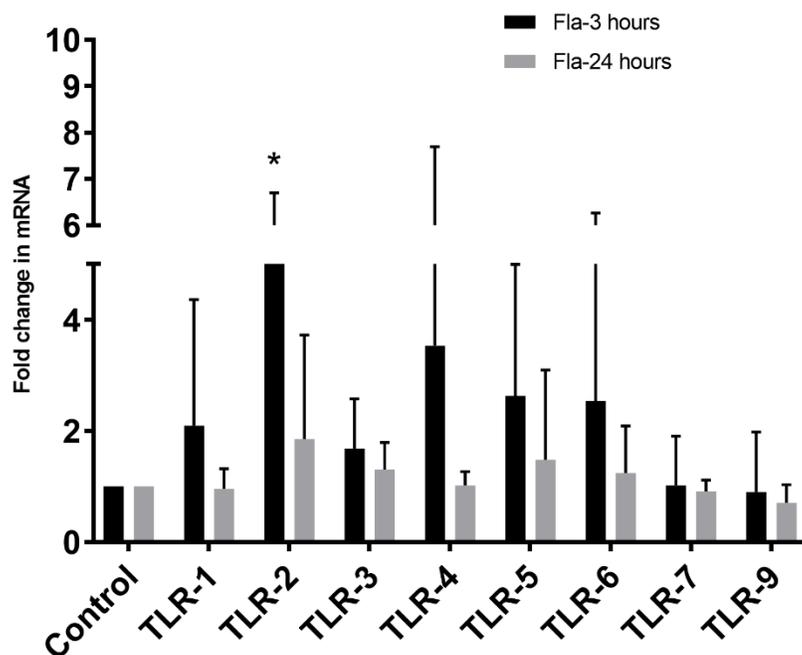
Figure 20: RLRs, NLRs and other PRRs, and their changes in gene expression based on MDP stimulation in PPNTECs. Bar graphs are the mean of three independent experiments and error bars represent the standard error of mean (SEM). Using delta-delta Ct method, fold change was calculated. Significant changes are represented by an asterisk (*), p<0.05.

Figure 21: RLRs, NLRs and other PRRs, and their changes in gene expression based on iE-dap stimulation in PPNTECs. Bar graphs are the mean of three independent experiments and error bars represent the standard error of mean (SEM). Using delta-delta Ct method, fold change was calculated. Significant changes are represented by an asterisk (*), $p < 0.05$.
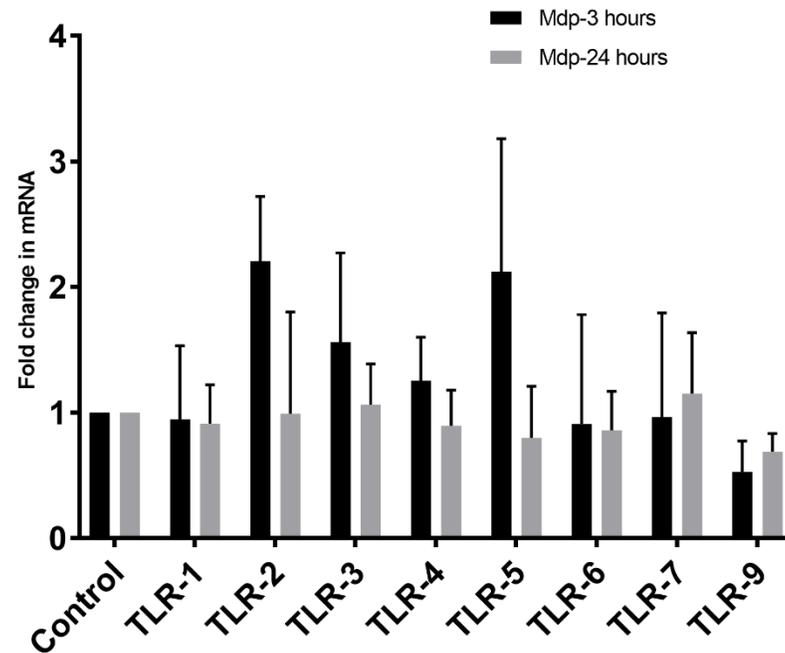
Figure 22: Cytokines/chemokines, and their changes in gene expression based on LPS stimulation in PPNTECs. Bar graphs are the mean of three independent experiments and error bars represent the standard error of mean (SEM). Using delta-delta Ct method, fold change was calculated. Significant changes are represented by an asterisk (*), $p < 0.05$.

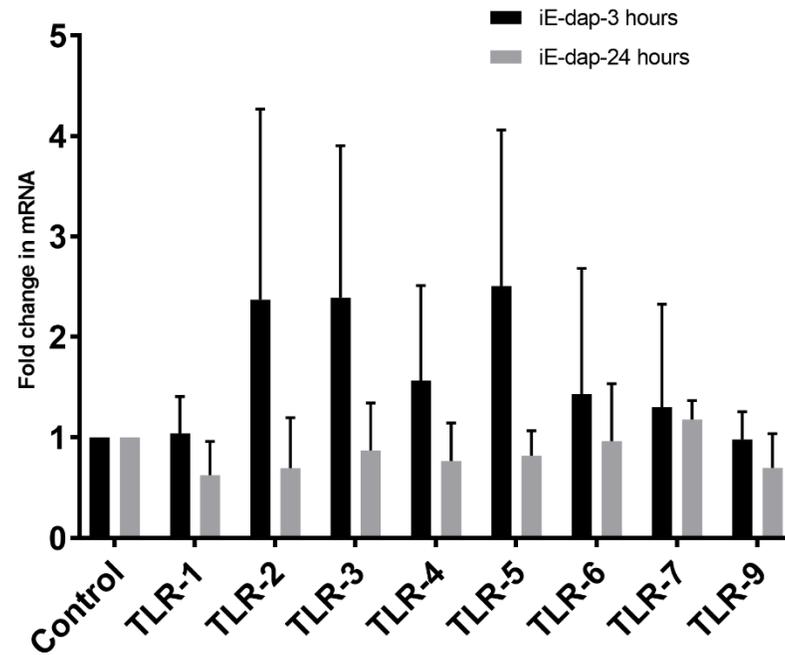Figure 23: Cytokines/chemokines, and their changes in gene expression based on PGN stimulation in PPNTECs. Bar graphs are the mean of three independent experiments and error bars represent the standard error of mean (SEM). Using delta-delta Ct method, fold change was calculated. Significant changes are represented by an asterisk (*), $p < 0.05$.

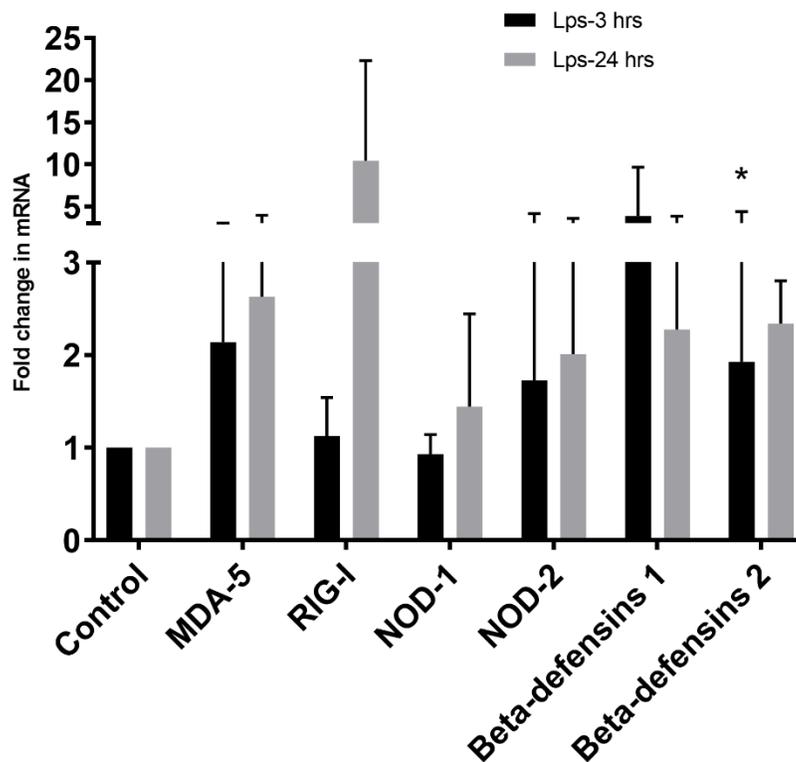Figure 24: Cytokines/chemokines, and their changes in gene expression based on FLA stimulation in PPNTECs. Bar graphs are the mean of three independent experiments and error bars represent the standard error of mean (SEM). Using delta-delta Ct method, fold change was calculated. Significant changes are represented by an asterisk (*), $p < 0.05$.

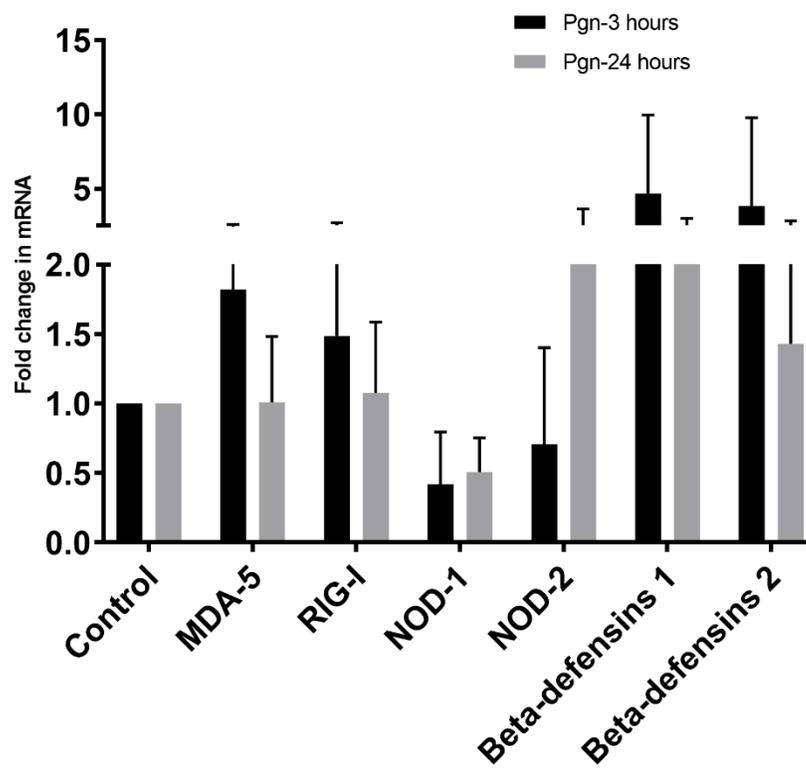Figure 25: Cytokines/chemokines, and their changes in gene expression based on MDP stimulation in PPNTECs. Bar graphs are the mean of three independent experiments and error bars represent the standard error of mean (SEM). Using delta-delta Ct method, fold change was calculated. Significant changes are represented by an asterisk (*), $p < 0.05$.

Figure 26: Cytokines/chemokines, and their changes in gene expression based on iE-dap stimulation in PPNTECs. Bar graphs are the mean of three independent experiments and error bars represent the standard error of mean (SEM). Using delta-delta Ct method, fold change was calculated. Significant changes are represented by an asterisk (*), $p < 0.05$.
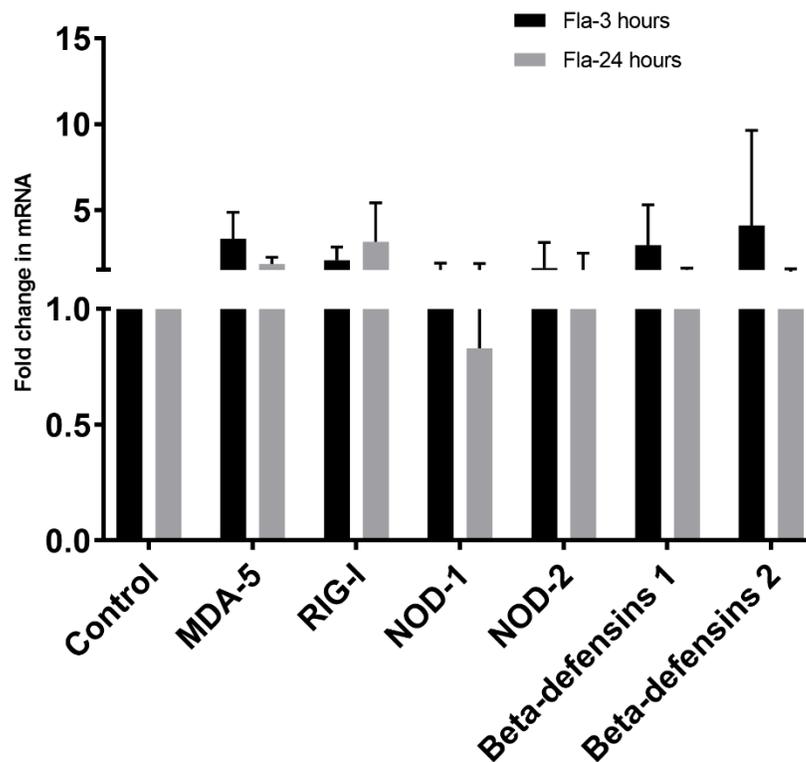
Figure 27: Various TLRs and their changes in gene expression based on Poly I:C stimulation in PPNTECs. Bar graphs are the mean of three independent experiments and error bars represent the standard error of mean (SEM). Using delta-delta Ct method, fold change was calculated. Significant changes are represented by an asterisk (*), p<0.05.

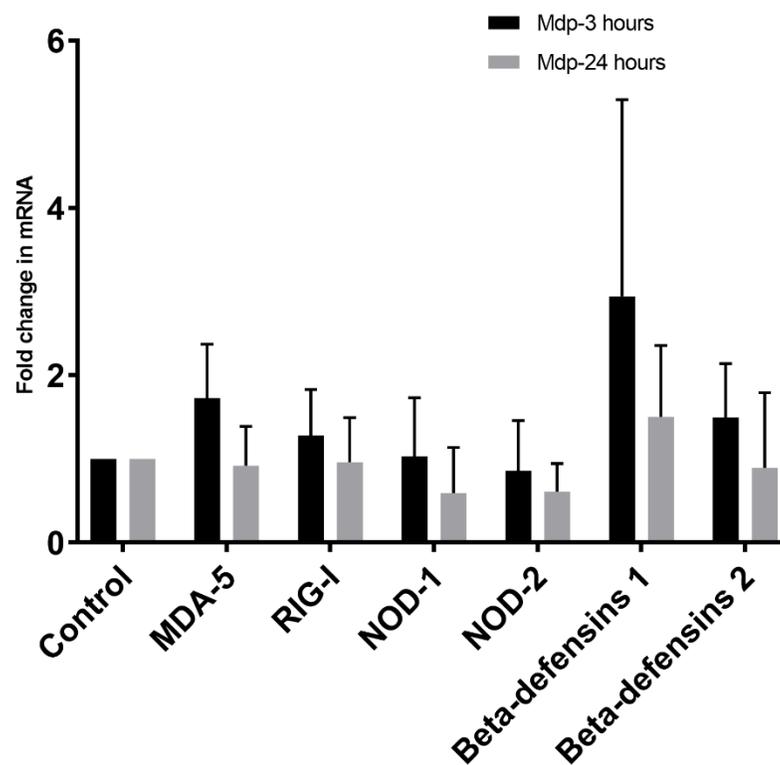Figure 28: Various TLRs and their changes in gene expression based on Poly I:C with lyovec stimulation in PPNTECs. Bar graphs are the mean of three independent experiments and error bars represent the standard error of mean (SEM). Using delta-delta Ct method, fold change was calculated. Significant changes are represented by an asterisk (*), $p<0.05$.
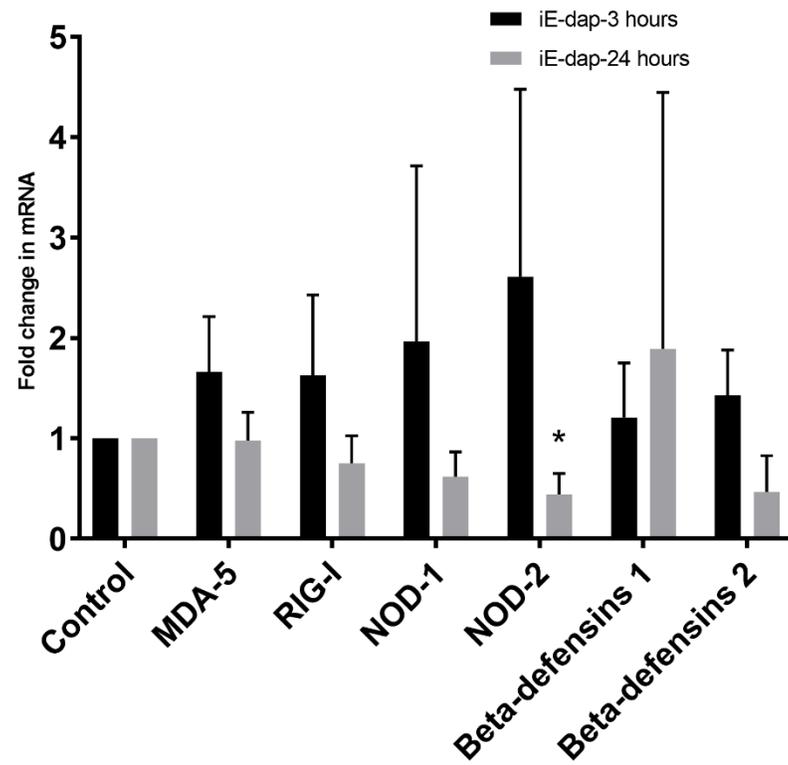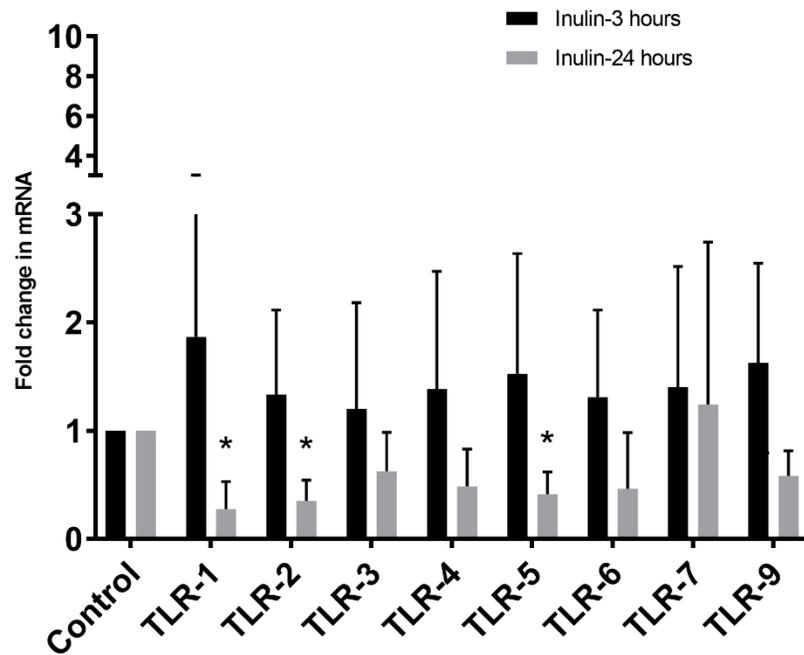
Figure 29: Various TLRs and their changes in gene expression based on Inulin acetate stimulation in PPNTECs. Bar graphs are the mean of three independent experiments and error bars represent the standard error of mean (SEM). Using delta-delta Ct method, fold change was calculated. Significant changes are represented by an asterisk (*), $p < 0.05$.
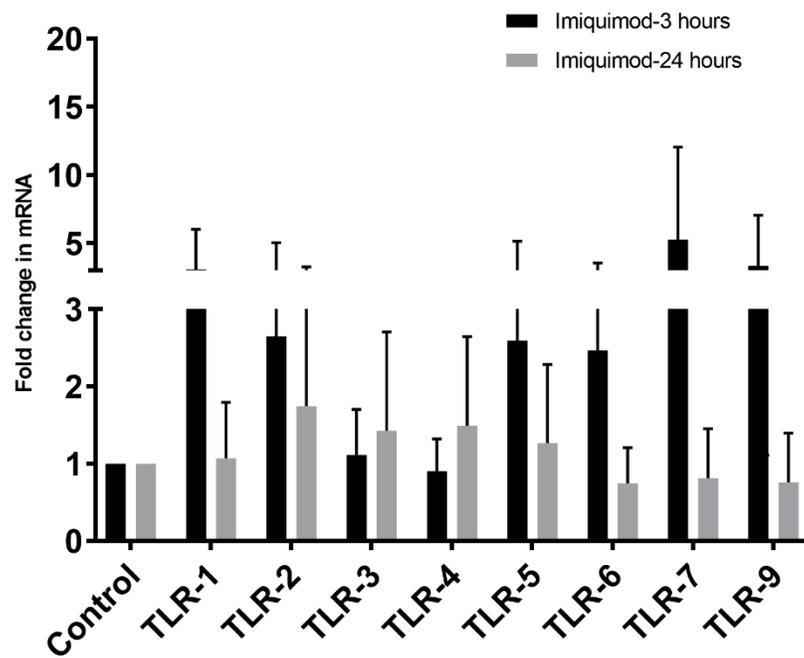
Figure 30: Various TLRs and their changes in gene expression based on imiquimod stimulation in PPNTECs. Bar graphs are the mean of three independent experiments and error bars represent the standard error of mean (SEM). Using delta-delta Ct method, fold change was calculated. Significant changes are represented by an asterisk (*), $p < 0.05$.
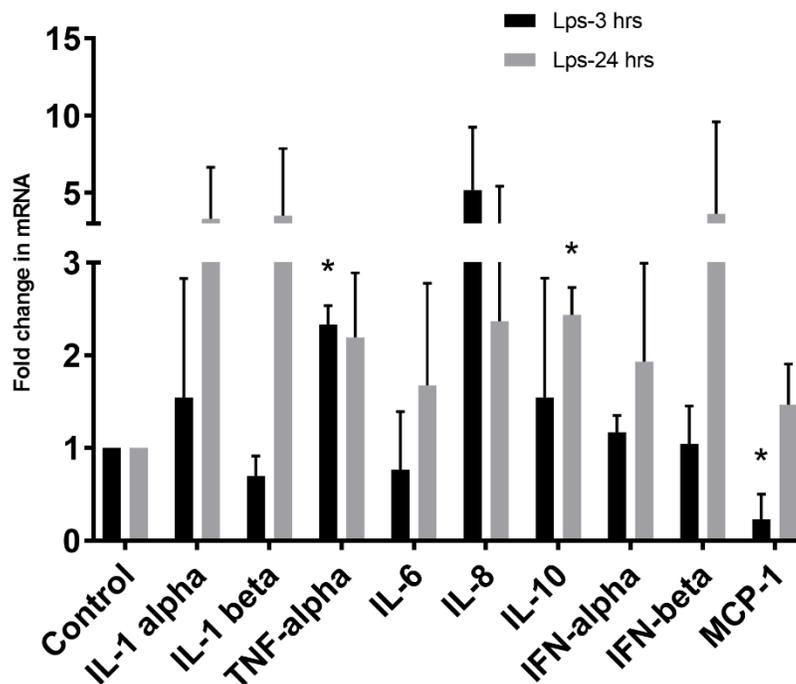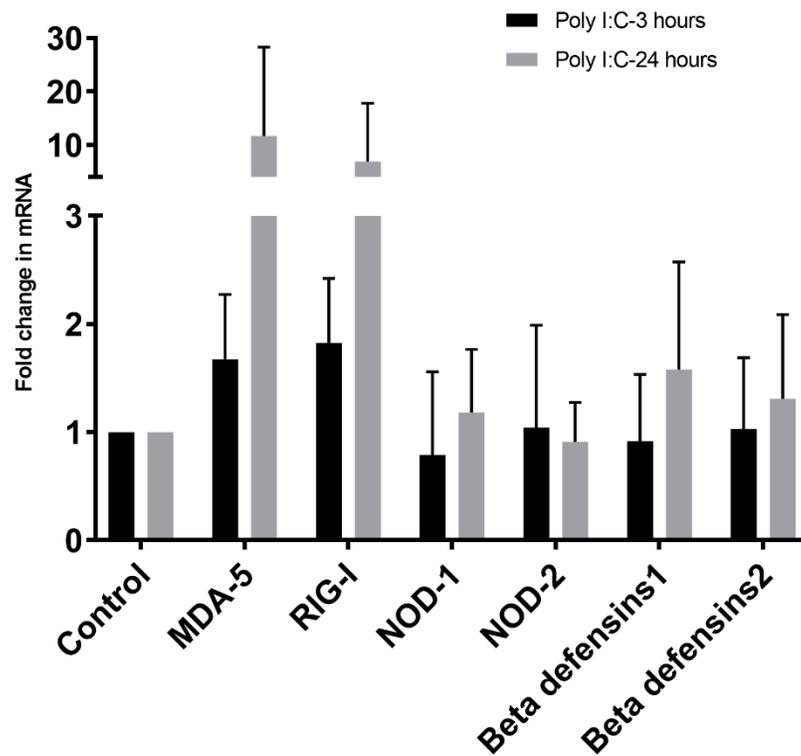
Figure 31: RLRs, NLRs, and other PRRs, and their changes in gene expression based on Poly I:C stimulation in PPNTECs. Bar graphs are the mean of three independent experiments and error bars represent the standard error of mean (SEM). Using delta-delta Ct method, fold change was calculated. Significant changes are represented by an asterisk (*), $p < 0.05$.
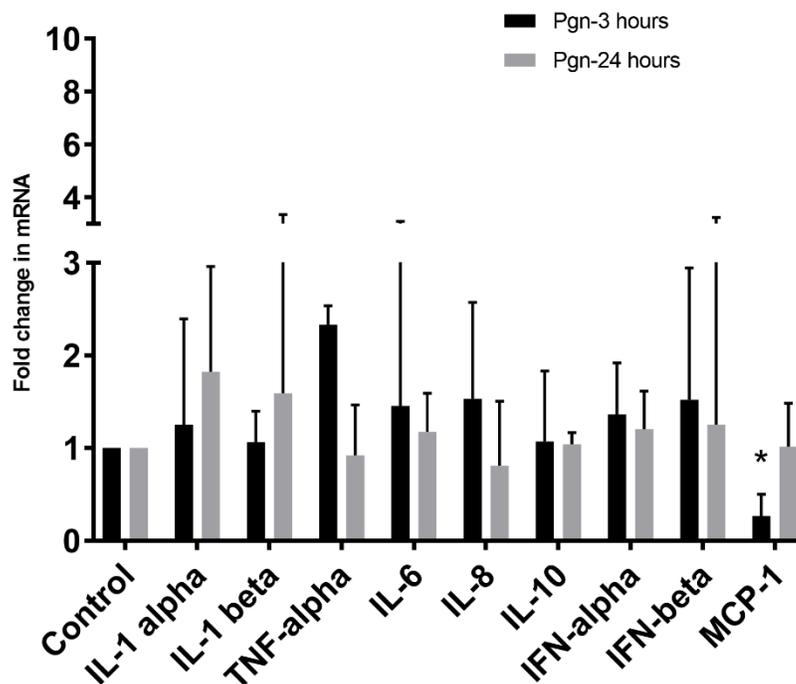
Figure 32: RLRs, NLRs, and other PRRs, and their changes in gene expression based on Poly I:C with lyovec stimulation in PPNTECs. Bar graphs are the mean of three independent experiments and error bars represent the standard error of mean (SEM). Using delta-delta Ct method, fold change was calculated. Significant changes are represented by an asterisk (*), $p < 0.05$.
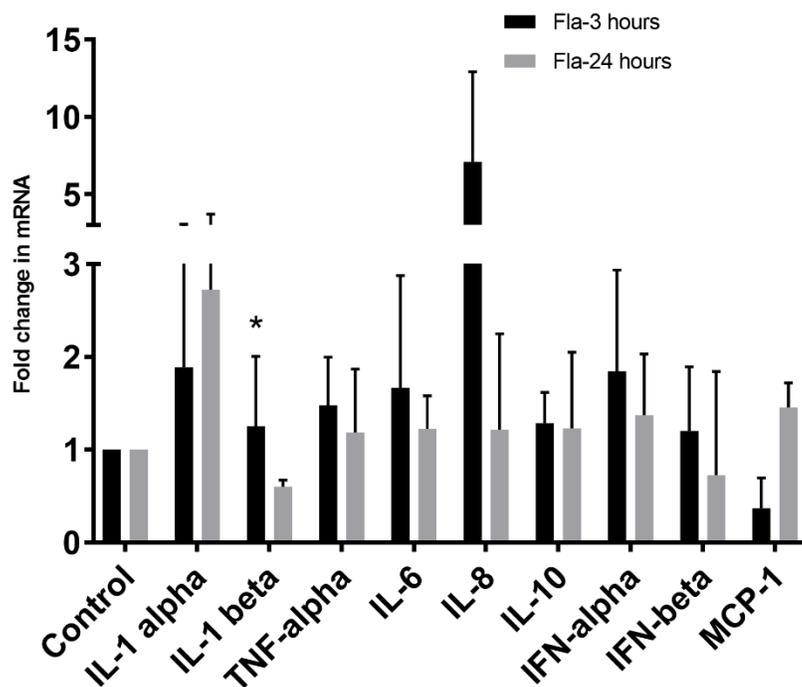
Figure 33: RLRs, NLRs, and other PRRs, and their changes in gene expression based on Inulin acetate stimulation in PPNTECs. Bar graphs are the mean of three independent experiments and error bars represent the standard error of mean (SEM). Using delta-delta Ct method, fold change was calculated. Significant changes are represented by an asterisk (*), $p < 0.05$.
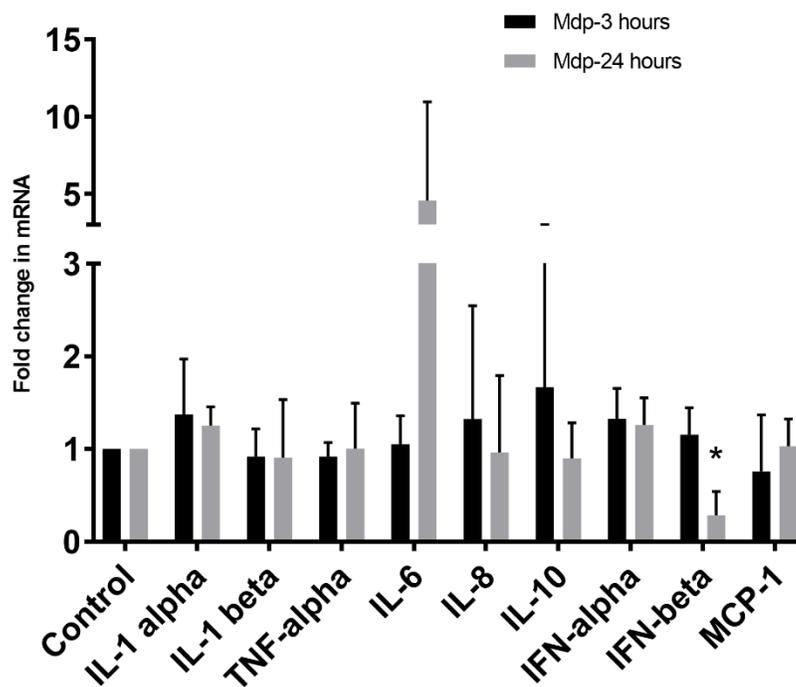
Figure 34: RLRs, NLRs, and other PRRs, and their changes in gene expression based on imiquimod stimulation in PPNTECs. Bar graphs are the mean of three independent experiments and error bars represent the standard error of mean (SEM). Using delta-delta Ct method, fold change was calculated. Significant changes are represented by an asterisk (*), $p < 0.05$.

Figure 35: Cytokines/chemokines, and their changes in gene expression based on Poly I:C stimulation in PPNTECs. Bar graphs are the mean of three independent experiments and error bars represent the standard error of mean (SEM). Using delta-delta Ct method, fold change was calculated. Significant changes are represented by an asterisk (*), $p < 0.05$.
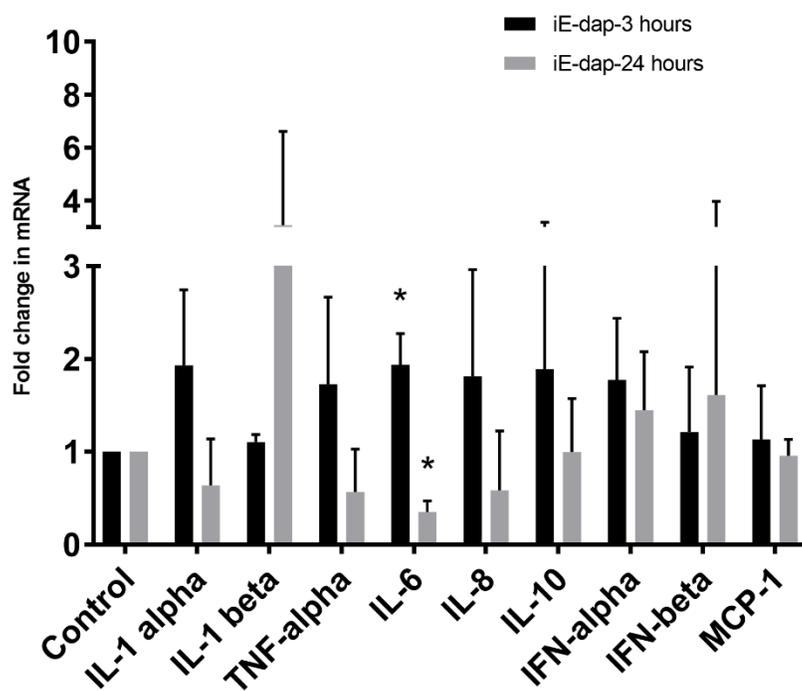
Figure 36: Cytokines/chemokines, and their changes in gene expression based on Poly I:C with lyovec stimulation in PPNTECs. Bar graphs are the mean of three independent experiments and error bars represent the standard error of mean (SEM). Using delta-delta Ct method, fold change was calculated. Significant changes are represented by an asterisk (*), $p < 0.05$.
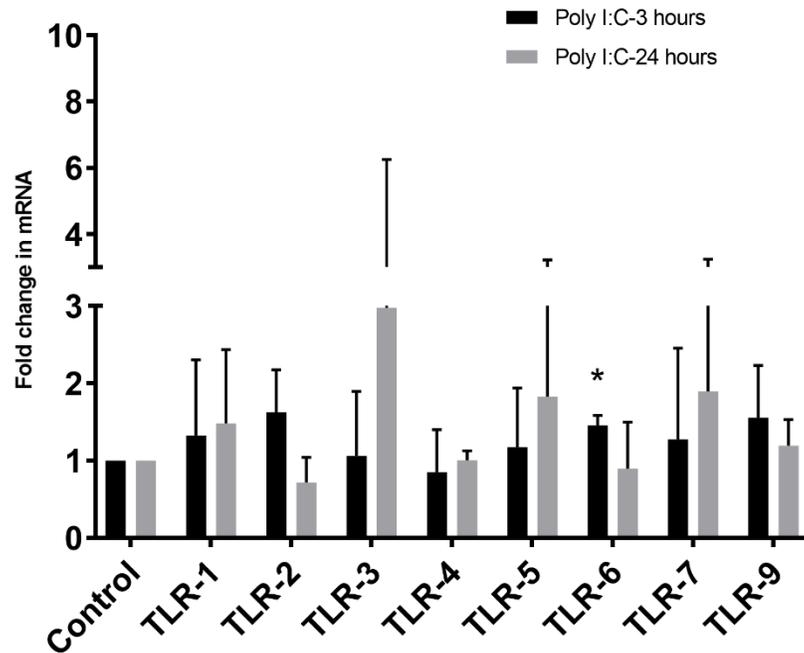
Figure 37: Cytokines/chemokines, and their changes in gene expression based on Inulin acetate stimulation in PPNTECs. Bar graphs are the mean of three independent experiments and error bars represent the standard error of mean (SEM). Using delta-delta Ct method, fold change was calculated. Significant changes are represented by an asterisk (*), $p < 0.05$.
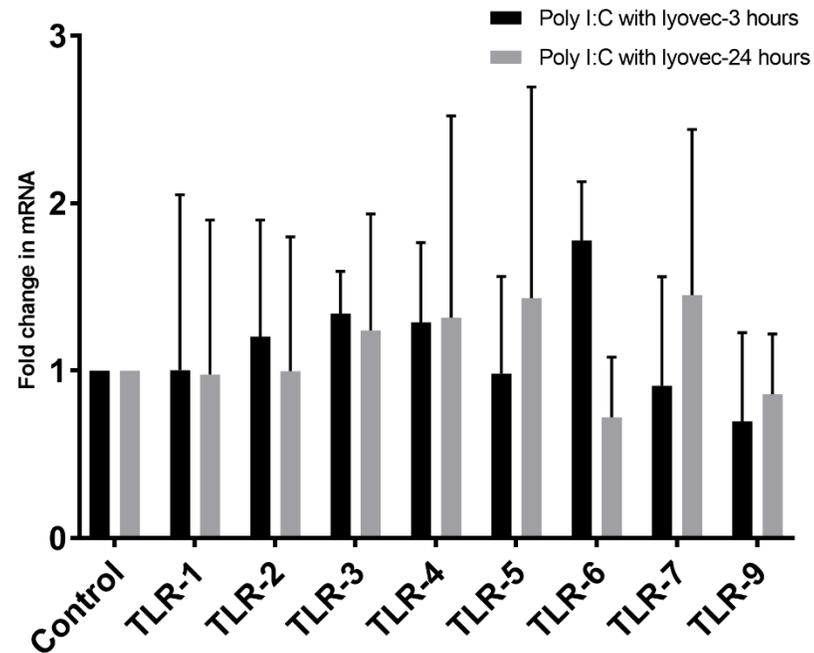
Figure 38: Cytokines/chemokines, and their changes in gene expression based on imiquimod stimulation in PPNTECs. Bar graphs are the mean of three independent experiments and error bars represent the standard error of mean (SEM). Using delta-delta Ct method, fold change was calculated. Significant changes are represented by an asterisk (*), $p<0.05$.

3.4.3 Changes in gene expression following bacterial ligand stimulation of pig primary tracheal epithelial cells

Except for upregulation of TLR-2 gene expression upon iE-dap stimulation for 24 hours, there were not any significant changes in gene expression of different TLRs upon bacterial ligand stimulation (Figure 43-47). While gene expression of RIG-I and NOD-1 upregulated significantly upon LPS stimulation for 3 hours (Figure 48), LPS downregulated IL-10 expression significantly after 24 hours of stimulation (Figure 53). PGN stimulation did not induce any significant changes in PRRs, cytokine and chemokine gene expression (Figure 44, 49 and 54).

NOD-2 gene expression decreased significantly after 3 hours of FLA stimulation. FLA caused RIG-I expression after 3 hours of stimulation to spike, but the change was not found to be statistically significant (Figure 50). MDP stimulation did not induce any changes in the expression of PRRs, cytokine and chemokine genes (Figure 46, 51 and 56). A significant increase in IL-6 and IL-1α gene expression was found after 3 hours and 24 hours of iE-dap stimulation respectively (Figure 57).

3.4.4 Changes in gene expression following viral ligand stimulation of pig primary tracheal epithelial cells

Only TNF-alpha showed a significant increase in gene expression upon Poly I:C stimulation after 24 hours. Expression of IFN-b skyrocketed after 24 hours of Poly I:C stimulation, but the change was found to be non-significant. Apart from that, Poly I:C stimulation did not induce any further statistically significant changes in gene expression of various PRRs, cytokine and chemokine genes (Figure 58, 62, 66).

Poly I:C with lyovec stimulation significantly decreased TLR-4 and TLR-5 gene expression after 3 hours (Figure 59). Significant downregulation of NOD-1 gene was observed after 3 and 24 hours of Poly I:C with lyovec stimulation. Consistent with NOD-1, Poly I:C with lyovec stimulation caused NOD-2 gene expression to go down significantly after 3 hours. MDA-5 gene expression increased significantly after 24 hours of Poly I:C with lyovec stimulation (Figure 63). IL-1B, IL-10, and IFN-A gene decreased significantly in their expression after 3 hours of Poly I:C with lyovec stimulation. Expression levels of TNF-A gene went up significantly after 24 hours of Poly I:C with lyovec stimulation (Figure 67). Both inulin acetate and imiquimod stimulation did not change the expression of PRRs (Figure 60, 61, 64 and 65); however, inulin acetate stimulation induced significant changes in beta defensin-1 and TNF-α gene expression (Figure 64 and 68).

Figure 39: Various TLRs and their changes in gene expression based on LPS stimulation in PPTECs. Bar graphs are the mean of three independent experiments and error bars represent the standard error of the mean (SEM). Using the delta-delta Ct method, fold change was calculated. Significant changes are represented by an asterisk (*), $p < 0.05$.
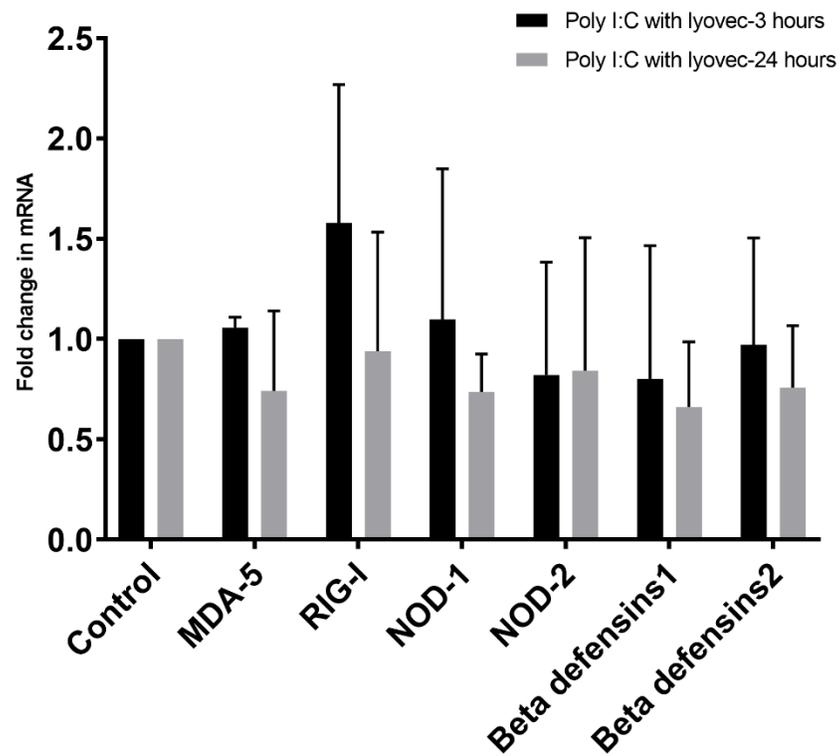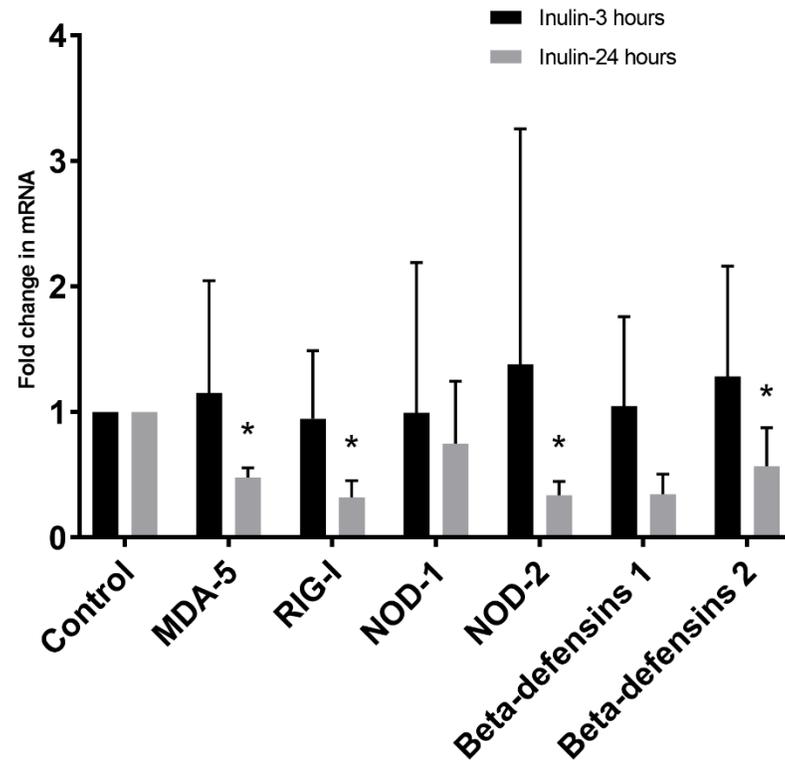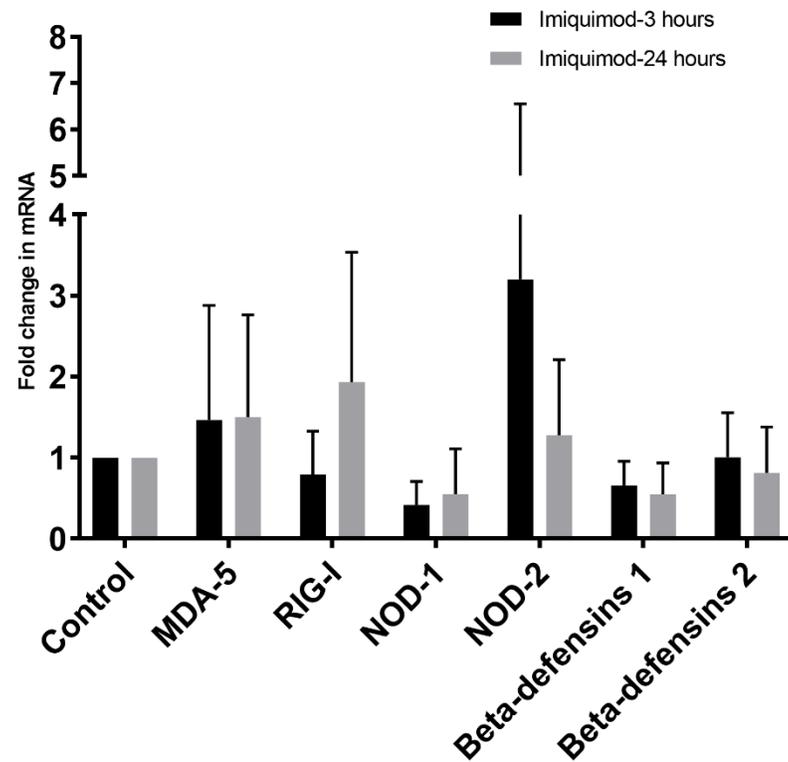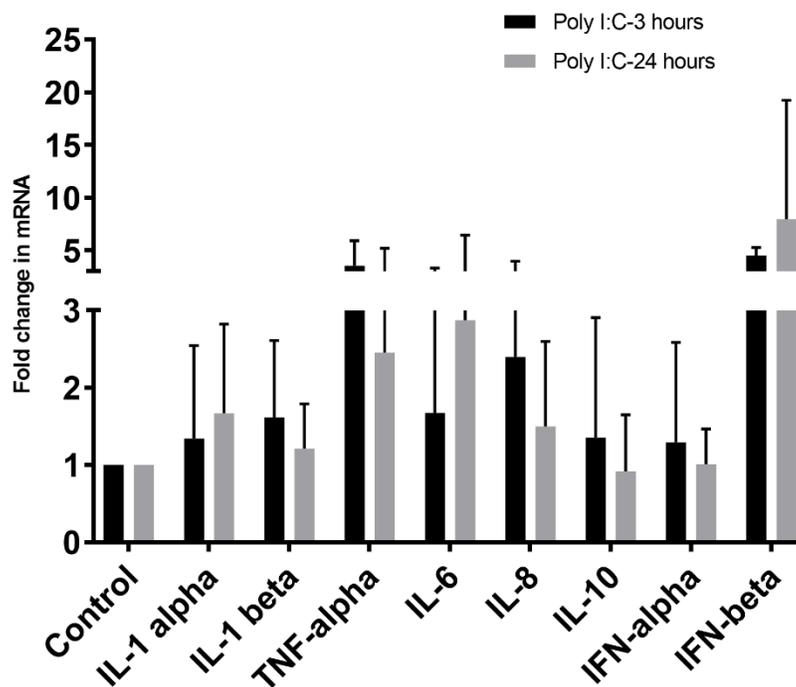
Figure 40: Various TLRs and their changes in gene expression based on PGN stimulation in PPTECs. Bar graphs are the mean of three independent experiments and error bars represent the standard error of the mean (SEM). Using the delta-delta Ct method, fold change was calculated. Significant changes are represented by an asterisk (*), p<0.05.
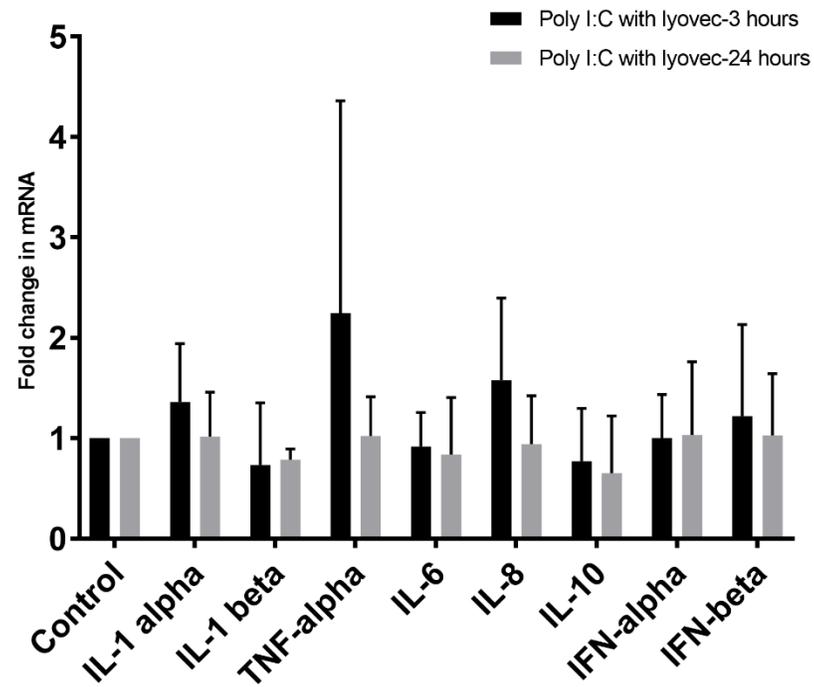
Figure 41: Various TLRs and their changes in gene expression based on FLA stimulation in PPTECs. Bar graphs are the mean of three independent experiments and error bars represent the standard error of the mean (SEM). Using the delta-delta Ct method, fold change was calculated. Significant changes are represented by an asterisk (*), p<0.05.

Figure 42: Various TLRs and their changes in gene expression based on MDP stimulation in PPTECs. Bar graphs are the mean of three independent experiments and error bars represent the standard error of the mean (SEM). Using the delta-delta Ct method, fold change was calculated. Significant changes are represented by an asterisk (*), p<0.05.
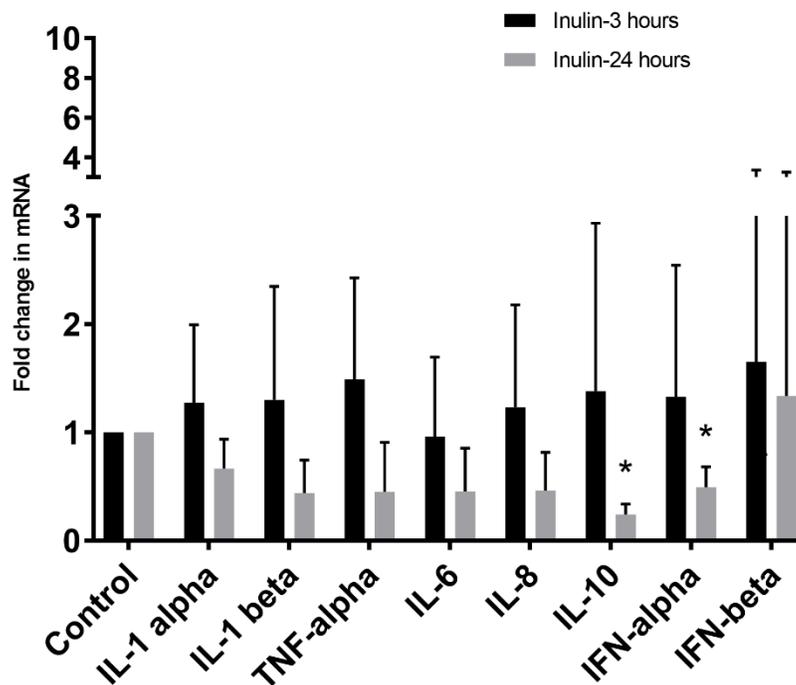
Figure 43: Various TLRs and their changes in gene expression based on iE-dap stimulation in PPTECs. Bar graphs are the mean of three independent experiments and error bars represent the standard error of the mean (SEM). Using the delta-delta Ct method, fold change was calculated. Significant changes are represented by an asterisk (*), $p < 0.05$.
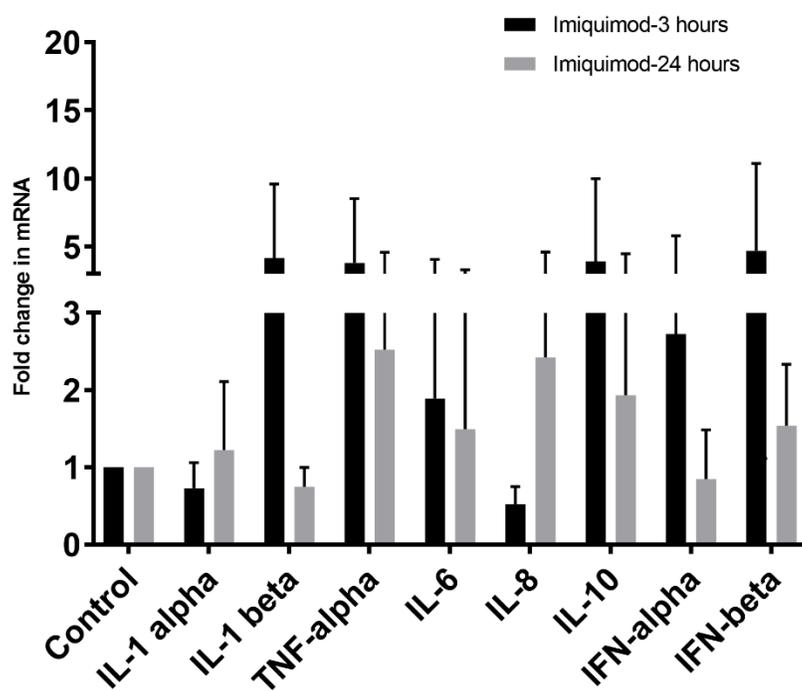
Figure 44: RLRs, NLRs, and other PRRs, and their changes in gene expression based on LPS stimulation in PPTECs. Bar graphs are the mean of three independent experiments and error bars represent the standard error of mean (SEM). Using delta-delta Ct method, fold change was calculated. Significant changes are represented by an asterisk (*), $p < 0.05$.

Figure 45: RLRs, NLRs, and other PRRs, and their changes in gene expression based on PGN stimulation in PPTECs. Bar graphs are the mean of three independent experiments and error bars represent the standard error of mean (SEM). Using delta-delta Ct method, fold change was calculated. Significant changes are represented by an asterisk (*), $p < 0.05$.

Figure 46: RLRs, NLRs, and other PRRs, and their changes in gene expression based on FLA stimulation in PPTECs. Bar graphs are the mean of three independent experiments and error bars represent the standard error of mean (SEM). Using delta-delta Ct method, fold change was calculated. Significant changes are represented by an asterisk (*), $p < 0.05$.

Figure 47: RLRs, NLRs, and other PRRs, and their changes in gene expression based on MDP stimulation in PPTECs. Bar graphs are the mean of three independent experiments and error bars represent the standard error of mean (SEM). Using delta-delta Ct method, fold change was calculated. Significant changes are represented by an asterisk (*), $p<0.05$.

Figure 48: RLRs, NLRs, and other PRRs, and their changes in gene expression based on iE-dap stimulation in PPTECs. Bar graphs are the mean of three independent experiments and error bars represent the standard error of mean (SEM). Using delta-delta Ct method, fold change was calculated. Significant changes are represented by an asterisk (*), $p < 0.05$.

Figure 49: Cytokines/chemokines, and their changes in gene expression based on LPS stimulation in PPTECs. Bar graphs are the mean of three independent experiments and error bars represent the standard error of the mean (SEM). Using the delta-delta Ct method, fold change was calculated. Significant changes are represented by an asterisk (*), $p < 0.05$.
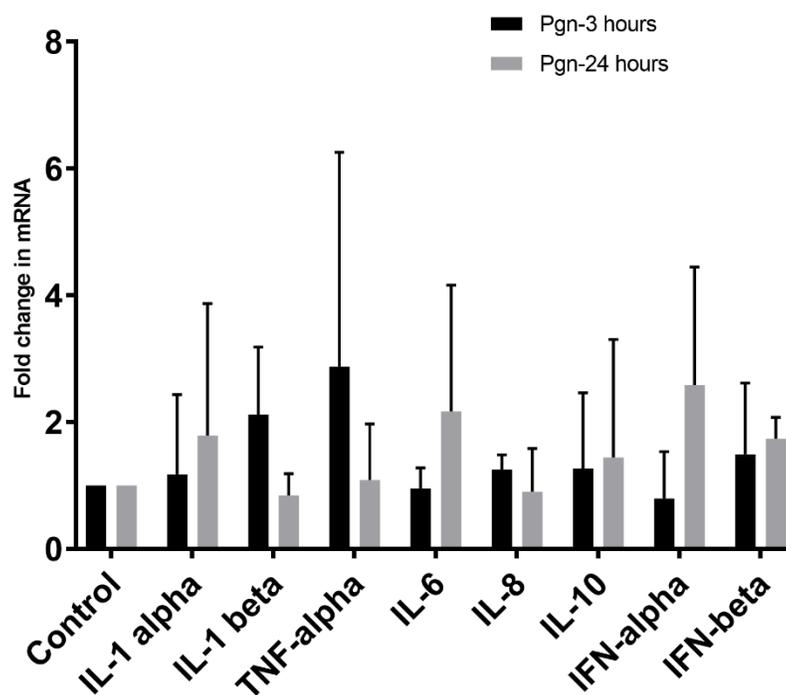
Figure 50: Cytokines/chemokines, and their changes in gene expression based on PGN stimulation in PPTECs. Bar graphs are the mean of three independent experiments and error bars represent the standard error of the mean (SEM). Using the delta-delta Ct method, fold change was calculated. Significant changes are represented by an asterisk (*), $p < 0.05$.
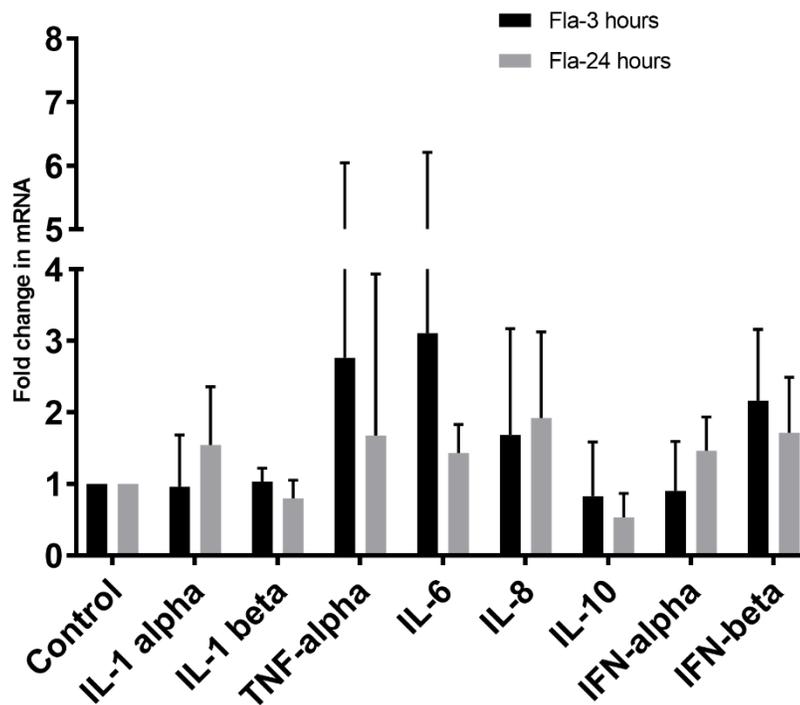
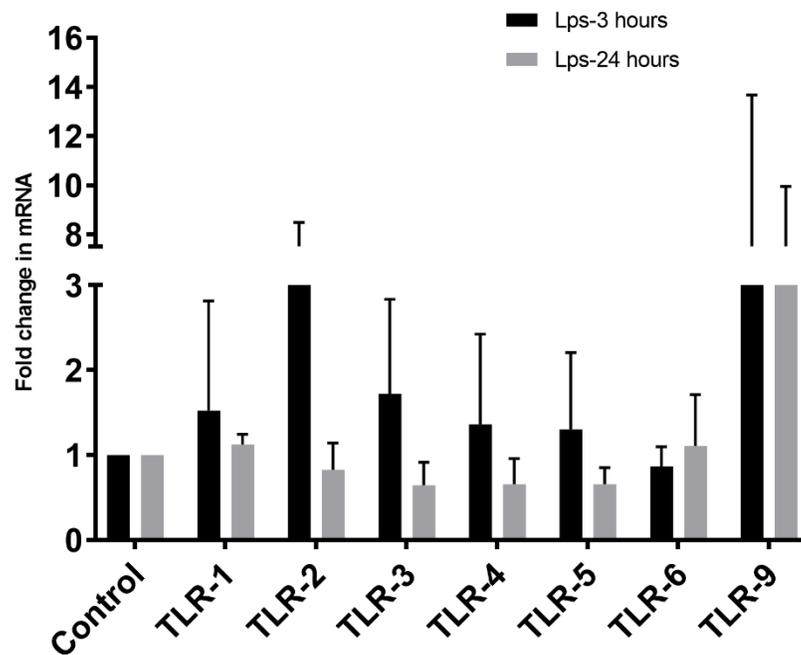Figure 51: Cytokines/chemokines, and their changes in gene expression based on FLA stimulation in PPTECs. Bar graphs are the mean of three independent experiments and error bars represent the standard error of the mean (SEM). Using the delta-delta Ct method, fold change was calculated. Significant changes are represented by an asterisk (*), p<0.05.
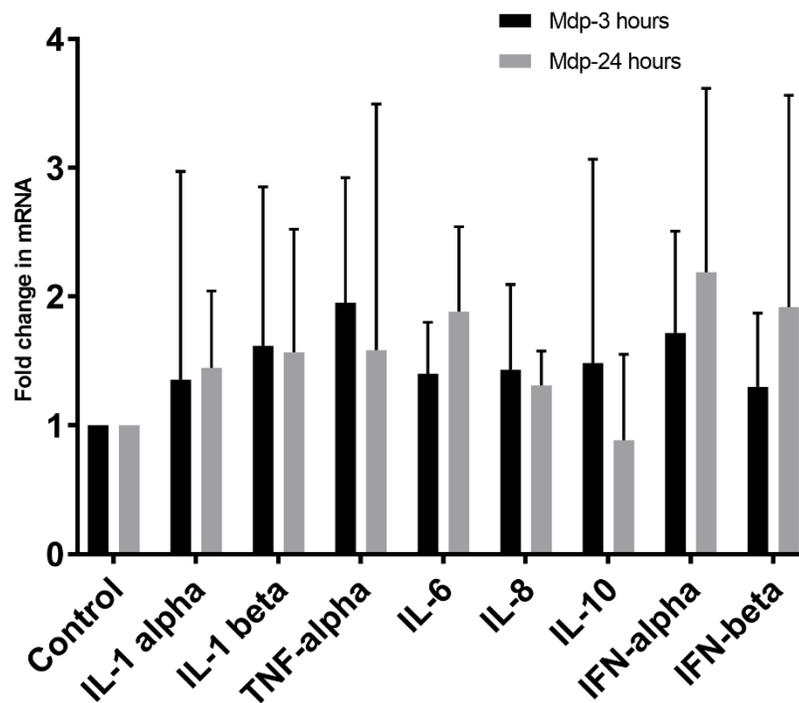
Figure 52: Cytokines/chemokines, and their changes in gene expression based on MDP stimulation in PPTECs. Bar graphs are the mean of three independent experiments and error bars represent the standard error of the mean (SEM). Using the delta-delta Ct method, fold change was calculated. Significant changes are represented by an asterisk (*), $p < 0.05$.
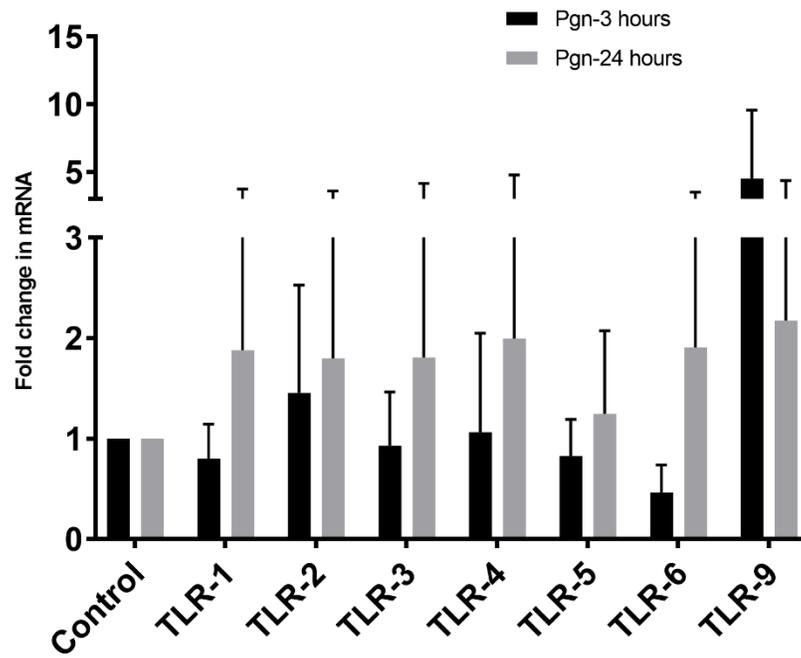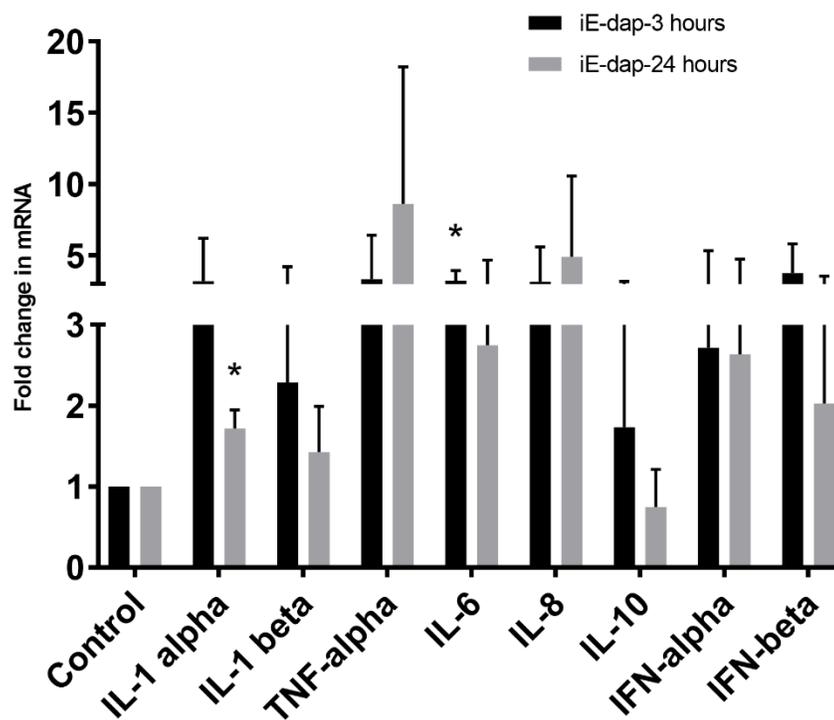
Figure 53: Cytokines/chemokines, and their changes in gene expression based on iE-dap stimulation in PPTECs. Bar graphs are the mean of three independent experiments and error bars represent the standard error of the mean (SEM). Using the delta-delta Ct method, fold change was calculated. Significant changes are represented by an asterisk (*), $p < 0.05$.
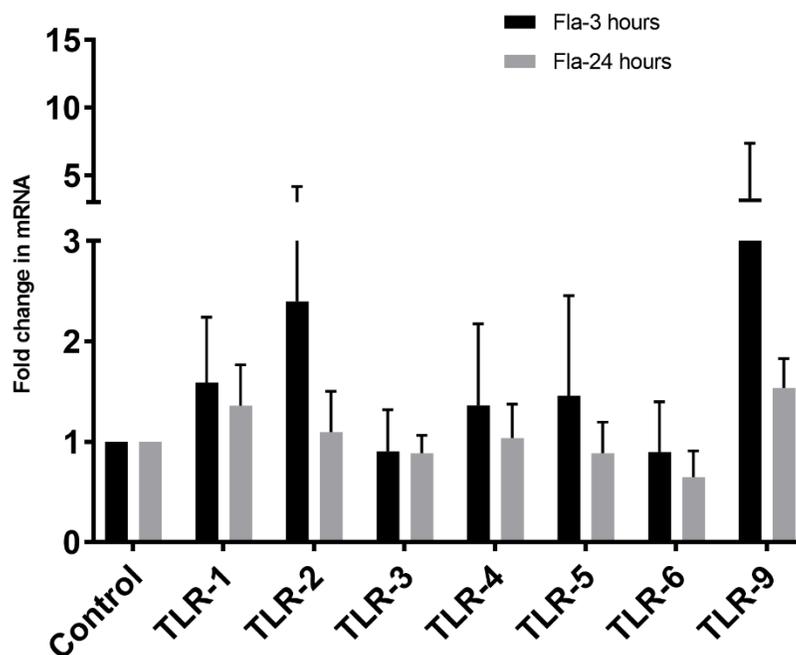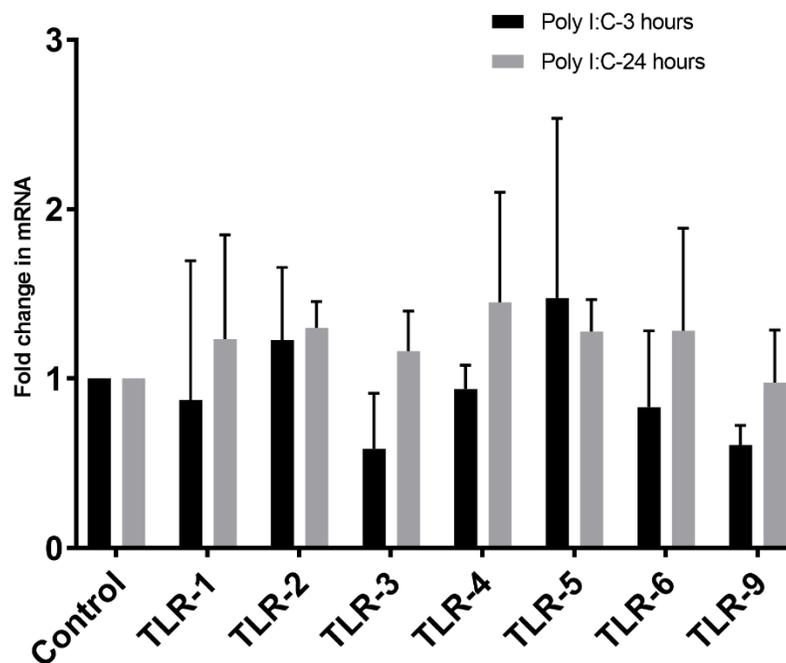
Figure 54: Various TLRs and their changes in gene expression based on Poly I:C stimulation in PPTECs. Bar graphs are the mean of three independent experiments and error bars represent the standard error of the mean (SEM). Using the delta-delta Ct method, fold change was calculated. Significant changes are represented by an asterisk (*), $p < 0.05$.
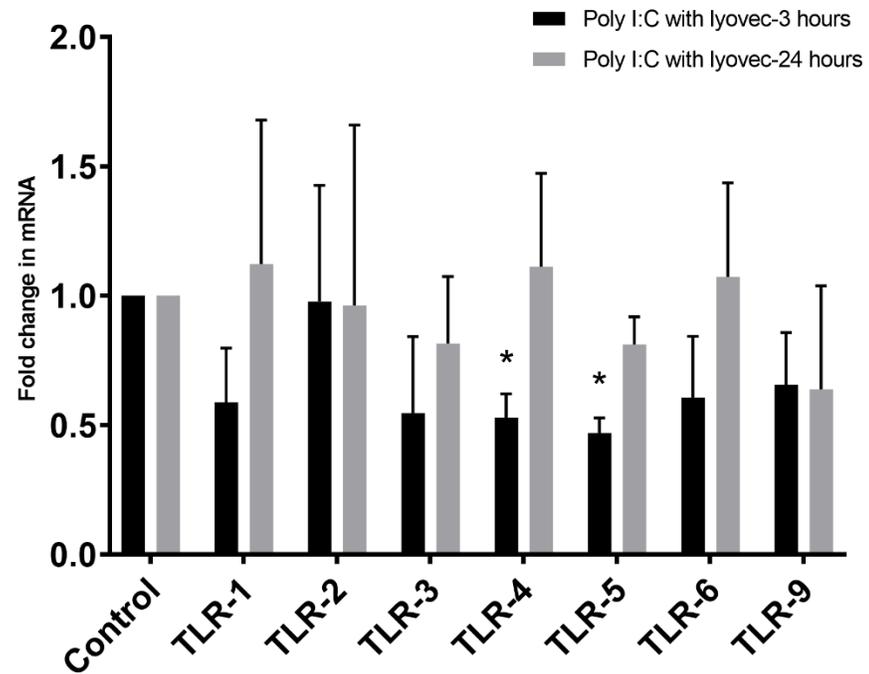
Figure 55: Various TLRs and their changes in gene expression based on Poly I:C with lyovec stimulation in PPTECs. Bar graphs are the mean of three independent experiments and error bars represent the standard error of the mean (SEM). Using the delta-delta Ct method, fold change was calculated. Significant changes are represented by an asterisk (*), $p < 0.05$.
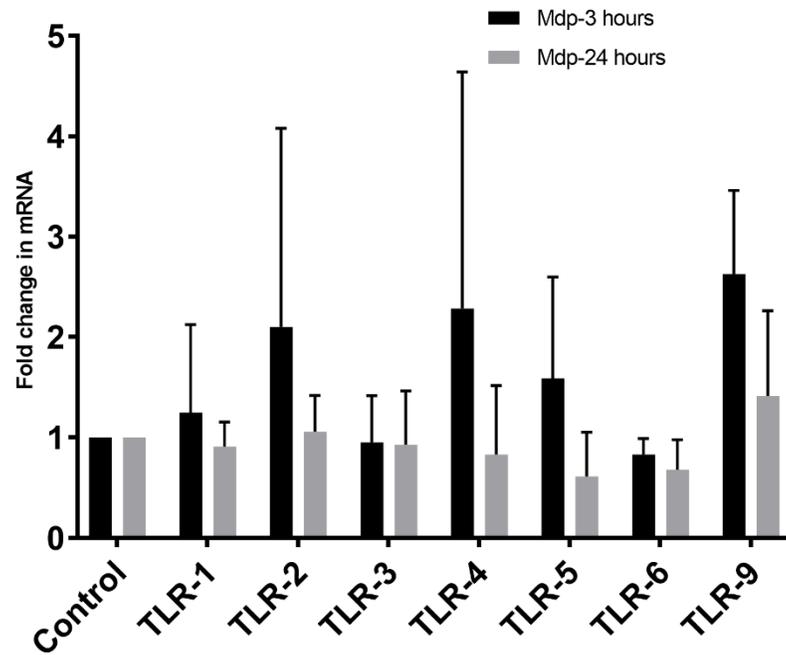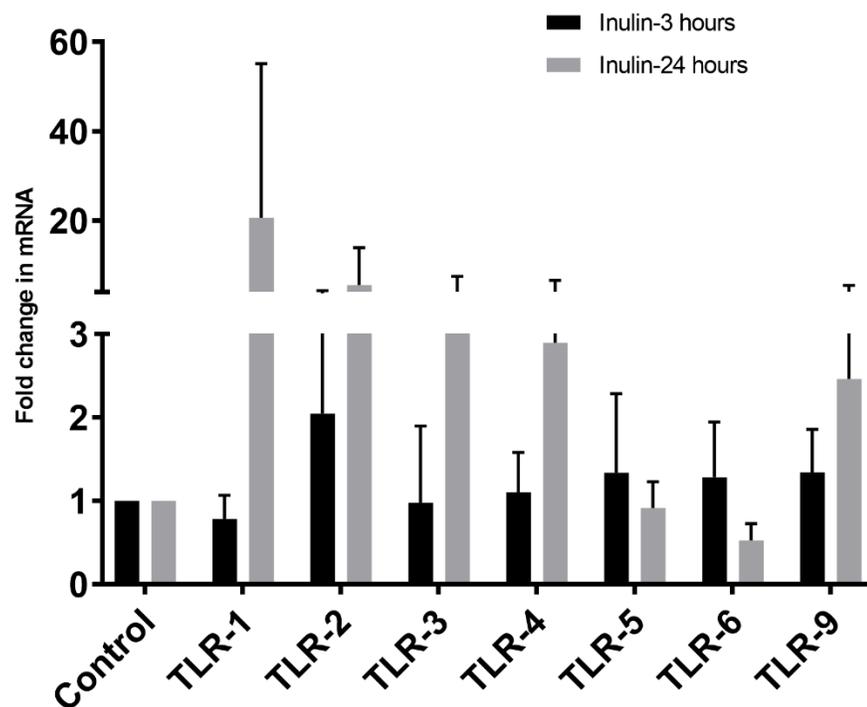
Figure 56: Various TLRs and their changes in gene expression based on Inulin acetate stimulation in PPTECs. Bar graphs are the mean of three independent experiments and error bars represent the standard error of the mean (SEM). Using the delta-delta Ct method, fold change was calculated. Significant changes are represented by an asterisk (*), $p < 0.05$.
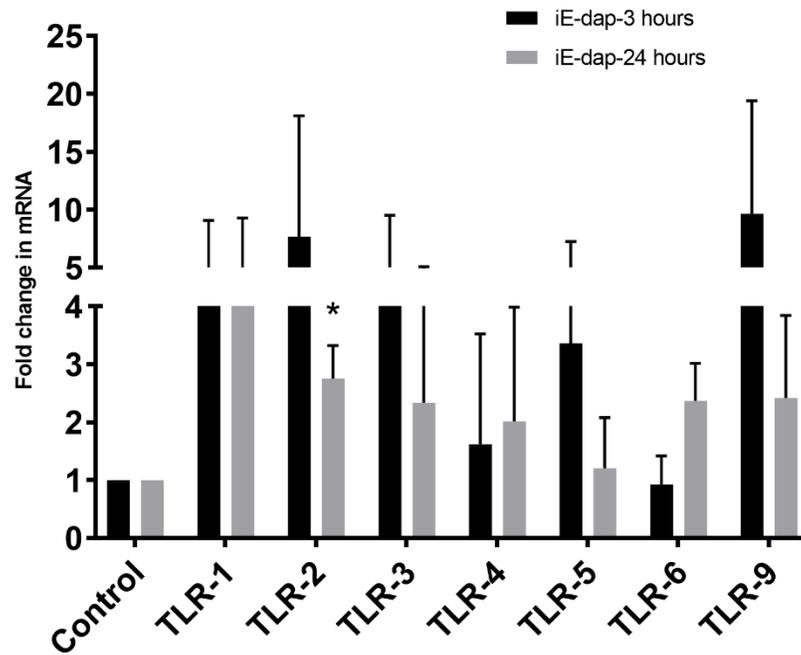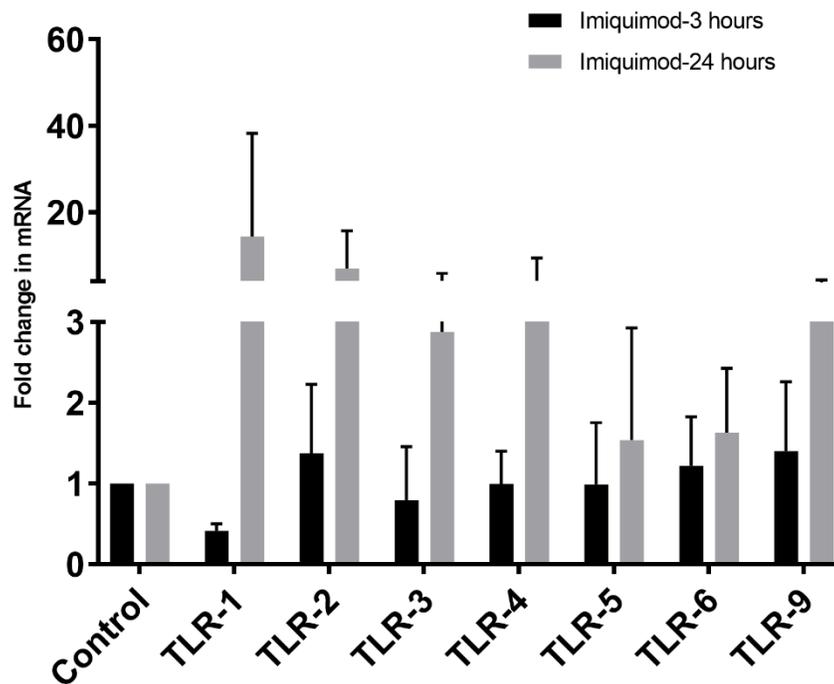
Figure 57: Various TLRs and their changes in gene expression based on imiquimod stimulation in PPTECs. Bar graphs are the mean of three independent experiments and error bars represent the standard error of the mean (SEM). Using the delta-delta Ct method, fold change was calculated. Significant changes are represented by an asterisk (*), $p<0.05$.
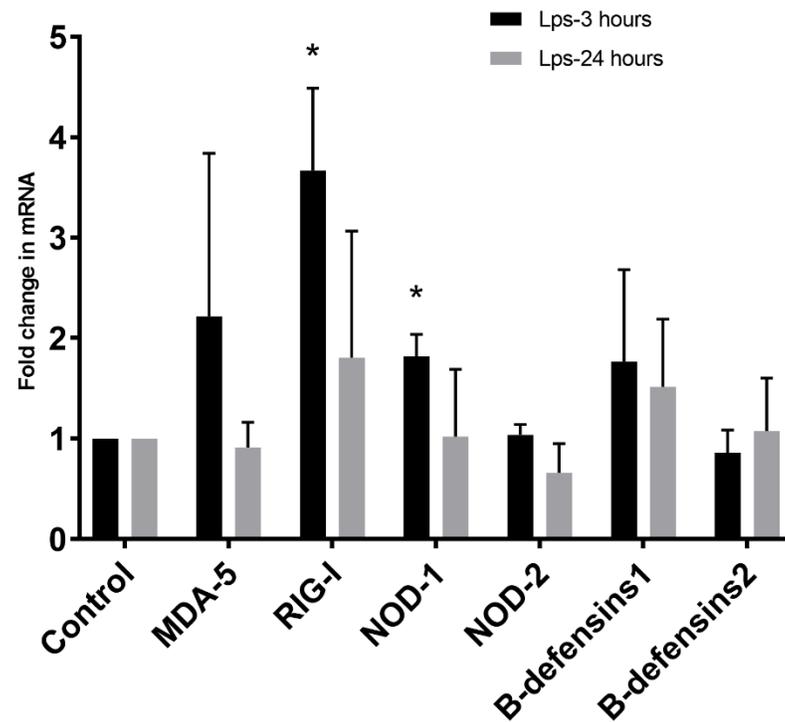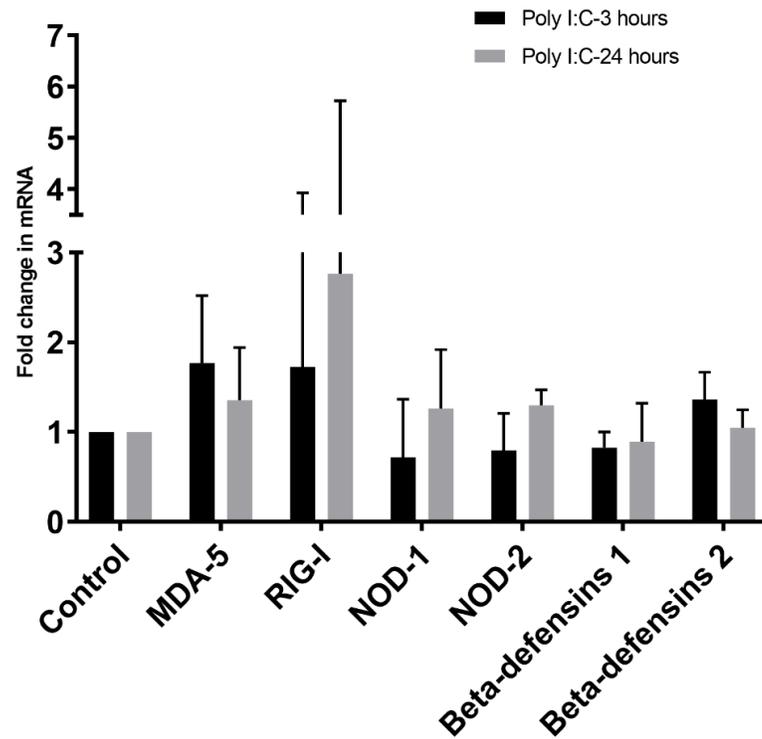
Figure 58: RLRs, NLRs, and other PRRs, and their changes in gene expression based on Poly I:C stimulation in PPTECs. Bar graphs are the mean of three independent experiments and error bars represent the standard error of mean (SEM). Using delta-delta Ct method, fold change was calculated. Significant changes are represented by an asterisk (*), $p < 0.05$.
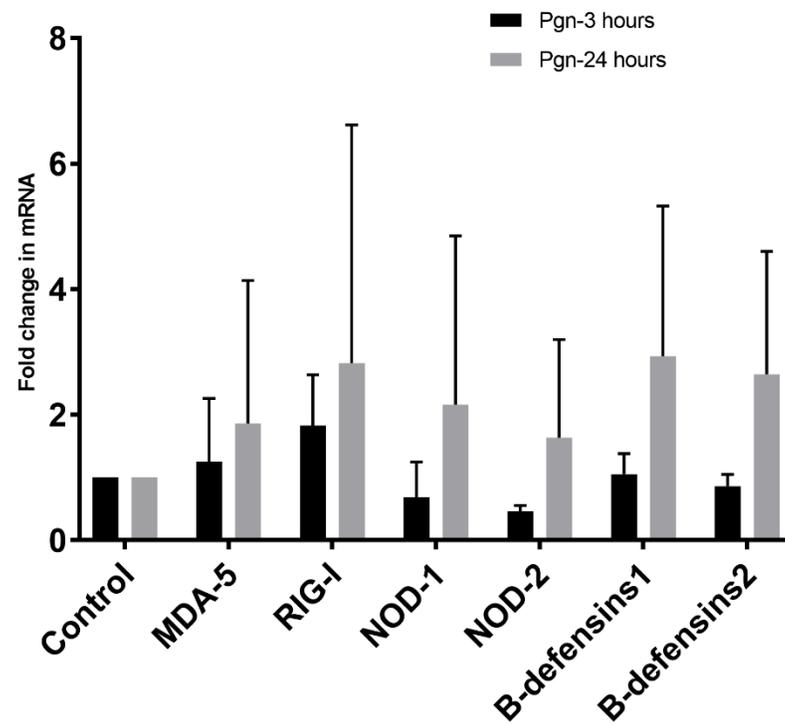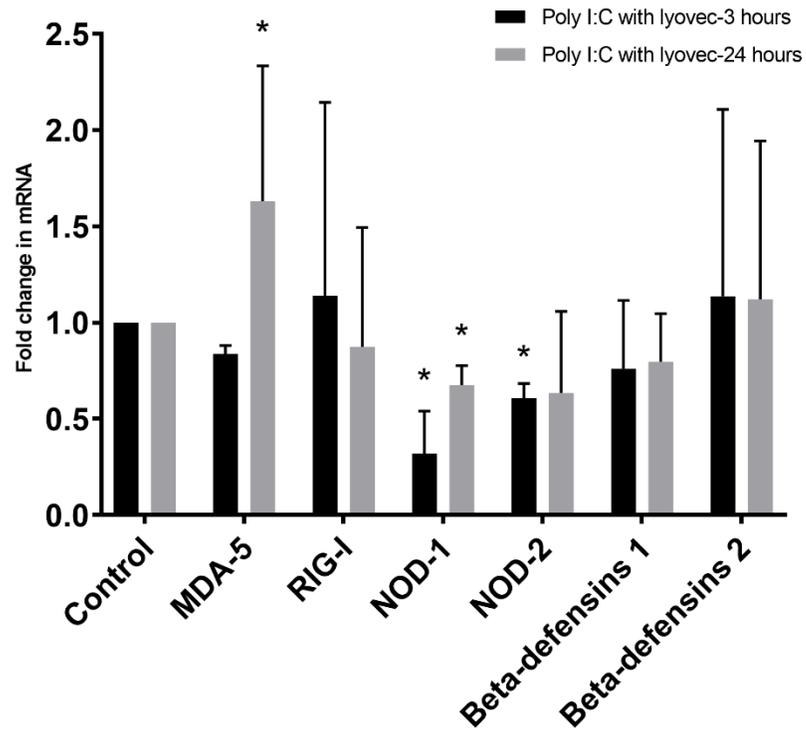
Figure 59: RLRs, NLRs, and other PRRs, and their changes in gene expression based on Poly I:C with lyovec stimulation in PPTECs. Bar graphs are the mean of three independent experiments and error bars represent the standard error of mean (SEM). Using delta-delta Ct method, fold change was calculated. Significant changes are represented by an asterisk (*), $p < 0.05$.
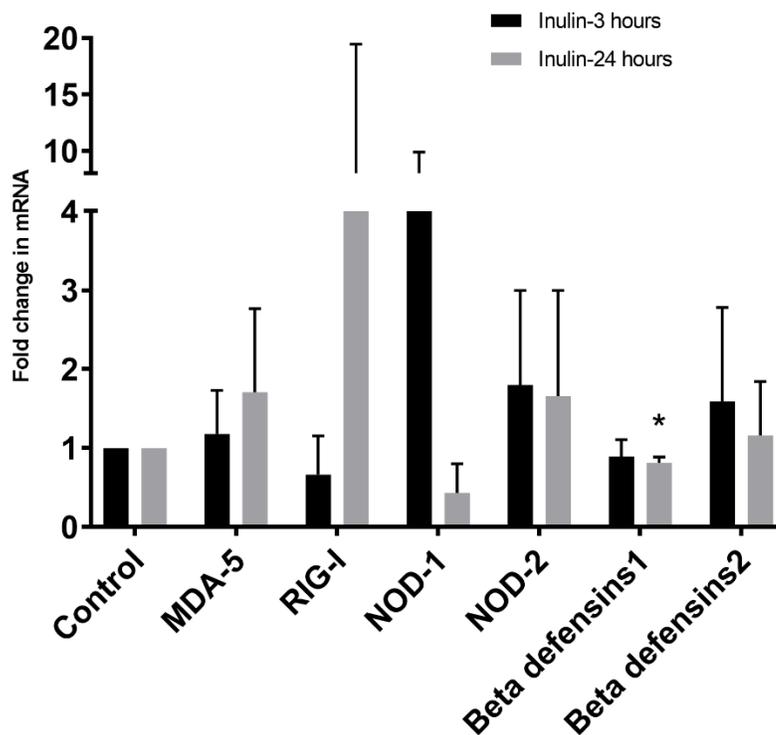
Figure 60: RLRs, NLRs, and other PRRs, and their changes in gene expression based on Inulin acetate nanoparticle stimulation in PPTECs. Bar graphs are the mean of three independent experiments and error bars represent the standard error of mean (SEM). Using delta-delta Ct method, fold change was calculated. Significant changes are represented by an asterisk (*), $p < 0.05$.
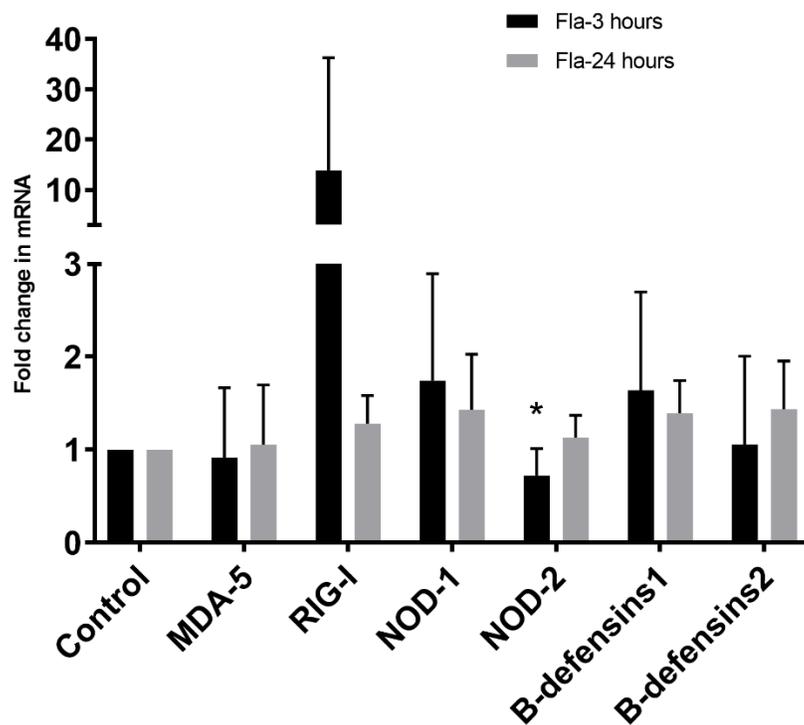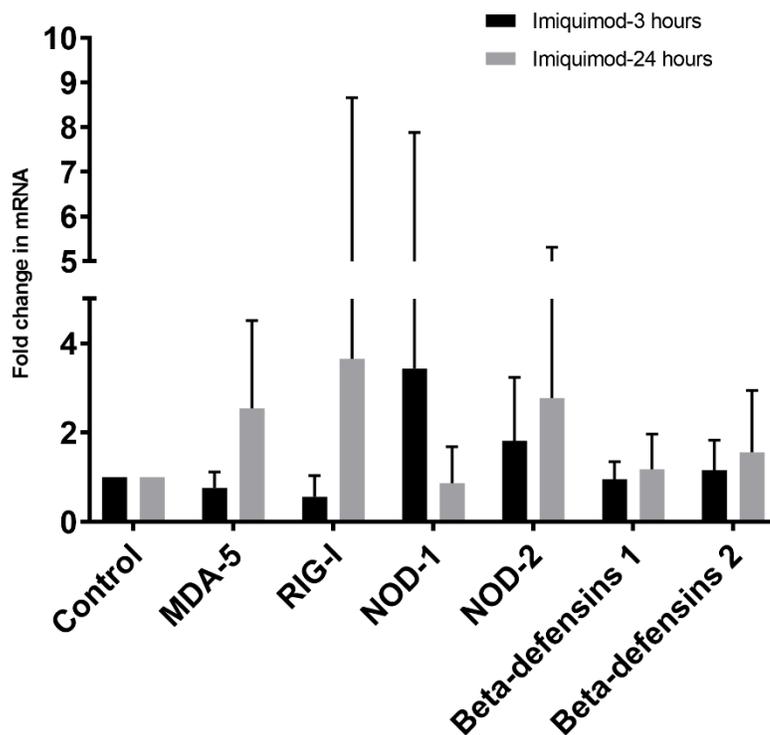
Figure 61: RLRs, NLRs, and other PRRs, and their changes in gene expression based on Imiquimod stimulation in PPTECs. Bar graphs are the mean of three independent experiments and error bars represent the standard error of mean (SEM). Using delta-delta Ct method, fold change was calculated. Significant changes are represented by an asterisk (*), $p < 0.05$.
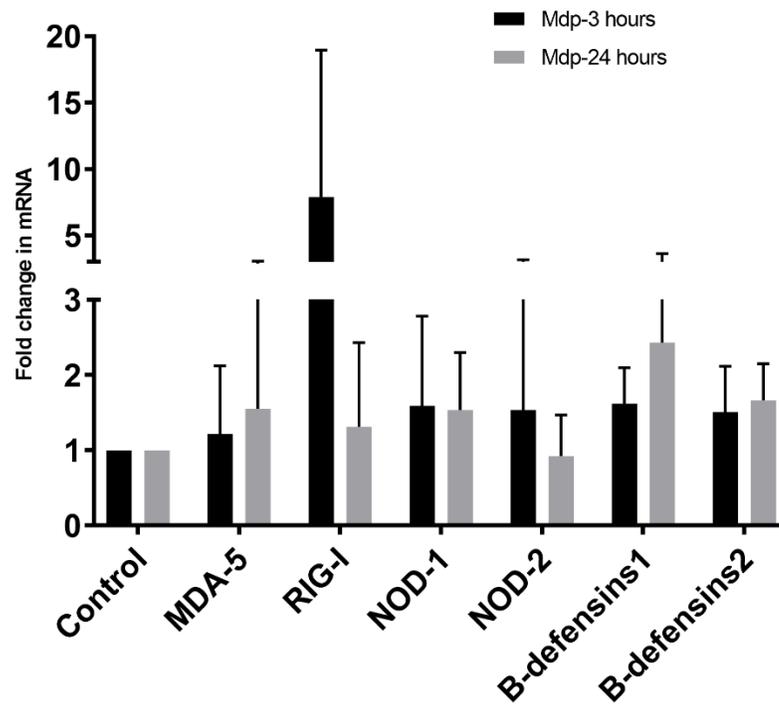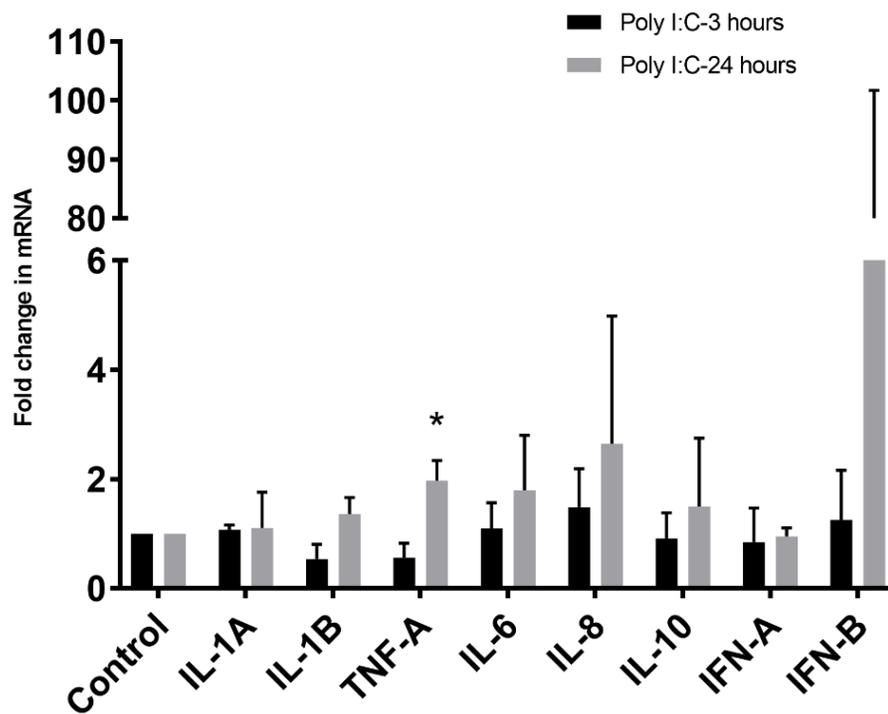
Figure 62: Cytokines/chemokines, and their changes in gene expression based on Poly I:C stimulation in PPTECs. Bar graphs are the mean of three independent experiments and error bars represent the standard error of the mean (SEM). Using the delta-delta Ct method, fold change was calculated. Significant changes are represented by an asterisk (*), p<0.05.
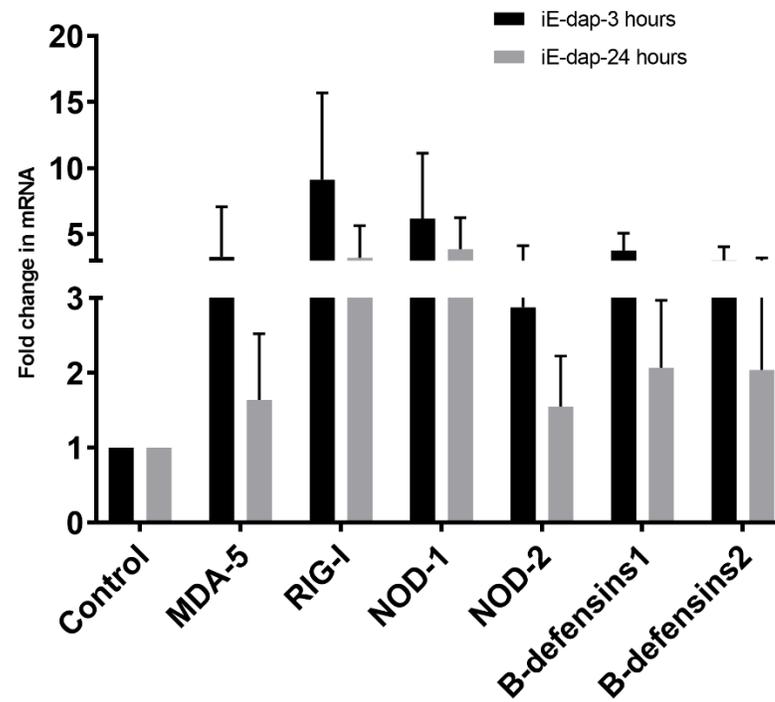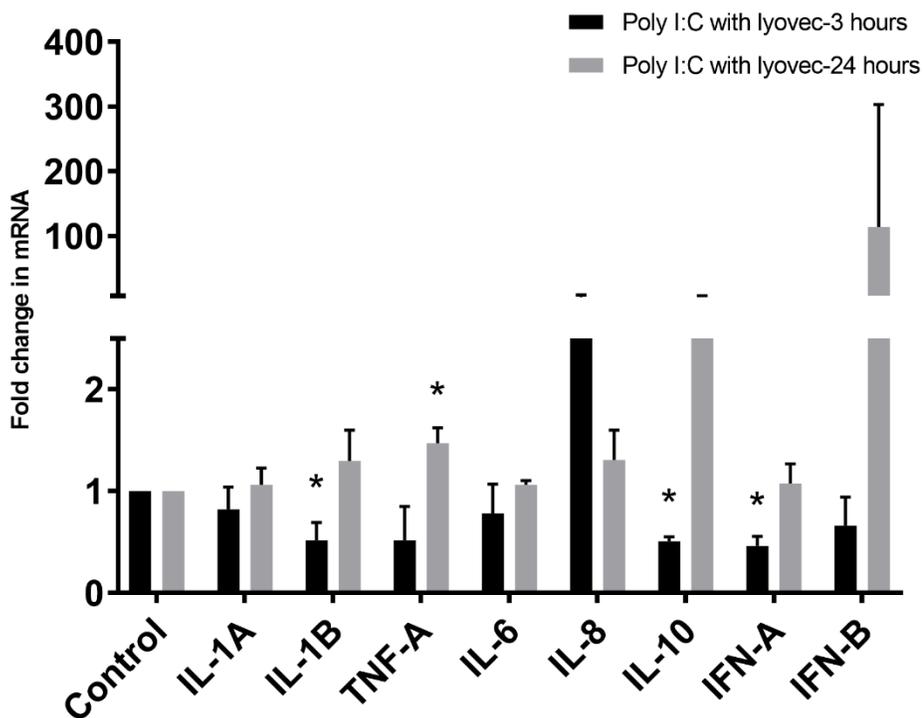
Figure 63: Cytokines/chemokines, and their changes in gene expression based on Poly I:C with lyovec stimulation in PPTECs. Bar graphs are the mean of three independent experiments and error bars represent the standard error of the mean (SEM). Using the delta-delta Ct method, fold change was calculated. Significant changes are represented by an asterisk (*), $p < 0.05$.
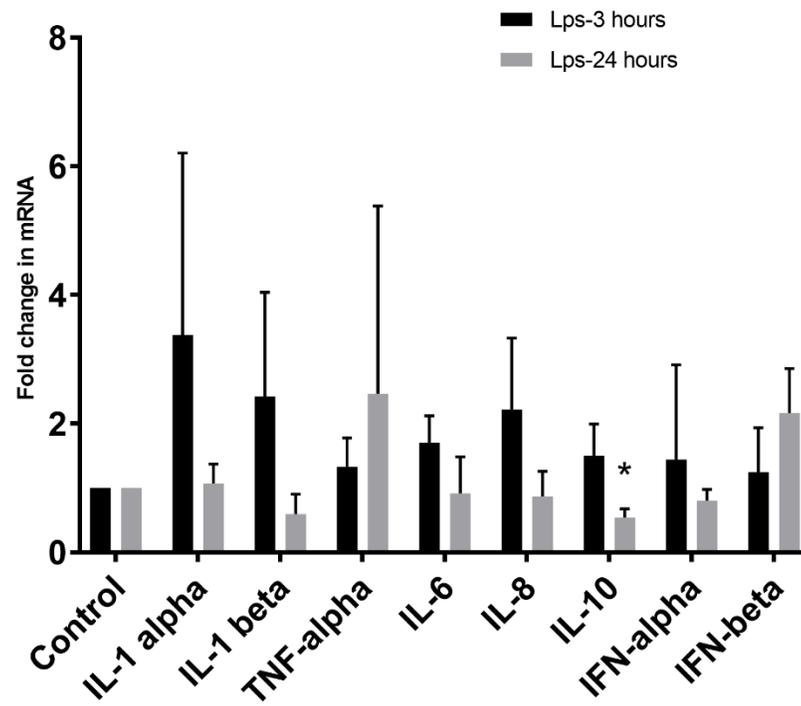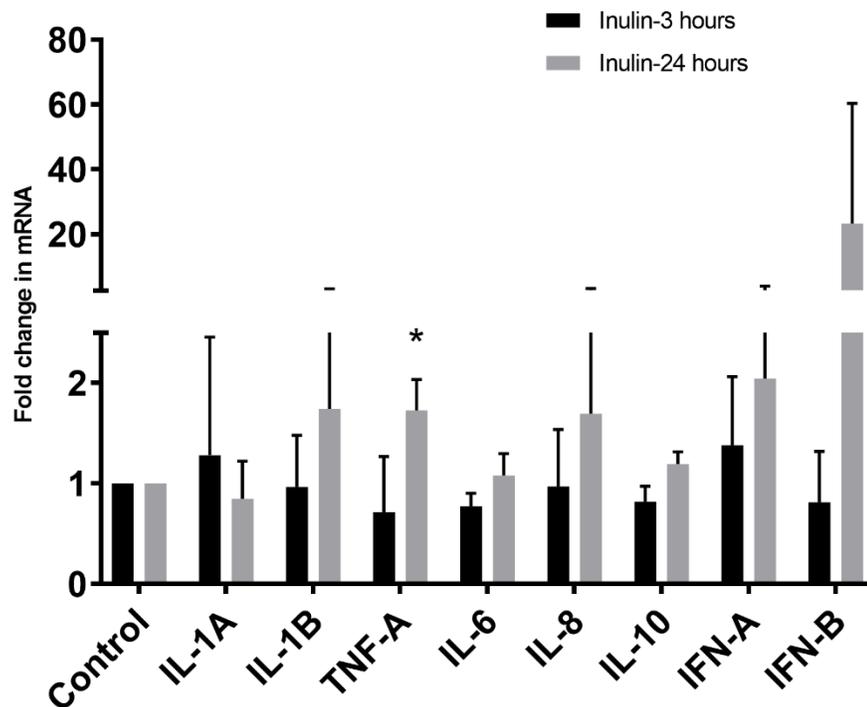
Figure 64: Cytokines/chemokines, and their changes in gene expression based on Inulin acetate nanoparticle stimulation in PPTECs. Bar graphs are the mean of three independent experiments and error bars represent the standard error of the mean (SEM). Using the delta-delta Ct method, fold change was calculated. Significant changes are represented by an asterisk (*), $p < 0.05$.
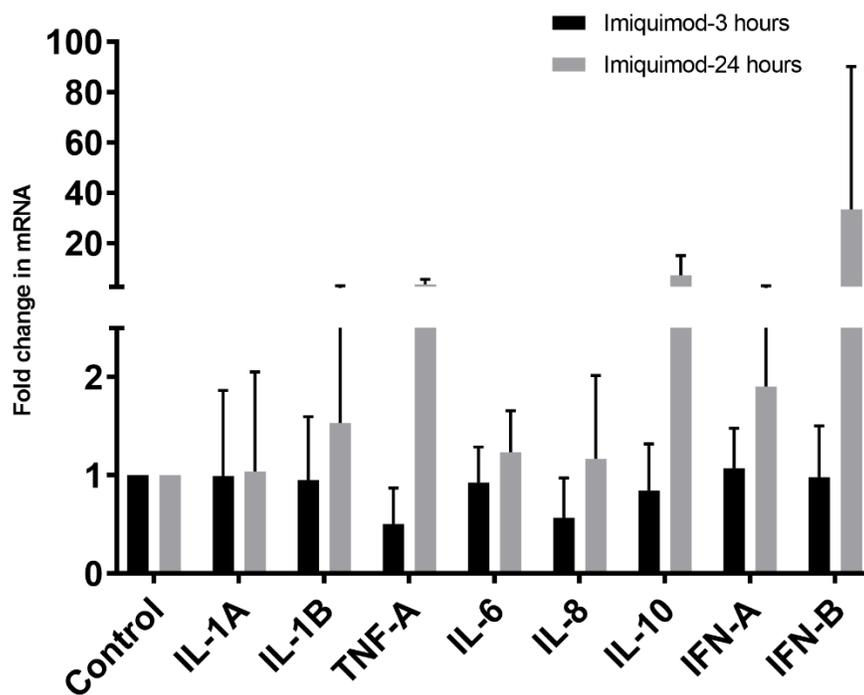
Figure 65: Cytokines/chemokines, and their changes in gene expression based on imiquimod stimulation in PPTECs. Bar graphs are the mean of three independent experiments and error bars represent the standard error of the mean (SEM). Using the delta-delta Ct method, fold change was calculated. Significant changes are represented by an asterisk (*), $p<0.05$.

3.5 Discussion

In this study, pig primary respiratory epithelial cells from the trachea (PPTECs) and nasal turbinate (PPNTECs) were stimulated with various bacterial and viral ligands to explore/identify whether these cells modulate the expression of various pathogen recognition receptors, cytokines and chemokines genes and if they do what roles these cells play in the innate immune responses associated with bacteria or viral pathogenic determinants. Primary cells from both trachea and nasal turbinate were stimulated with bacterial ligands LPS, PGN, FLA, MDP, and i.E.-DAP and, viral ligands Poly I:C, Poly I:C with lyovec, and imiquimod. In addition, inulin acetate nanoparticles, known to be agonist of TLR4, were also used to stimulate these cells.

RT-qPCR data analysis revealed that both PPTECs and PPNTECs express various TLRs, NLRS, RLRs, defensins, cytokines and chemokine genes constitutively. The very fact that these cells express various PRRs, cytokines and chemokines genes render them relevant and effective in studying respiratory disease pathogenesis and the innate immune system.

LPS, an outer surface membrane component of almost all gram-negative bacteria, has an immunostimulatory lipid A component that acts as a strong innate immunity stimulator. The extracellular involvement of LPS binding protein (LBP), CD14, and TLR4/MD-2 complex results in LPS recognition leading to the activation of MyD88 or TRIF pathways (130).

In the stimulation assay conducted with PPNTECs, LPS caused upregulation of TNF-A and MCP-1-proinflammatory cytokines/chemokines, at 3 hours' time point. Previous studies have shown that TNF- alpha and MCP-1 production is triggered or upregulated upon LPS stimulation (131, 132). Apart from B-defensin 2 and TLR-1 upregulation after

3 and 24 hours of stimulation respectively, LPS did not induce any changes in the gene expression of other TLRs including TLR-4. To our knowledge, this is the first ligand stimulation assay conducted on pig respiratory epithelial cells, but our findings are consistent with studies conducted on IPEC-J2 cell lines (132, 133). IL-10 is an anti-inflammatory and immunosuppressive cytokine and is highly regulated at the transcription level. LPS stimulation of PPNTECs caused the significant upregulation of IL-10 gene expression. Consistent with this, in another study, LPS is known to cause the increased IL-10 gene expression (134). Activation of MyD88 or TRIF signaling pathway after LPS-TLR4/MD-2 binding causes the production of proinflammatory cytokines. To contain the inflammation, anti-inflammatory cytokines are released into the system, and this creates a balance between pro-inflammatory and anti-inflammatory cytokines (85). An imbalance between pro-inflammatory and anti-inflammatory cytokines is attributed to bipolar disorder (135).

In the stimulation assay conducted with PPTECs, LPS caused significant upregulation of RIG-I and NOD-1 genes. NOD-1 upregulation might be because LPS is a PAMP or a danger signal, and NOD-1 serves to identify the presence of danger signals to restore homeostasis. Encounter with a danger signal results in the activation of NOD-1 signaling cascades (136). Unlike in PPNTECs, LPS caused significant downregulation of IL-10 in PPTECs after 3 hours of stimulation. A possible explanation might be that IL-10 expression is highly regulated and only proceeds when there are hyper levels of pro-inflammatory cytokines. However, in this study based on gene expression levels, none of the pro-inflammatory cytokines were significantly upregulated upon LPS stimulation in PPTECs. Most of the gene expression patterns in response to LPS were similar between PPNTECs

and PPTECs except for a few differences. The differences might be a result of their different anatomical location, physiological properties, and variation in the receptors they express.

PGN is a major cell wall component derived from a Gram-positive bacterium. PGN is known to activate TLR-2 and NOD-2. While TLR-2 binds to PGN, NOD-2 binds to MDP, a PGN breakdown component thus can also detect PGN (137). Even though both TLR-2 and NOD-2 sense PGN, no or very few significant changes in mRNA gene expression for various PRRs were observed upon PGN stimulation. Having said that, in PPTECs, after 24 hours of PGN stimulation, both TLR-2 and NOD-2 gene expression levels were upregulated. Even in PPNTECs, 24 hours of PGN stimulation yielded higher expression of NOD-2 compared to 3 hours. The insignificant but increased expression after 24 hours of stimulation may be a result of the insufficient PGN dose used or inadequate time for PGN to produce significant effects. A higher dose and a longer stimulation time may produce better results. Another possible reason could be the use of the purified version of PGN in our study as it has been observed that the purification process renders PGN to become less effective (137).

MCP-1 is a chemokine involved in the migration of monocytes and lymphocytes in case of an injury or an infection and helps in promoting inflammation. It also regulates monocyte differentiation into dendritic cells (138). In this study, the PGN significantly downregulated MCP-1 expression after 3 hours of stimulation in PPNTECs. In a study conducted on microglial cells of mice, PGN successfully downregulated the expression of MCP-1 along with TLR-2 and TNF-alpha expression upregulated by LPS challenge (139).

While this study was conducted on already induced microglial cells, the fact that PGN downregulated MCP-1 expression is consistent with our observation. PGN produced little to no effect on other cytokines and chemokines genes.

FLA is a structural component of bacterial flagella that binds to TLR-5 and activates NF-kB signaling which results in the generation of innate immune responses through proinflammatory gene expression against flagellated bacterium (140, 141). FLA stimulation of PPNTECs resulted in increased expression of IL-1b. As stated above, IL-1b is a proinflammatory cytokine and FLA/TLR5 downstream signaling induces increased expression of proinflammatory cytokines. PPNTECs constitutively expressed TLR-5 but FLA did not upregulate TLR-5 gene expression. It suggests that the high levels of IL-1b are a result of FLA/TLR-5 binding and activation of downstream signaling.

In PPNTECs, FLA caused significant upregulation of TLR-2 after 3 hours of stimulation. Previous studies have shown that gastric epithelial cells make use of TLR-2 and TLR-5 to respond against *Helicobacter pylori*, a Gram-negative, flagellated bacterial infection (142). Even though the cells used in this study are from the respiratory tract of pigs, the correlation between TLR-2 and flagellated bacterial infection might be a factor behind elevated levels of TLR-2 gene expression upon FLA stimulation. On the contrary, a study conducted on human airway epithelial cells infection via flagellin of *Pseudomonas aeruginosa* demonstrated that TLR-2 dependent immune responses are flagellin independent. Another study conducted with *Haemophilus influenzae*, a flagellum-free bacteria, demonstrated that lack of flagella did not induce TLR-5 but significantly stimulated TLR-2 citing TLR-5, not TLR-2, as a receptor for flagellin (143).

In PPTECs, FLA induced significant NOD-2 downregulation after 3 hours of stimulation. There's no direct link between FLA stimulation and NOD-2 downregulation. NODs are cytosolic receptors important in recognizing intracellular ligands. NODs are shown to be involved in binding with flagellin and activation of the NF-kB pathway (144, 145). RIG-I levels were spiked upon 3 hours of FLA stimulation, but the upregulation was statistically insignificant. RIG-I is a cytoplasmic viral recognition molecule that activates Type I IFN responses.

MDP is a bacterial cell wall component that is recognized by NOD-2, and this binding activates the NF-kB pathway to produce pro-inflammatory cytokines (146). MDP stimulation of PPNTECs and PPTECs did not modulate PRRs, cytokines and chemokines genes except the downregulation of IFN-b gene expression after 24 hours in PPNTECs. A study conducted on the rat cardiac fibroblast showed that IFN-b can act as both pro-inflammatory and anti-inflammatory cytokine (147). Overall, MDP's inability to modulate PPRs, cytokines and chemokines genes in respiratory epithelial cells may be related to dose of MDP used for stimulation or nature and physiology of these cells.

iE-DAP is derived from bacterial peptidoglycan and acts as a ligand for the NOD-1 receptor. Upon receptor binding, the NF-kB pathway is activated and leads to the induction of the inflammatory responses characterized by elevated levels of IL-6 and MCP-1 (148, 149). iE-DAP stimulation of PPNTECs induced significant upregulation of IL-6 after 3 hours. Our findings are consistent with the findings of a study conducted in human alveolar epithelial cells where they found that iE-DAP treatment of alveolar epithelial cells increased the expression levels of IL-6 (150). However, after 24 hours of stimulation, expression levels of IL-6 decreased significantly. Consistent with IL-6, IL-8 and IL-1a

gene expression also produced similar results. Both IL-8 and IL-1a gene expression were upregulated after 3 hours of stimulation and downregulated after 24 hours of stimulation, but the changes were statistically insignificant. IL-6, IL-8, and IL-1a, are proinflammatory cytokines and it is no surprise to see a similar trend in their gene expression pattern upon iE-DAP stimulation because iE-DAP causes inflammatory responses through elevated pro-inflammatory cytokine production via the NF-kB pathway (148, 151). iE-DAP stimulation of PPTECs produced similar IL-6 gene expression changes as observed in PPNTECs. The similarity in gene expression patterns between PPNTECs and PPTECs can be attributed to the similar physiological properties, anatomical proximity, and similar receptor expression.

Poly I:C is a double-stranded viral RNA analog and mimics the dsRNA viral genome. Poly I:C is detected mainly by TLR-3, and by MDA-5, an RLRs family receptor in a cell-specific manner. Poly I:C/MDA5 association activates NF-kB pathway through RLR-dependent signaling pathway and IFN-promoter-stimulator-1 (IPS-1). Similarly, TLR-3 activates the NF-kB pathway through Toll/IL-1R domain-containing adaptor inducing IFN (TRIF). Both pathways lead to the activation of Natural Killer (NK) cells (152-154). We stimulated both PPNTECs and PPTECs with Poly I:C for 3 hours and 24 hours respectively.

After 3 hours of Poly I:C stimulation, TLR-6 gene expression was upregulated significantly. TLR-6 is known to recognize lipids and is located on the cell surface (155). Upregulation of TLR-6 upon RNA analog stimulation is hard to explain without further study. However, none of the other PRRs showed significant changes upon stimulation. mRNA levels of IFN-B were high on both 3 hours and 24 hours' time points in both cell types, but the changes were insignificant. Though statistically insignificant, upregulated IFN-B gene expression can be attributed to the innate immune responses by these cells.

IFN-B is produced as a defense mechanism to fight against viral infections. IFNs interfere with various viral replication stages to halt the replication and stop the viral infection from growing (156). Like PPNTECs, Poly I:C stimulation caused a huge spike in mRNA levels of IFN-B after 24 hours in PPTECs, but the change was insignificant.

Poly I:C stimulation of PPTECs had an upregulating effect on TNF-a as TNF-a mRNA levels were upregulated after 24 hours of stimulation. Association of Poly I:C and TNF-a have been demonstrated by previous studies. A study conducted in glial cells demonstrated that Poly I:C stimulated activation of glial cells promoted TNF-a production (157). TNF-a is one of the cytokines produced as an innate immune defense mechanism during an infection or invasion.

Poly I:C with lyovec is a complex of Poly I:C and transfection reagent lyovec. Complexing Poly I:C with lyovec is believed to effectively deliver Poly I:C into the cytoplasm. Unlike naked Poly I:C which is mainly recognized by TLR-3, transfected Poly I:C is mainly recognized by RIG-I and MDA-5, and activation of NF-kB proceed through the RIG-I/MDA-5 pathway (158). This pathway leads to the production of Type I IFNs against viral infection. Use of Poly I:C complexed with lyovec has been common and used in multiple studies like for the stimulation of human lung adenocarcinoma cells (159), human nasal epithelial cells (160), chicken embryo kidney cells (161). In our lab, previous studies conducted on bovine and ovine ileal myofibroblast cells (data not published) used Poly I:C with lyovec for the stimulation assay. In this study, we used Poly I:C with lyovec to stimulate both PPNTECs and PPTECs.

In PPTECs, Poly I:C with lyovec stimulation caused significant downregulation of TLR-4 and TLR-5 after 3 hours. Both NOD-1 and NOD-2 gene expression levels were also

downregulated significantly after 3 hours of stimulation by Poly I:C-lyovec complex. Poly I:C with lyovec stimulation ends up with robust antiviral immune response generation mediated by the production of Type I IFNs. For TLR-4 and TLR-5, LPS and FLA are the ligands respectively. For NOD-1 and NOD-2, iE-DAP and MDP are the ligands respectively. All four ligands are bacterial pathogenic determinants. Because these four receptors namely TLR-4, TLR-5, NOD1, and NOD-2 are involved in or responsible for the induction of immune response against bacterial attack, their downregulation upon Poly I:C with lyovec stimulation is although hard to explain but may signal downregulated responses to bacterial infections upon viral infections. After 24 hours of stimulation, NOD-1 expression was downregulated significantly. Since upregulated NOD-1 is responsible for activation of NF-kB pathway and production of pro-inflammatory cytokines (148, 149), this downregulation after 24 hours of stimulation might be important in anti-inflammatory responses against pathogens including viruses because NLRs have been identified to either positively or negatively modulate the inflammatory responses. A study has found NOD-1 to be involved in augmenting inflammatory responses. In contrast to our findings, according to a study, NOD-1 had been found to form a multicomplex protein NODosome upon their activation and this protein complex then activates IFN and NF-kB pathways to provide immune responses following a viral infection (162).

As expected, after 24 hours of Poly I:C with lyovec stimulation of PPTECs, MDA-5, which is one of the receptors for lyovec complexed Poly I:C, upregulated significantly. Consistent with our findings, previous studies have shown the induction of MDA-5 gene expression after Poly I:C with lyovec stimulation. A study conducted on human nasal epithelial cells demonstrated the recognition of RLRs (RIG-I and MDA-5) by Poly I:C complexed with

lyovec followed by IFN-b secretion in nasal mucosa (160). Another study conducted on mice showed that Poly I:C is responsible for the activation of mice's NK cells through MDA-5 binding and downstream signaling through IPS- 1 (163). Poly I:C lyovec stimulation for 24 hours produced TNF-a mRNA upregulation on PPTECs. Consistent with our finding, a study conducted on human bronchial epithelial cells showed a dose-dependent increased production of inflammatory cytokines including TNF-a after Poly I:C activation (164). Similarly, a study conducted on microglial cells has also shown similar effects (157).

Furthermore, in PPTECs, Poly I:C with lyovec induced significant downregulation of IL-1b, IFN-a, and IL-10 after 3 hours of stimulation. However, IFN-a and IL-1b levels were increased by more than 2 folds after 24 hours, even though statistically insignificant. Both IL-1b and IFN-a are correlated to inflammation following viral infection (165, 166). Their initial downregulation and rapid upregulation after 24 hours of stimulation might suggest that either they need longer stimulation for their activation or the doses of Poly I:C with lyovec we used were inadequate and took time before these genes were activated. IL-10 is an anti-inflammatory cytokine (167), just opposite of inflammatory cytokines IL-1b and IFN-α. In a previous study conducted in our lab on ovine intestinal sub-epithelial myofibroblasts (ISEMFs), IFN-b expression was increased by at least 150-fold after 24 hours of stimulation (unpublished data). Consistent with the previous study, IFN-b expression rose by at least 100 folds in this study after 24 hours of stimulation, though the change was statistically insignificant. The rapid increase in mRNA levels of IFN-b can be attributed to the generation of a strong anti-viral immune response triggered by Poly I:C with lyovec stimulation of PPTECs. Surprisingly, no significant changes were observed on

PPNTECs following Poly I:C with lyovec stimulation at both time points. Even though PPNTECs and PNTECs share few similarities, we also need to account at what stages the cells were in during the stimulation assay, their age/passage number, and culture conditions. These factors along with their innate differences may account for the observed differences.

Imiquimod is a nucleoside analogue belonging to the imidazoquinoline family. Imiquimod is sensed by TLR-7 and TLR-8. Recognition of Imiquimod by TLR-7/8 induces activation of the TLR signaling pathway leading to the activation and nuclear translocation of NF-kB and production of pro-inflammatory cytokines. The transcribed cytokines activate APCs and play role in generating the immune response against tumors through T-helper (Th1) cells (168). However, Imiquimod has been found to work independently of TLR-7/8. In the adenosine receptor signaling pathway, imiquimod can cause a reduction of adenylyl cyclase activity independent of TLR-7/8 (169). Moreover, imiquimod, because of its ability to induce both the innate and adaptive immune response, is seen as a potent vaccine adjuvant to increase the efficiency of DC-based tumor immunotherapy (170).

Imiquimod stimulation of PPNTECs produced no significant changes on all PRRs tested. However, even though the change was statistically insignificant, we saw at least a 5-fold increase in TLR-7 expression only after 3 hours of imiquimod stimulation. Few other TLRs also showed a similar effect after 3 hours of treatment. We did not test for TLR-7 expression on PPTECs. On PPNTECs, pro-inflammatory cytokines like IFN-a, TNF-a, IL-6, and IFN-b and their expression were rapidly upregulated after 3 hours of imiquimod treatment, but the changes were statistically insignificant. Even though insignificant, Imiquimod is known to cause the upregulated expression of pro-inflammatory cytokines

(169). Stimulation of PPTECs produced similar, statistically insignificant, upregulation of pro-inflammatory cytokines but after 24 hours of imiquimod stimulation.

Inulin acetate nanoparticle (InAc) is a polymer designed for use as a vaccine adjuvant in a pathogen-mimicking vaccine delivery system (PMDVS) to significantly stimulate the innate immune system against various diseases. InAc was developed from a plant polysaccharide called inulin (120). InAc is believed to be an agonist of TLR-4. A study conducted in mice demonstrated that the use of PMDVS with inulin as the delivery system caused induction of both the cell-mediated and humoral immune response (171). TLR-4 agonistic property of InAc has been verified in a study conducted with cells like microglial, dendritic, blood mononuclear, and HEK293 where InAc was able to stimulate the cells followed by the production of cytokines (172).

In this study, we used InAc to stimulate both PPNTECs and PPTECs at 3 hours and 24 hours' time points at a concentration of 250 microgram/ml. In PPTECs, InAc stimulation for 3 hours did not induce any significant changes in gene regulation of the PRRs tested. Upon 24 hours of stimulation, TLR-4 did upregulate by around 2 folds, but the change was statistically insignificant. Since InAc is known as a TLR-4 agonist and has been seen causing induction of TLR-4 mediated signaling (171), the observed upregulation might be a result of InAc stimulation. In PPTECs, InAc did cause significant downregulation of beta defensins-1 after 24 hours, but it caused statistically significant upregulation of TNF-a. Since InAc works through the TLR-4 signaling pathway, the production of TNF-a might be a result of TLR-4 signaling pathway activation followed by NF-kB activation, and the production of cytokines like TNF-a. Association between TLR-4 activation and TNF-a gene expression has been demonstrated in previous studies (173, 174).

Surprisingly, InAc stimulation of PPNTECs resulted in the downregulation of various TLRs, NLRS, RLRs, and different cytokines/chemokines after 24 hours. PRRs like TLR-1, TLR-2, TLR-3, NOD-2, RIG-I, beta defensins-2, and MDA-5 were significantly downregulated after 24 hours of InAc stimulation. Similarly, cytokines like IL-10 and IFN-a were also downregulated significantly. Such downregulation of PRRs from different categories could be a result of insufficient dose. Further studies with a higher dose of InAc is highly recommended and might produce different results.

4   Conclusions and Future Directions

In this study, the established and characterized PPNTECs and PPTECs were used to explore their roles in the induction of immune responses upon stimulation by the bacterial or viral ligands. From the broader perspective, the main goal was to get an insight into how these cells might react during a pathogenic infection or invasion, and how they modulate the innate immune response during a disease progression or pathogenesis. Contrary to the plethora of research on pig intestinal mucosal cells, only a handful of published research studies have been conducted on pig respiratory mucosal cells, even though respiratory mucosal cells play an indispensable role in the respiratory immune system and respiratory disease pathogenesis. To our knowledge, this is the first study conducted on pig respiratory epithelial cells from the trachea and nasal turbinate of a day-old piglet. Because there's not much information about how these cells impact the innate immune system, our study will provide a better understanding of the involvement of respiratory epithelial cells in the respiratory immune system and the maintenance of homeostasis in case of a respiratory infection or invasion.

In this study, pig respiratory epithelial cells obtained from the trachea and nasal turbinate of a day-old piglet had some fibroblast contamination. A pure culture of pig respiratory epithelial cells was established by removing fibroblast contamination using the trypsin treatment method by exploiting their adherence properties. The established pure epithelial cultures of both PPNTECs and PPTECs, are verified by IHC (cytokeratin expression >90%) and were immortalized using hTERT and SV-40 large T-antigen. The epithelial nature of the cells was examined after the immortalization as well, and there were no significant changes in their phenotypic and biochemical properties. Unlike primary cells,

immortalized cells grew much faster as indicated by their shorter mean doubling time. Immortalized cells lines were established successfully as verified by a positive gel image and an immunofluorescence test for SV40 protein expression for SV40 immortalized cells and ICC for hTERT cells immortalized with hTERT gene. Along with the primary cells, these immortalized cells can serve as a good model for use in future studies on pig respiratory immune system and respiratory disease pathogenesis.

The established PPNTECs and PPTECs were stimulated with various bacterial and viral ligands to understand their role in modulating the innate immune responses in the respiratory immune system. Cells were tested for expression/modulation of PRRs like TLRs, RLRs, NLRs, defensins along with genes encoding for various chemokines/cytokines at two different time points of 3 hours and 24 hours. After RNA isolation, cDNA synthesis, and RT-qPCR, CT values were analyzed for changes in gene expression of various PRRs, cytokines and chemokines genes. Based on data obtained from RT-qPCR, both cell lines were found to express various PRRs, cytokine and chemokine genes. Different PRRs gene and their expression were modulated by the bacterial and viral ligands by either upregulating the gene expression or downregulating it. Not only the PRRs but the expression of various cytokine/chemokine genes were also modulated after the stimulation with different bacterial and viral ligands. This is an important finding and will immensely help future studies on these cells and their role in the respiratory immune system, and the respiratory disease pathogenesis. Knowing how the cells behave or react upon stimulation with different pathogenic determinants will certainly help and bolster future research on these cells to a greater extent. The immortalized PPNTECs and PPTECs could serve as a continuous cell culture model for the study of respiratory diseases and

disease pathogenesis. Immortalization wipes out the cell senescence issues and provides security against the unexpected hindrance of the research work because of the aging of the primary cells.

Our study was mostly descriptive, and we did not explore the mechanistic details of our findings especially for the ligand stimulation assay. Our stimulation assay findings are based on the assumption that any observed changes in the gene expression are directly caused by the stimulating agents we added without accounting for other possible reasons for observed changes like culture environment, cellular stages, or any external stress. Further studies with a focus on mechanistic details are recommended to fully validate our findings at the molecular level.

5   References

1.   Kraehenbuhl JP, Pringault E, Neutra M. Intestinal epithelia and barrier functions. Alimentary pharmacology & therapeutics. 1997;11:3-9.

2.   Branca JJV, Gulisano M, Nicoletti C. Intestinal epithelial barrier functions in ageing. Ageing Research Reviews. 2019;54:100938.

3.   Chase C, Kaushik RS. Mucosal Immune System of Cattle: All Immune Responses Begin Here. Veterinary Clinics: Food Animal Practice. 2019;35(3):431-51.

4.   Ganesan S, Comstock AT, Sajjan US. Barrier function of airway tract epithelium. Tissue barriers. 2013;1(4):e24997.

5.   Cario E. Innate immune signalling at intestinal mucosal surfaces: a fine line between host protection and destruction. Current Opinion in Gastroenterology. 2008;24(6):725-32.

6.   Thaiss CA, Zmora N, Levy M, Elinav E. The microbiome and innate immunity. Nature. 2016;535(7610):65-74.

7.   Davis CP. Normal flora. Medical Microbiology 4th edition. 1996.

8.   McFarland LV. Normal flora: diversity and functions. Microbial ecology in health and disease. 2000;12(4):193-207.

9.   Rakoff-Nahoum S, Paglino J, Eslami-Varzaneh F, Edberg S, Medzhitov R. Recognition of commensal microflora by toll-like receptors is required for intestinal homeostasis. Cell. 2004;118(2):229-41.

10.   J Philpott D, E Girardin S, J Sansonetti P. Innate immune responses of epithelial cells following infection with bacterial pathogens. Current Opinion in Immunology. 2001;13(4):410-6.

11. Cario E, Podolsky DK. Intestinal epithelial Tollerance versus inTollerance of commensals. Molecular Immunology. 2005;42(8):887-93.

12. Medzhitov R, Janeway Jr C. Innate immune recognition: mechanisms and pathways. Immunological reviews. 2000;173:89-97.

13. Cooper MD, Alder MN. The evolution of adaptive immune systems. Cell. 2006;124(4):815-22.

14. Barton GM, Medzhitov R. Control of adaptive immune responses by Toll-like receptors. Current opinion in immunology. 2002;14(3):380-3.

15. Kumagai Y, Akira S. Identification and functions of pattern-recognition receptors. Journal of Allergy and Clinical Immunology. 2010;125(5):985-92.

16. Kawai T, Akira S. Antiviral signaling through pattern recognition receptors. The Journal of Biochemistry. 2007;141(2):137-45.

17. Zipfel C. Plant pattern-recognition receptors. Trends in immunology. 2014;35(7):345-51.

18. Li D, Wu M. Pattern recognition receptors in health and diseases. Signal transduction and targeted therapy. 2021;6(1):1-24.

19. Akira S, Uematsu S, Takeuchi O. Pathogen Recognition and Innate Immunity. Cell. 2006;124(4):783-801.

20. O'Neill LAJ, Golenbock D, Bowie AG. The history of Toll-like receptors — redefining innate immunity. Nature Reviews Immunology. 2013;13(6):453-60.

21. Takeda K, Kaisho T, Akira S. Toll-Like Receptors. Annual Review of Immunology. 2003;21(1):335-76.

22. Chuang T-H, Ulevitch RJ. Cloning and characterization of a sub-family of human

toll-like receptors: hTLR7, hTLR8 and hTLR9. European cytokine network. 2000;11(3):372-8.

23. Armant MA, Fenton MJ. Toll-like receptors: a family of pattern-recognition receptors in mammals. Genome Biology. 2002;3(8):reviews3011.1.

24. Takeuchi O, Kawai T, Sanjo H, Copeland NG, Gilbert D, Jenkins NA, et al. TLR6: A novel member of an expanding toll-like receptor family. Gene. 1999;231(1-2):59-65.

25. Kimbrell DA, Beutler B. The evolution and genetics of innate immunity. Nature Reviews Genetics. 2001;2(4):256-67.

26. O'Neill LAJ. TLRs: Professor Mechnikov, sit on your hat. Trends in Immunology. 2004;25(12):687-93.

27. Medzhitov R, Preston-Hurlburt P, Janeway CA. A human homologue of the Drosophila Toll protein signals activation of adaptive immunity. Nature. 1997;388(6640):394-7.

28. Katwal P, Thomas M, Uprety T, Hildreth MB, Kaushik RS. Development and biochemical and immunological characterization of early passage and immortalized bovine intestinal epithelial cell lines from the ileum of a young calf. (0920-9069 (Print)).

29. Joosten LAB, Abdollahi-Roodsaz S, Dinarello CA, O'Neill L, Netea MG. Toll-like receptors and chronic inflammation in rheumatic diseases: new developments. Nature Reviews Rheumatology. 2016;12(6):344-57.

30. Yang Y, Jobin C. Microbial imbalance and intestinal pathologies: connections and contributions. Disease Models & Mechanisms. 2014;7(10):1131-42.

31.   Török HP, Glas J, Endres I, Tonenchi L, Teshome MY, Wetzke M, et al. Epistasis Between Toll-Like Receptor-9 Polymorphisms and Variants in NOD2 and IL23R Modulates Susceptibility to Crohn's Disease. Official journal of the American College of Gastroenterology | ACG. 2009;104(7).

32.   Pierik M, Joossens S, Van Steen K, Van Schuerbeek N, Vlietinck R, Rutgeerts P, et al. Toll-Like Receptor-1, -2, and -6 Polymorphisms Influence Disease Extension in Inflammatory Bowel Diseases. Inflammatory Bowel Diseases. 2006;12(1):1-8.

33.   Price AE, Shamardani K, Lugo KA, Deguine J, Roberts AW, Lee BL, et al. A Map of Toll-like Receptor Expression in the Intestinal Epithelium Reveals Distinct Spatial, Cell Type-Specific, and Temporal Patterns. Immunity. 2018;49(3):560-75.e6.

34.   Muzio M, Bosisio D, Polentarutti N, D'Amico G, Stoppacciaro A, Mancinelli R, et al. Differential expression and regulation of toll-like receptors (TLR) in human leukocytes: selective expression of TLR3 in dendritic cells. J Immunol. 2000;164(11):5998-6004.

35.   Visintin A, Mazzoni A, Spitzer JH, Wyllie DH, Dower SK, Segal DM. Regulation of Toll-like receptors in human monocytes and dendritic cells. J Immunol. 2001;166(1):249-55.

36.   Supajatura V, Ushio H, Nakao A, Okumura K, Ra C, Ogawa H. Protective roles of mast cells against enterobacterial infection are mediated by Toll-like receptor 4. J Immunol. 2001;167(4):2250-6.

37.   McCurdy JD, Lin TJ, Marshall JS. Toll-like receptor 4-mediated activation of murine mast cells. J Leukoc Biol. 2001;70(6):977-84.

38. McNamara PS, Fonceca AM, Howarth D, Correia JB, Slupsky JR, Trinick RE, et al. Respiratory syncytial virus infection of airway epithelial cells, in vivo and in vitro, supports pulmonary antibody responses by inducing expression of the B cell differentiation factor BAFF. Thorax. 2013;68(1):76-81.

39. Svanborg C, Godaly G, Hedlund M. Cytokine responses during mucosal infections: role in disease pathogenesis and host defence. Current Opinion in Microbiology. 1999;2(1):99-103.

40. Kawasaki T, Kawai T. Toll-like receptor signaling pathways. Front Immunol. 2014;5:461-.

41. Botos I, Segal DM, Davies DR. The structural biology of Toll-like receptors. Structure. 2011;19(4):447-59.

42. El-Zayat SR, Sibaii H, Mannaa FA. Toll-like receptors activation, signaling, and targeting: an overview. Bulletin of the National Research Centre. 2019;43(1):187.

43. Deguine J, Barton GM. MyD88: a central player in innate immune signaling. F1000Prime Rep. 2014;6:97-.

44. Muzio M, Ni J, Feng P, Dixit VM. IRAK (Pelle) family member IRAK-2 and MyD88 as proximal mediators of IL-1 signaling. Science. 1997;278(5343):1612-5.

45. Martin M, Böl GF, Eriksson A, Resch K, Brigelius-Flohé R. Interleukin-1-induced activation of a protein kinase co-precipitating with the type I interleukin-1 receptor in T cells. Eur J Immunol. 1994;24(7):1566-71.

46. Kanakaraj P, Schafer PH, Cavender DE, Wu Y, Ngo K, Grealish PF, et al. Interleukin (IL)-1 receptor-associated kinase (IRAK) requirement for optimal induction of multiple IL-1 signaling pathways and IL-6 production. J Exp Med.

1998;187(12):2073-9.

47.   Aravind L, Dixit VM, Koonin EV. Apoptotic molecular machinery: vastly
increased complexity in vertebrates revealed by genome comparisons. Science.
2001;291(5507):1279-84.

48.   Li S, Strelow A, Fontana EJ, Wesche H. IRAK-4: a novel member of the IRAK
family with the properties of an IRAK-kinase. Proc Natl Acad Sci U S A.
2002;99(8):5567-72.

49.   Wesche H, Gao X, Li X, Kirschning CJ, Stark GR, Cao Z. IRAK-M is a novel
member of the Pelle/interleukin-1 receptor-associated kinase (IRAK) family. J Biol
Chem. 1999;274(27):19403-10.

50.   Dhillon B, Aleithan F, Abdul-Sater Z, Abdul-Sater AA. The Evolving Role of
TRAFs in Mediating Inflammatory Responses. Front Immunol. 2019;10:104-.

51.   Medzhitov R, Preston-Hurlburt P, Kopp E, Stadlen A, Chen C, Ghosh S, et al.
MyD88 is an adaptor protein in the hToll/IL-1 receptor family signaling pathways.
Mol Cell. 1998;2(2):253-8.

52.   Oshiumi H, Sasai M, Shida K, Fujita T, Matsumoto M, Seya T. TIR-containing
adapter molecule (TICAM)-2, a bridging adapter recruiting to toll-like receptor 4
TICAM-1 that induces interferon-beta. J Biol Chem. 2003;278(50):49751-62.

53.   Oshiumi H, Matsumoto M, Funami K, Akazawa T, Seya T. TICAM-1, an adaptor
molecule that participates in Toll-like receptor 3-mediated interferon-beta
induction. Nat Immunol. 2003;4(2):161-7.

54.   Ullah MO, Sweet MJ, Mansell A, Kellie S, Kobe B. TRIF-dependent TLR
signaling, its functions in host defense and inflammation, and its potential as a

therapeutic target. J Leukoc Biol. 2016;100(1):27-45.

55. Meylan E, Burns K, Hofmann K, Blancheteau V, Martinon F, Kelliher M, et al. RIP1 is an essential mediator of Toll-like receptor 3-induced NF-kappa B activation. Nat Immunol. 2004;5(5):503-7.

56. Shalova IN, Kajiji T, Lim JY, Gómez-Piña V, Fernández-Ruíz I, Arnalich F, et al. CD16 regulates TRIF-dependent TLR4 response in human monocytes and their subsets. J Immunol. 2012;188(8):3584-93.

57. Lee HK, Dunzendorfer S, Soldau K, Tobias PS. Double-stranded RNA-mediated TLR3 activation is enhanced by CD14. Immunity. 2006;24(2):153-63.

58. Di Gioia M, Zanoni I. Toll-like receptor co-receptors as master regulators of the immune response. Mol Immunol. 2015;63(2):143-52.

59. Zanoni I, Granucci F. Role of CD14 in host protection against infections and in metabolism regulation. Front Cell Infect Microbiol. 2013;3:32-.

60. Palsson-McDermott EM, Doyle SL, McGettrick AF, Hardy M, Husebye H, Banahan K, et al. TAG, a splice variant of the adaptor TRAM, negatively regulates the adaptor MyD88-independent TLR4 pathway. Nature immunology. 2009;10(6):579-86.

61. Doyle SL, Husebye H, Connolly DJ, Espevik T, O'Neill LA, McGettrick AF. The GOLD domain-containing protein TMED7 inhibits TLR4 signalling from the endosome upon LPS stimulation. Nat Commun. 2012;3:707.

62. Xue Q, Zhou Z, Lei X, Liu X, He B, Wang J, et al. TRIM38 negatively regulates TLR3-mediated IFN-β signaling by targeting TRIF for degradation. PLoS One. 2012;7(10):e46825-e.

63. Kanneganti T-D, Lamkanfi M, Núñez G. Intracellular NOD-like receptors in host defense and disease. Immunity. 2007;27(4):549-59.

64. Lamkanfi M, Kanneganti T-D. Regulation of immune pathways by the NOD-like receptor NLRC5. Immunobiology. 2012;217(1):13-6.

65. Inohara N, Ogura Y, Chen FF, Muto A, Nuñez G. Human Nod1 confers responsiveness to bacterial lipopolysaccharides. J Biol Chem. 2001;276(4):2551-4.

66. Chamaillard M, Philpott D, Girardin SE, Zouali H, Lesage S, Chareyre F, et al. Gene–environment interaction modulated by allelic heterogeneity in inflammatory diseases. Proceedings of the National Academy of Sciences. 2003;100(6):3455-60.

67. Girardin SE, Boneca IG, Carneiro LA, Antignac A, Jéhanno M, Viala J, et al. Nod1 detects a unique muropeptide from gram-negative bacterial peptidoglycan. Science. 2003;300(5625):1584-7.

68. Inohara N, Koseki T, Del Peso L, Hu Y, Yee C, Chen S, et al. Nod1, an Apaf-1-like activator of caspase-9 and nuclear factor-κB. Journal of Biological Chemistry. 1999;274(21):14560-7.

69. Loo Y-M, Gale M. Immune Signaling by RIG-I-like Receptors. Immunity. 2011;34(5):680-92.

70. Yoneyama M, Kikuchi M, Natsukawa T, Shinobu N, Imaizumi T, Miyagishi M, et al. The RNA helicase RIG-I has an essential function in double-stranded RNA-induced innate antiviral responses. Nature Immunology. 2004;5(7):730-7.

71. Cui S, Eisenächer K, Kirchhofer A, Brzózka K, Lammens A, Lammens K, et al. The C-terminal regulatory domain is the RNA 5'-triphosphate sensor of RIG-I. Mol Cell. 2008;29(2):169-79.

72.   Paz S, Sun Q, Nakhaei P, Romieu-Mourez R, Goubau D, Julkunen I, et al. Induction of IRF-3 and IRF-7 phosphorylation following activation of the RIG-I pathway. Cell Mol Biol (Noisy-le-grand). 2006;52(1):17-28.

73.   Liu HM, Gale M. Hepatitis C Virus Evasion from RIG-I-Dependent Hepatic Innate Immunity. Gastroenterol Res Pract. 2010;2010:548390.

74.   Drickamer K. C-type lectin-like domains. Curr Opin Struct Biol. 1999;9(5):585-90.

75.   Cambi A, Koopman M, Figdor CG. How C-type lectins detect pathogens. Cell Microbiol. 2005;7(4):481-8.

76.   Ley K, Kansas GS. Selectins in T-cell recruitment to non-lymphoid tissues and sites of inflammation. Nat Rev Immunol. 2004;4(5):325-35.

77.   Geijtenbeek TB, Torensma R, van Vliet SJ, van Duijnhoven GC, Adema GJ, van Kooyk Y, et al. Identification of DC-SIGN, a novel dendritic cell-specific ICAM-3 receptor that supports primary immune responses. Cell. 2000;100(5):575-85.

78.   El-Awady AR, Miles B, Scisci E, Kurago ZB, Palani CD, Arce RM, et al. Porphyromonas gingivalis evasion of autophagy and intracellular killing by human myeloid dendritic cells involves DC-SIGN-TLR2 crosstalk. PLoS pathogens. 2015;11(2):e1004647.

79.   Kawai T, Akira S. Toll-like receptors and their crosstalk with other innate receptors in infection and immunity. Immunity. 2011;34(5):637-50.

80.   Cookson WO, Ubhi B, Lawrence R, Abecasis GR, Walley AJ, Cox HE, et al. Genetic linkage of childhood atopic dermatitis to psoriasis susceptibility loci. Nat Genet. 2001;27(4):372-3.

81.   Ablasser A, Bauernfeind F, Hartmann G, Latz E, Fitzgerald KA, Hornung V. RIG-

I-dependent sensing of poly(dA:dT) through the induction of an RNA polymerase III-transcribed RNA intermediate. Nat Immunol. 2009;10(10):1065-72.

82.   Rathinam VAK, Fitzgerald KA. Innate immune sensing of DNA viruses. Virology. 2011;411(2):153-62.

83.   Nathan C, Sporn M. Cytokines in context. J Cell Biol. 1991;113(5):981-6.

84.   Dinarello CA. Proinflammatory cytokines. Chest. 2000;118(2):503-8.

85.   Dinarello CA. Role of pro- and anti-inflammatory cytokines during inflammation: experimental and clinical findings. J Biol Regul Homeost Agents. 1997;11(3):91-103.

86.   Wormald S, Hilton DJ. Inhibitors of Cytokine Signal Transduction *. Journal of Biological Chemistry. 2004;279(2):821-4.

87.   Rollins BJ. Chemokines. Blood. 1997;90(3):909-28.

88.   Ernst CA, Zhang YJ, Hancock PR, Rutledge BJ, Corless CL, Rollins BJ. Biochemical and biologic characterization of murine monocyte chemoattractant protein-1. Identification of two functional domains. The Journal of Immunology. 1994;152(7):3541-9.

89.   Sullivan TP, Eaglstein WH, Davis SC, Mertz P. The pig as a model for human wound healing. Wound repair and regeneration. 2001;9(2):66-76.

90.   Nielsen KL, Hartvigsen ML, Hedemann MS, Lærke HN, Hermansen K, Bach Knudsen KE. Similar metabolic responses in pigs and humans to breads with different contents and compositions of dietary fibers: a metabolomics study. The American journal of clinical nutrition. 2014;99(4):941-9.

91.   Pan C, Kumar C, Bohl S, Klingmueller U, Mann M. Comparative proteomic

phenotyping of cell lines and primary cells to assess preservation of cell type-specific functions. Mol Cell Proteomics. 2009;8(3):443-50.

92. Alge CS, Hauck SM, Priglinger SG, Kampik A, Ueffing M. Differential protein profiling of primary versus immortalized human RPE cells identifies expression patterns associated with cytoskeletal remodeling and cell survival. J Proteome Res. 2006;5(4):862-78.

93. Segeritz C-P, Vallier L. Chapter 9 - Cell Culture: Growing Cells as Model Systems In Vitro. In: Jalali M, Saldanha FYL, Jalali M, editors. Basic Science Methods for Clinical Researchers. Boston: Academic Press; 2017. p. 151-72.

94. Takeuchi O, Akira S. Innate immunity to virus infection. Immunol Rev. 2009;227(1):75-86.

95. Takeuchi O, Akira S. Pattern recognition receptors and inflammation. Cell. 2010;140(6):805-20.

96. Khan R, Petersen FC, Shekhar S. Commensal Bacteria: An Emerging Player in Defense Against Respiratory Pathogens. Frontiers in immunology. 2019;10:1203-.

97. Santagati M, Scillato M, Patanè F, Aiello C, Stefani S. Bacteriocin-producing oral streptococci and inhibition of respiratory pathogens. FEMS Immunol Med Microbiol. 2012;65(1):23-31.

98. Manning J, Dunne EM, Wescombe PA, Hale JD, Mulholland EK, Tagg JR, et al. Investigation of Streptococcus salivarius-mediated inhibition of pneumococcal adherence to pharyngeal epithelial cells. BMC Microbiol. 2016;16(1):225.

99. Shay JW, Wright WE. Hayflick, his limit, and cellular ageing. Nat Rev Mol Cell Biol. 2000;1(1):72-6.

100. Bodnar AG, Ouellette M, Frolkis M, Holt SE, Chiu C-P, Morin GB, et al. Extension of life-span by introduction of telomerase into normal human cells. science. 1998;279(5349):349-52.

101. Irfan Maqsood M, Matin MM, Bahrami AR, Ghasroldasht MM. Immortality of cell lines: challenges and advantages of establishment. Cell biology international. 2013;37(10):1038-45.

102. Lee KM, Choi KH, Ouellette MM. Use of exogenous hTERT to immortalize primary human cells. Cytotechnology. 2004;45(1):33-8.

103. Bryan T, Redder RR. SV40-lnduced Immortalization of Human Cells. Critical Reviews™ in Oncogenesis. 1994;5(4).

104. Oda D, Bigler L, Lee P, Blanton R. HPV immortalization of human oral epithelial cells: a model for carcinogenesis. Experimental cell research. 1996;226(1):164-9.

105. Pan C, Kumar C, Bohl S, Klingmueller U, Mann M. Comparative proteomic phenotyping of cell lines and primary cells to assess preservation of cell type-specific functions. Molecular & Cellular Proteomics. 2009;8(3):443-50.

106. Henderson JR. Applications of primary cell cultures in the study of animal viruses. II. Variations in host responses to infection by certain arthropod-borne viruses. Yale J Biol Med. 1961;33(5):350-8.

107. Sato S, Kiyono H. The mucosal immune system of the respiratory tract. Current Opinion in Virology. 2012;2(3):225-32.

108. Murphy TF, Bakaletz LO, Smeesters PR. Microbial interactions in the respiratory tract. Pediatr Infect Dis J. 2009;28(10 Suppl):S121-6.

109. Brundage JF. Interactions between influenza and bacterial respiratory pathogens:

implications for pandemic preparedness. The Lancet Infectious Diseases. 2006;6(5):303-12.

110. Li Z, Lu G, Meng G. Pathogenic Fungal Infection in the Lung. Frontiers in immunology. 2019;10:1524-.

111. Kash JC, Taubenberger JK. The Role of Viral, Host, and Secondary Bacterial Factors in Influenza Pathogenesis. The American Journal of Pathology. 2015;185(6):1528-36.

112. Sreenivasan C, Thomas M, Sheng Z, Hause BM, Collin EA, Knudsen DE, et al. Replication and transmission of the novel bovine influenza D virus in a guinea pig model. Journal of virology. 2015;89(23):11990-2001.

113. Sreenivasan CC, Thomas M, Antony L, Wormstadt T, Hildreth MB, Wang D, et al. Development and characterization of swine primary respiratory epithelial cells and their susceptibility to infection by four influenza virus types. Virology. 2019;528:152-63.

114. Jha KK, Banga S, Palejwala V, Ozer HL. SV40-Mediated Immortalization. Experimental Cell Research. 1998;245(1):1-7.

115. Wright W, Shay J. Wright, W.E. & Shay, J.W. The two-stage mechanism controlling cellular senescence and immortalization. Exp. Gerontol. 27, 383-389. Experimental gerontology. 1992;27:383-9.

116. Toouli CD, Huschtscha LI, Neumann AA, Noble JR, Colgin LM, Hukku B, et al. Comparison of human mammary epithelial cells immortalized by simian virus 40 T-Antigen or by the telomerase catalytic subunit. Oncogene. 2002;21(1):128-39.

117. Sack GH, Jr. Human cell transformation by simian virus 40--a review. In Vitro.

1981;17(1):1-19.

118.   Chopra DP, Dombkowski AA, Stemmer PM, Parker GC. Intestinal epithelial cells in vitro. Stem Cells Dev. 2010;19(1):131-42.

119.   Kaushik RS, Begg AA, Wilson HL, Aich P, Abrahamsen MS, Potter A, et al. Establishment of fetal bovine intestinal epithelial cell cultures susceptible to bovine rotavirus infection. Journal of Virological Methods. 2008;148(1):182-96.

120.   Kumar S, Tummala H. Development of Soluble Inulin Microparticles as a Potent and Safe Vaccine Adjuvant and Delivery System. Molecular Pharmaceutics. 2013;10(5):1845-53.

121.   Chang J-S, Russell GC, Jann O, Glass EJ, Werling D, Haig DM. Molecular cloning and characterization of Toll-like receptors 1-10 in sheep. Veterinary Immunology and Immunopathology. 2009;127(1):94-105.

122.   Pacheco IL, Abril N, Zafra R, Molina-Hernández V, Morales-Prieto N, Bautista MJ, et al. Fasciola hepatica induces Foxp3 T cell, proinflammatory and regulatory cytokine overexpression in liver from infected sheep during early stages of infection. Veterinary Research. 2018;49(1):56.

123.   Jin X, Zhang M, Zhu X-m, Fan Y-r, Du C-g, Bao H-e, et al. Modulation of ovine SBD-1 expression by Saccharomyces cerevisiae in ovine ruminal epithelial cells. BMC Veterinary Research. 2018;14(1):134.

124.   Arce C, Ramirez-Boo M, Lucena C, Garrido J. Innate immune activation of swine intestinal epithelial cell lines (IPEC-J2 and IPI-2I) in response to LPS from Salmonella typhimurium. Comparative immunology, microbiology and infectious diseases. 2010;33(2):161-74.

125. Meurens F, Girard-Misguich F, Melo S, Grave A, Salmon H, Guillén N. Broad early immune response of porcine epithelial jejunal IPI-2I cells to Entamoeba histolytica. Molecular immunology. 2009;46(5):927-36.

126. Sargeant HR, Miller HM, Shaw M-A. Inflammatory response of porcine epithelial IPEC J2 cells to enterotoxigenic E. coli infection is modulated by zinc supplementation. Molecular immunology. 2011;48(15-16):2113-21.

127. Moue M, Tohno M, Shimazu T, Kido T, Aso H, Saito T, et al. Toll-like receptor 4 and cytokine expression involved in functional immune response in an originally established porcine intestinal epitheliocyte cell line. Biochimica et Biophysica Acta (BBA)-General Subjects. 2008;1780(2):134-44.

128. Sreenivasan C, Zhao M, Francis D, Kaushik RS, editors. PROINFLAMMATORY CYTOKINE PROFILE OF PORCINE INTESTINAL EPITHELIAL CELLS UPON STIMULATION WITH ENTEROTOXIGENIC ESCHERICHIA COLI AND HEAT LABILE TOXIN. Proceedings of the South Dakota Academy of Science; 2011.

129. Veldhuizen EJ, Hendriks HG, Hogenkamp A, Van Dijk A, Gaastra W, Tooten PC, et al. Differential regulation of porcine β-defensins 1 and 2 upon Salmonella infection in the intestinal epithelial cell line IPI-2I. Veterinary immunology and immunopathology. 2006;114(1-2):94-102.

130. Alexander C, Rietschel ET. Bacterial lipopolysaccharides and innate immunity. Journal of endotoxin research. 2001;7(3):167-202.

131. van der Bruggen T, Nijenhuis S, van Raaij E, Verhoef J, van Asbeck BS. Lipopolysaccharide-induced tumor necrosis factor alpha production by human

monocytes involves the raf-1/MEK1-MEK2/ERK1-ERK2 pathway. Infect Immun. 1999;67(8):3824-9.

132. Abreu MT, Vora P, Faure E, Thomas LS, Arnold ET, Arditi M. Decreased Expression of Toll-Like Receptor-4 and MD-2 Correlates with Intestinal Epithelial Cell Protection Against Dysregulated Proinflammatory Gene Expression in Response to Bacterial Lipopolysaccharide. The Journal of Immunology. 2001;167(3):1609-16.

133. Burkey T, Skjolaas K, Dritz S, Minton J. Expression of porcine Toll-like receptor 2, 4 and 9 gene transcripts in the presence of lipopolysaccharide and Salmonella enterica serovars Typhimurium and Choleraesuis. Veterinary immunology and immunopathology. 2009;130(1-2):96-101.

134. Benkhart EM, Siedlar M, Wedel A, Werner T, Ziegler-Heitbrock HWL. Role of Stat3 in Lipopolysaccharide-Induced IL-10 Gene Expression. The Journal of Immunology. 2000;165(3):1612-7.

135. Kim Y-K, Jung H-G, Myint A-M, Kim H, Park S-H. Imbalance between pro-inflammatory and anti-inflammatory cytokines in bipolar disorder. Journal of Affective Disorders. 2007;104(1):91-5.

136. Zhong Y, Kinio A, Saleh M. Functions of NOD-Like Receptors in Human Diseases. Frontiers in Immunology. 2013;4(333).

137. Travassos LH, Girardin SE, Philpott DJ, Blanot D, Nahori M-A, Werts C, et al. Toll-like receptor 2-dependent bacterial sensing does not occur via peptidoglycan recognition. EMBO reports. 2004;5(10):1000-6.

138. Singh S, Anshita D, Ravichandiran V. MCP-1: Function, regulation, and

involvement in disease. Int Immunopharmacol. 2021;101(Pt B):107598-.

139. Laflamme N, Echchannaoui H, Landmann R, Rivest S. Cooperation between toll-like receptor 2 and 4 in the brain of mice challenged with cell wall components derived from gram-negative and gram-positive bacteria. European Journal of Immunology. 2003;33(4):1127-38.

140. Yoon SI, Kurnasov O, Natarajan V, Hong M, Gudkov AV, Osterman AL, et al. Structural basis of TLR5-flagellin recognition and signaling. Science. 2012;335(6070):859-64.

141. Hayashi F, Smith KD, Ozinsky A, Hawn TR, Yi EC, Goodlett DR, et al. The innate immune response to bacterial flagellin is mediated by Toll-like receptor 5. Nature. 2001;410(6832):1099-103.

142. Smith MF, Jr., Mitchell A, Li G, Ding S, Fitzmaurice AM, Ryan K, et al. Toll-like receptor (TLR) 2 and TLR5, but not TLR4, are required for Helicobacter pylori-induced NF-kappa B activation and chemokine expression by epithelial cells. J Biol Chem. 2003;278(35):32552-60.

143. Zhang Z, Louboutin J-P, Weiner DJ, Goldberg JB, Wilson JM. Human Airway Epithelial Cells Sense <i>Pseudomonas aeruginosa</i> Infection via Recognition of Flagellin by Toll-Like Receptor 5. Infection and Immunity. 2005;73(11):7151-60.

144. Rietdijk ST, Burwell T, Bertin J, Coyle AJ. Sensing intracellular pathogens—NOD-like receptors. Current Opinion in Pharmacology. 2008;8(3):261-6.

145. Amer A, Franchi L, Kanneganti T-D, Body-Malapel M, Özören N, Brady G, et al. Regulation of Legionella Phagosome Maturation and Infection

through Flagellin and Host Ipaf *. Journal of Biological Chemistry. 2006;281(46):35217-23.

146. Lécine P, Esmiol S, Métais JY, Nicoletti C, Nourry C, McDonald C, et al. The NOD2-RICK complex signals from the plasma membrane. J Biol Chem. 2007;282(20):15197-207.

147. Bolívar S, Anfossi R, Humeres C, Vivar R, Boza P, Muñoz C, et al. IFN-β Plays Both Pro- and Anti-inflammatory Roles in the Rat Cardiac Fibroblast Through Differential STAT Protein Activation. Frontiers in Pharmacology. 2018;9(1368).

148. Bi D, Gao Y, Chu Q, Cui J, Xu T. NOD1 is the innate immune receptor for iE-DAP and can activate NF-κB pathway in teleost fish. Developmental & Comparative Immunology. 2017;76:238-46.

149. Cardenas I, Mulla MJ, Myrtolli K, Sfakianaki AK, Norwitz ER, Tadesse S, et al. Nod1 activation by bacterial iE-DAP induces maternal-fetal inflammation and preterm labor. J Immunol. 2011;187(2):980-6.

150. Takano M, Takeuchi T, Kuriyama S, Yumoto R. Role of peptide transporter 2 and MAPK signaling pathways in the innate immune response induced by bacterial peptides in alveolar epithelial cells. Life Sciences. 2019;229:173-9.

151. Rosenzweig HL, Galster KT, Planck SR, Rosenbaum JT. NOD1 expression in the eye and functional contribution to IL-1beta-dependent ocular inflammation in mice. Invest Ophthalmol Vis Sci. 2009;50(4):1746-53.

152. Zou J, Kawai T, Tsuchida T, Kozaki T, Tanaka H, Shin KS, et al. Poly IC triggers a cathepsin D- and IPS-1-dependent pathway to enhance cytokine production and mediate dendritic cell necroptosis. Immunity. 2013;38(4):717-28.

153. Miyake T, Kumagai Y, Kato H, Guo Z, Matsushita K, Satoh T, et al. Poly I:C-Induced Activation of NK Cells by CD8α[+] Dendritic Cells via the IPS-1 and TRIF-Dependent Pathways. The Journal of Immunology. 2009;183(4):2522-8.

154. Lundberg AM, Drexler SK, Monaco C, Williams LM, Sacre SM, Feldmann M, et al. Key differences in TLR3/poly I:C signaling and cytokine induction by human primary cells: a phenomenon absent from murine cell systems. Blood. 2007;110(9):3245-52.

155. Sameer AS, Nissar S. Toll-Like Receptors (TLRs): Structure, Functions, Signaling, and Role of Their Polymorphisms in Colorectal Cancer Susceptibility. Biomed Res Int. 2021;2021:1157023-.

156. McNab F, Mayer-Barber K, Sher A, Wack A, O'Garra A. Type I interferons in infectious disease. Nature Reviews Immunology. 2015;15(2):87-103.

157. Steelman AJ, Li J. Poly(I:C) promotes TNFα/TNFR1-dependent oligodendrocyte death in mixed glial cultures. Journal of Neuroinflammation. 2011;8(1):89.

158. Liu J, Guo Y-M, Hirokawa M, Iwamoto K, Ubukawa K, Michishita Y, et al. A synthetic double-stranded RNA, poly I:C, induces a rapid apoptosis of human CD34^{+} cells. Experimental Hematology. 2012;40(4):330-41.

159. Sato Y, Yoshino H, Kashiwakura I, Tsuruga E. DAP3 is involved in modulation of cellular radiation response by RIG-I-Like receptor agonist in human lung adenocarcinoma cells. International Journal of Molecular Sciences. 2021;22(1):420.

160. Tengroth L, Millrud CR, Kvarnhammar AM, Kumlien Georén S, Latif L, Cardell

L-O. Functional Effects of Toll-Like Receptor (TLR)3, 7, 9, RIG-I and MDA-5 Stimulation in Nasal Epithelial Cells. PLOS ONE. 2014;9(6):e98239.

161.   Zhu J, Xu S, Li X, Wang J, Jiang Y, Hu W, et al. Infectious bronchitis virus inhibits activation of the TLR7 pathway, but not the TLR3 pathway. Archives of Virology. 2020;165(9):2037-43.

162.   Coutermarsh-Ott S, Eden K, Allen IC. Beyond the inflammasome: regulatory NOD-like receptor modulation of the host immune response following virus exposure. J Gen Virol. 2016;97(4):825-38.

163.   Miyake T, Kumagai Y, Kato H, Guo Z, Matsushita K, Satoh T, et al. Poly I:C-induced activation of NK cells by CD8 alpha+ dendritic cells via the IPS-1 and TRIF-dependent pathways. J Immunol. 2009;183(4):2522-8.

164.   Lever AR, Park H, Mulhern TJ, Jackson GR, Comolli JC, Borenstein JT, et al. Comprehensive evaluation of poly(I:C) induced inflammatory response in an airway epithelial model. Physiol Rep. 2015;3(4):e12334.

165.   Altomonte L, Zoli A, Mirone L, Scolieri P, Magaró M. Serum levels of interleukin-1b, tumour necrosis factor-a and interleukin-2 in rheumatoid arthritis. Correlation with disease activity. Clinical Rheumatology. 1992;11(2):202-5.

166.   Langevin C, Boudinot P, Collet B. IFN Signaling in Inflammation and Viral Infections: New Insights from Fish Models. Viruses. 2019;11(3).

167.   Ip WKE, Hoshi N, Shouval DS, Snapper S, Medzhitov R. Anti-inflammatory effect of IL-10 mediated by metabolic reprogramming of macrophages. Science. 2017;356(6337):513-9.

168.   Chi H, Li C, Zhao FS, Zhang L, Ng TB, Jin G, et al. Anti-tumor Activity of Toll-

Like Receptor 7 Agonists. Front Pharmacol. 2017;8:304.

169. Schön MP, Schön M. Imiquimod: mode of action. British Journal of Dermatology. 2007;157(s2):8-13.

170. Ma F, Zhang J, Zhang J, Zhang C. The TLR7 agonists imiquimod and gardiquimod improve DC-based immunotherapy for melanoma in mice. Cell Mol Immunol. 2010;7(5):381-8.

171. Kumar S, Kesharwani SS, Kuppast B, Bakkari MA, Tummala H. Pathogen-mimicking vaccine delivery system designed with a bioactive polymer (inulin acetate) for robust humoral and cellular immune responses. Journal of Controlled Release. 2017;261:263-74.

172. Kumar S, Kesharwani SS, Kuppast B, Rajput M, Bakkari MA, Tummala H. Discovery of inulin acetate as a novel immune-active polymer and vaccine adjuvant: synthesis, material characterization, and biological evaluation as a toll-like receptor-4 agonist. Journal of Materials Chemistry B. 2016;4(48):7950-60.

173. Frasnelli SCT, de Medeiros MC, Bastos AdS, Costa DL, Orrico SRP, Rossa Junior C. Modulation of Immune Response by RAGE and TLR4 Signalling in PBMCs of Diabetic and Non-Diabetic Patients. Scandinavian Journal of Immunology. 2015;81(1):66-71.

174. Wu D-M, Wang Y-J, Han X-R, Wen X, Li L, Xu L, et al. Retracted: Tanshinone IIA prevents left ventricular remodelling via the TLR4/MyD88/NF-κB signalling pathway in rats with myocardial infarction. Journal of Cellular and Molecular Medicine. 2018;22(6):3058-72.